

THE UNIVERSITY OF CALGARY

DYNAMIC ANALYSIS OF A SPHERICAL MEMBRANE WITH A HEAVY  
PLATE AT THE TOP

BY

SHAO-SHAN TANG

A THESIS

SUBMITTED TO THE FACULTY OF GRADUATE STUDIES  
IN PARTIAL FULFILMENT OF THE REQUIREMENTS  
FOR THE DEGREE OF MASTER OF SCIENCE

DEPARTMENT OF MECHANICAL ENGINEERING

CALGARY, ALBERTA

FEBRUARY, 1993

© SHAO-SHAN TANG 1993



National Library  
of Canada

Acquisitions and  
Bibliographic Services Branch

395 Wellington Street  
Ottawa, Ontario  
K1A 0N4

Bibliothèque nationale  
du Canada

Direction des acquisitions et  
des services bibliographiques

395, rue Wellington  
Ottawa (Ontario)  
K1A 0N4

*Your file* *Votre référence*

*Our file* *Notre référence*

The author has granted an irrevocable non-exclusive licence allowing the National Library of Canada to reproduce, loan, distribute or sell copies of his/her thesis by any means and in any form or format, making this thesis available to interested persons.

L'auteur a accordé une licence irrévocable et non exclusive permettant à la Bibliothèque nationale du Canada de reproduire, prêter, distribuer ou vendre des copies de sa thèse de quelque manière et sous quelque forme que ce soit pour mettre des exemplaires de cette thèse à la disposition des personnes intéressées.

The author retains ownership of the copyright in his/her thesis. Neither the thesis nor substantial extracts from it may be printed or otherwise reproduced without his/her permission.

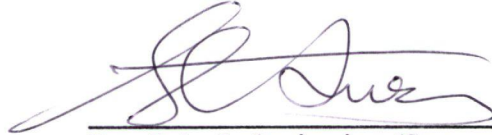
L'auteur conserve la propriété du droit d'auteur qui protège sa thèse. Ni la thèse ni des extraits substantiels de celle-ci ne doivent être imprimés ou autrement reproduits sans son autorisation.

ISBN 0-315-83265-7

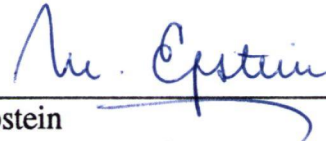
Canada

The University of Calgary  
Faculty of Graduate Studies


The undersigned certify that they have read, and recommend to the Faculty of Graduate Studies for acceptance, a thesis entitled, "Dynamic Analysis of a Spherical Membrane With a Heavy Plate at the Top", submitted by Shao-shan Tang in partial fulfilment of the requirements for the degree of Master of Science in Mechanical Engineering.



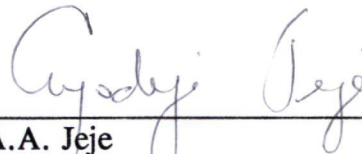
Dr. S.A. Lukasiewicz (Supervisor)  
Department of Mechanical Engineering



Dr. M. Epstein  
Department of Mechanical Engineering



Dr. M.C. Singh  
Department of Mechanical Engineering



Dr. A.A. Jeje  
Department of Chemical Engineering

# Acknowledgements

The author wishes to express his sincere gratitude and appreciation to his supervisor, Dr. S. Lukasiewicz, for his conscientious guidance, support and encouragement throughout the course of this work.

Thanks are also due to the fellow students of the Department of Mechanical Engineering for their advice and cooperation. The author is profoundly grateful to his sister, Ying Tang, who rendered great assistance in typing and editing this thesis. The financial assistance provided by the Department of Mechanical Engineering of the University of Calgary, and as well as by Dr. S. Lukasiewicz, are gratefully appreciated and acknowledged.

# Abstract

This thesis presents an investigation of large deflection and dynamic behaviour of a pneumatic, non-shallow spherical membrane, subjected to axisymmetric loading. The membrane is assumed to be inextensible and without mass. The round rigid plate built in at the top of the membrane is the only part of the structure that has mass and weight. The exact geometry of deformations is the starting point of the mathematic formulation. Numerical computational approaches are applied to establish the load and deflection relationship of the membrane structures. The relationship between the plate displacement and the applied load shows a peculiar discontinuity across the initial no-load position. Furthermore, across the no-load position, there is a significant difference in stiffness in the inward and outward displacement directions.

The dynamic behaviour of membrane structures is studied based on the structural stiffness results obtained from the static analysis. Free vibration frequencies are dependent not only on mass of the plate and stiffness of the membrane shell, but also on the oscillation amplitude. Nonlinear, chaotic vibration responses to periodic load inputs have been observed and analyzed.

The bisection method is used in the root finding process. Trapezoidal and Simpson's schemes are applied in numerical integration of wrinkled membrane length and its enclosed volume. Runge-Kutta approach has been employed to determine the dynamic behaviour of the structures.

# Table of Contents

Acknowledgements . . . . .	iii
Abstract . . . . .	iv
List of Tables . . . . .	vi
List of Figures . . . . .	vii
Nomenclature . . . . .	x
Chapter 1 Introduction . . . . .	1
1.1 General Background . . . . .	1
1.2 Literature Review . . . . .	5
1.2.1 Review on the analysis of air-supported structures . . . . .	5
1.2.2 Review on the study of the large deflection behaviour of spherical inflatables . . . . .	11
1.3 Objectives . . . . .	13
1.4 Assumptions . . . . .	14
Chapter 2 Formulation of the Theoretical Model . . . . .	15
2.1 The differential geometry of revolutes . . . . .	15
2.2 Static Analysis . . . . .	20
2.3 Dynamic Response of the Plate . . . . .	32
Chapter 3 Numerical Solutions and Techniques . . . . .	37
3.1 Static Analysis . . . . .	37
3.2 Dynamic Analysis . . . . .	47
Chapter 4 Numerical Results and Analysis . . . . .	54
4.1 Static Loading and Deformation . . . . .	54
4.2 Dynamic Behaviour . . . . .	68
Chapter 5 Concluding Remarks and Summary . . . . .	84
5.1 Summary and Limitations . . . . .	84
5.2 Concluding Remarks . . . . .	89
References . . . . .	90
Appendix . . . . .	95

# List of Tables

Table 1	Parameters to define a deformed configuration of semi-spherical dome . . . . .	36
Table 2	Parameters At $P_2$ Approaches Negative Infinity . . . . .	42
Table 3	The effect of inner pressure on the membrane deformation . . . . .	57
Table 4	Oscillation Frequency Affected By The Plate Mass . . . . .	71

# List of Figures

Figure 1 Prestressed membranes . . . . .	2
Figure 2 Two types of support of a spherical membrane . . . . .	7
Figure 3 Three modes of symmetric deformation of cylindrical inflatables . . . . .	9
Figure 4a Geometry of membrane of revolution . . . . .	16
Figure 4b Stress resultants and surface load on a differential element . . . . .	16
Figure 5a Initial cross-section of a spherical inflatable . . . . .	19
Figure 5b Spherical inflatable in 3-dimensional view . . . . .	19
Figure 6 A membrane segment in its meridian plane . . . . .	21
Figure 7 A point on a deformed membrane surface . . . . .	31
Figure 8 Free body diagram of the plate in vibration . . . . .	33
Figure 9 Angle $\phi_1$ as function of the height of the plate . . . . .	35
Figure 10 Parameters defining a deformed spherical inflatable . . . . .	43
Figure 11 Three modes of deformation of a low profile spherical membrane . . . . .	44
Figure 12 Flow Chart of Root Finding Routine . . . . .	45
Figure 13 Deformed membrane by infinite suction at the plate . . . . .	46
Figure 14 Phase plane of the plate in free vibration . . . . .	50
Figure 15 Phase plane of the plate in forced vibration . . . . .	51
Figure 16 Phase plane of the plate at the resonant state . . . . .	52
Figure 17 Vibration of the plate at the resonant state . . . . .	53

## List of Figures (cont'd)

Figure 18	Load-displacement relations in 3 different configurations (Downward displacement: Domes subjected to push-in load at the plate) . .	55
Figure 19	Load-displacement relations in 3 different configurations (Upward displacement: Domes subjected to pull-out load at the plate) . . .	56
Figure 20	Deformed semi-spherical membranes . . . . .	58
Figure 21	The distinct load-deflection curve of a high profile dome . . . . .	59
Figure 22a	Schematic diagram of a deformed spherical membrane in high profile . . . . .	60
Figure 22b	Schematic diagram of a deformed spherical membrane in high profile . . . . .	61
Figure 23a	Formation of wrinkles near the plate . . . . .	63
Figure 23b	Formation of wrinkles near the support . . . . .	63
Figure 24	Comparison of the results to the earlier data curves from ref. [10] . .	67
Figure 25	Free oscillation patterns with different magnitudes . . . . .	69
Figure 26	An approximated spring-mass model of the dome . . . . .	72
Figure 27	Time - displacement curve from the approx. mass-spring model . . . .	73
Figure 28	Free vibration frequency as function of vibration amplitude . . . . .	74
Figure 29	Forced vibration of the plate . . . . .	76
Figure 30	Free oscillation of a plate with different internal pressure assumptions . . . . .	77
Figure 31	Spectrum analysis of a spherical dome . . . . .	78

## List of Figures (cont'd)

Figure 32	Spectrum analysis of a spherical dome: upward motion . . . . .	79
Figure 33	The max. upward motion amplitude in forced vibration away from the resonance . . . . .	80
Figure 34	Meridian force $N_\varphi$ around the plate edge in free vibration . . . . .	82
Figure 35	Meridian force $N_\varphi$ around the plate edge in forced vibration . . . . .	83

:

# Nomenclature

$\Phi_0$	Central half angle of a spherical inflatable before deformation
$\Phi$	Central half angle of a spherical inflatable after deformation
$W, P$	Concentrated load applied at the spherical apex
$R_0$	Radius of cylindrical tubes
$R$	Radius of a spherical surface
$P_1$	Internal pressure(absolute) of a deformed inflatable
$P_2$	Applied pressure on the rigid plate
$r_0$	Radius of the rigid plate
$r$	Radius of point on the deformed membrane, measured from the central axis
$R_1, R_2$	Principal radii at a surface point
$\varphi$	Angle between the principal normal to the meridian and the axis of revolution
$\theta$	Azimuth angle measured from a reference plane in the static analysis section
$\phi_1$	The meridian angle measured at the plate edge
$\phi_2$	The meridian angle measured at the boundary separating the wrinkled and unwrinkled region
$N_\phi$	Principal force/unit length in the meridional plane
$N_\theta$	Principal force/unit length in the parallel plane
$N_{\phi\theta}$	Shearing force/unit length in the parallel and meridional plane

## Nomenclature (cont'd)

$q_1$	Surface load in the meridian direction
$q_2$	Surface load in the circumferential direction
$q_n$	Surface load in the principal normal direction
$u, v, w$	Displacement in meridional, circumferential and normal direction
$\ddot{u}, \ddot{v}, \ddot{w}$	Acceleration in meridional, circumferential and normal direction
$t$	Time in the dynamic analysis
$\rho$	Density/unit area of the membrane
$s$	Meridian length in the wrinkled region
$S$	Initial meridian length of the wrinkled material
$C$	Integration constant
$V_0, P_0$	Initial volume and pressure of an inflatable
$h$	The height of the plate measured from a reference point
$\delta$	Displacement of the plate from the original position
$m$	Mass of the plate
$g$	Gravity acceleration
$F(t)$	Dynamic force applied at the plate
$y$	Displacement coordinate, defined outward direction as positive
$\dot{y}_0$	Initial velocity of the plate
$y_0$	Initial location of the plate
$\varepsilon_c$	Tolerance of $C$ value
$\varepsilon_y$	Tolerance in evaluation of meridian curve length

# Chapter 1 Introduction

## 1.1 General Background

Inflatable membrane structures have come into practical use since the Second World War as one form of tension structures. These pneumatic structures are well suited to support broadly distributed loads and live load. They are lightweight, low-cost and collapsible when deflated and therefore easy to transport and erect. With the appearance of translucent, high-strength, polyvinyl-chloride plastic sheets on the market inflatables, such as bubble structures, have become common in the last two decades. They are regularly used for temporary or semi-permanent enclosures. Land based applications include temporary shelters and warehouse tents. Sea based applications are such as moored vessels and buoys, floating hospitals and other logistical support facilities. Fig.<sup>1</sup> 1 shows various shapes of prestressed membrane structures in practical applications. The history of early applications of inflatables as architectural forms and as engineering systems is described and summarized in ref<sup>2</sup> [1]<sup>3</sup> to [8].

These inflated structures have characteristics that the load-carrying members transmit applied loads to either the foundation or other supporting structures by direct tensile stress without flexure and compression. Their cross sectional dimensions and

---

<sup>1</sup>For simplicity the word "Figure" is abbreviated as "Fig." in this thesis.

<sup>2</sup>Similar as "Figure", Reference is shortened as "ref".

<sup>3</sup>Numbers in square brackets refer to articles listed under References.

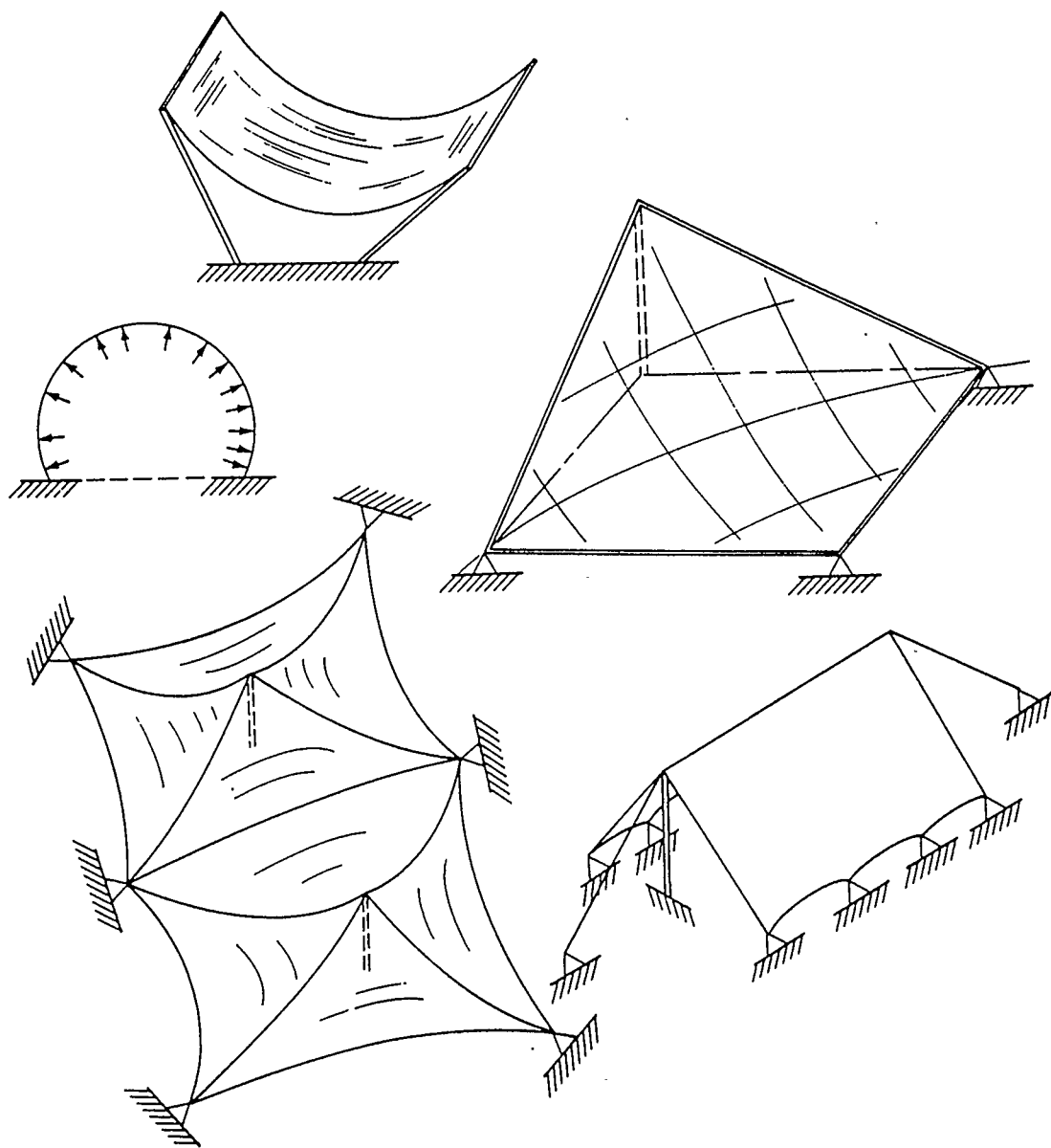


Figure 1 Prestressed membranes

methods of fabrication are such that their shear and flexural rigidities, as well as their buckling resistance, are negligible. Because of their reduced stiffness characteristics, these membrane structures are susceptible to large motions due to external loads and dynamic effects. They respond in a non-linear fashion to both prestressing forces such as internal pressure and in service loads, regardless of linearity of materials or loads.

Spherical pneumatics are now used for enclosing large unobstructed areas for recreational facilities such as tennis courts, swimming pools, skating rinks, etc. and for creation of large-scale temporary or semi-permanent enclosures in connection with exploration and work sites in the far north of Canada and the United States. The application of such structures is also seen in agricultural areas where bubble-form green houses are constructed using translucent plastic sheets, which possess relatively high tensile and tear strength and good transmissivity as well.

Over the past two decades there has been a considerable development of analysis techniques and computer codes for membrane structures. Free vibration modes and corresponding frequencies of inextensible, air-inflated, cylindrical membranes have been determined[9]. In this thesis it is attempted to uncover and understand the large deflection dynamic behaviour of inextensible, air-inflated spherical membrane shells subjected to axisymmetric loads. Although similar studies in areas such as collapse of spherical air supported membranes by static loads and instability of spherical membranes have been carried out and reported in ref. [11] to [18], investigation of the response of

spherical inflatable membranes to the dynamic load at the apex has not been reported in previous works.

In the present study the problem of the large deflection and dynamic behaviour of an air-inflated spherical dome with a round rigid plate built in at the top is investigated. Deflections are allowed to become large compared to the initial configurations of the inflatables. The study is based on an exact geometrically non-linear analysis, admitting deflections to the order of the initial height of the structure. Because of the inextensible nature of the pneumatic shells, wrinkles are always developed in the deformed region where circumferential stress (or "hoop" stress) vanishes. Both cases where the internal pressure obeys Boyle's Law and remains constant are studied and significant differences are observed in large deformation behaviour. The problem is defined by a set of integral-differential equations which are derived based on the membrane theory and combined with Gauss-Codazzi condition. The governing differential equation to describe the wrinkled region is solved in a closed form. The constant of integration is determined by numerical approaches for given boundary conditions together with the compatibility equation. The obtained results are verified by comparing to the available published values; a close agreement is observed. Based on the static load-displacement relationship of the structure, the structural response to the dynamic loads is analyzed. The mass of the membrane is neglected and the interaction between the fluid and the structure is not included.

## 1.2 Literature Review

### 1.2.1 Review on the analysis of air-supported structures

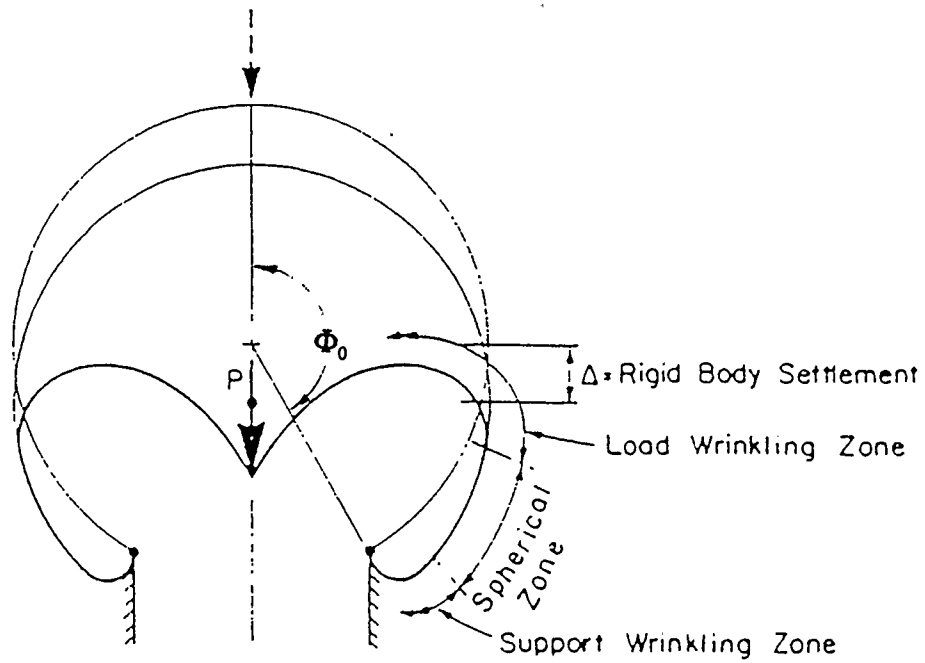
The development of pneumatic structures started out shortly after the Second World War. One of the first air structures was a radome -- a semi-spherical dome housing radar devices, which was conceived and developed to meet the needs of the British Royal Air Force for a thin, non-metallic protective covering for the large ground radar installations. As a result, a study program was carried out which included analytical design studies, model construction and testing.

Since then many research projects in air-inflatables have been undertaken over the years. Based on the membrane theory of small deformations, many problems such as stability of the membrane structures have been solved. The best overview of these is presented by Frei Otto in ref. [5].

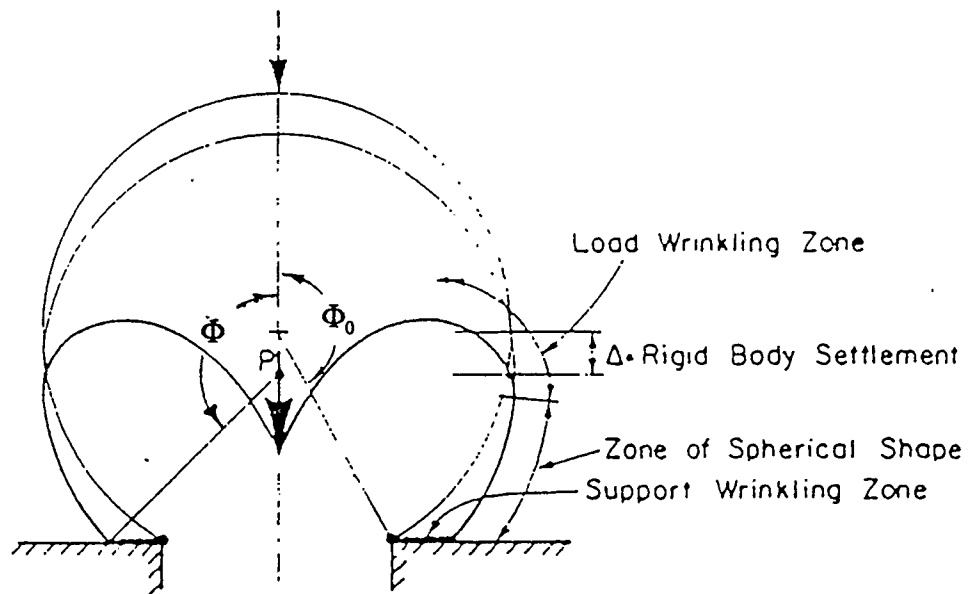
Although air-supported structures are designed not to deform to the point where membrane wrinkling is caused under normal working conditions, they are sometimes subjected to excessive loading due to ice, snow or water accumulation. The aspect of collapse by ponding of air-supported structures has gained a considerable interest from researchers. D.J. Malcolm investigated the possibility of collapse through an accumulation of rain. His studies were limited to symmetric problems including the collapse of axisymmetric membranes[17] subjected to a static axisymmetric load in the presence of a ponding medium.

S. Lukasiewicz and P.G. Glockner [11,12,13] extended the analysis to the non-symmetrically loaded cylindrical and spherical membranes and admitted the extensibility of the inflatable structure. Simple analysis was presented to investigate the behaviour of a spherical membrane subjected to an increasing concentrated force applied non-symmetrically to the structure. The dead weight of the structure was also included in the analysis. They concluded that applying the concentrated line load non-symmetrically would decrease the value of the critical load. They also found that the effect of the elasticity of the membrane material is to decrease the value of the critical load. They approached the membrane stability problem using Lagrangian variational principle, i.e. the variation of the total potential energy of the system is zero. Investigation was also conducted in the ponding instability of air-supported spherical membranes with initial imperfections. Simple formulae for the critical load were obtained. It was found that, in the symmetrically loaded cases, the effect of the ponding fluid accumulating in the initial depression reduces the value of the critical load significantly. Their results also indicated that, if the ponding takes place non-symmetrically, the eccentricity causes a significant increase in the value of the critical load thereby making the axisymmetric loading the governing configuration.

P.G. Glockner and W. Szyszkowski[18,19,20,21] analyzed spherical membranes as shown in Fig. 2 undergoing very large axisymmetric deformations and wrinkling under the action of concentrated loads applied at the apex using equations of equilibrium and the Gauss-Codazzi relations. The deflections of the membrane were allowed to grow larger than the initial height of the structure, and even larger than the initial radius of



a) 'Stove pipe' Support



b) Support with adjacent horizontal surface

Fig. 2 Two types of support of a spherical membrane

curvature  $R_0$ . The analysis established certain height to span ratios above which there existed critical loads beyond which the structure would 'snap-through' and collapse. They concluded that for central half angle  $\Phi_0$  less than  $90^\circ$  the equilibrium was always stable under concentrated load at the apex. If, in addition to a concentrated load, an accumulating medium was also present, filling the depression completely, the instability may have occurred even for central angles  $\Phi_0$  less than  $90^\circ$ .

A complete analysis of the nonlinear load-deflection and stability behaviour of cylindrical membranes without end 'shear walls' subjected to longitudinal symmetric line loads is presented in [18] by W. Szyszkowski and P.G. Glockner. The analysis includes low and high profile structures as well as lateral stability behaviour. The analyses were carried out for two different support characteristics with the cross-sectional shapes same as in Fig. 2:

- a support which is raised above the exterior ground surface adjacent to the structure and above the interior floor surface so as to allow arbitrary deflections and rotations of the membrane at the support as well as to permit vertical deflections under the line load which are equal to or larger than the initial rise of the structure, Fig. 3a.
- a support where a horizontal ground surface exists next to and at the elevation of the support thereby restricting the rotation and deflection of the membrane at the support to  $\Phi_0 > 0^\circ$ , shown in Fig. 3a,b.

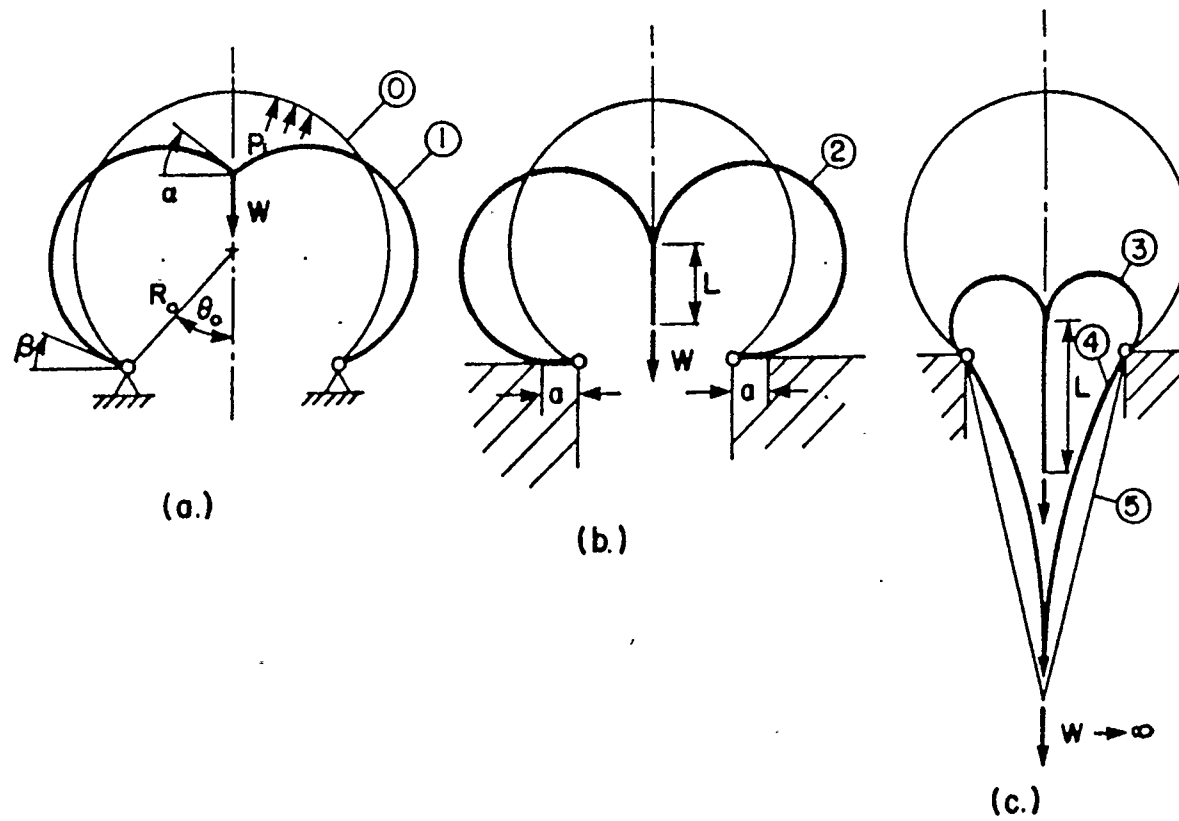


Figure 3 Three modes of symmetric deformation of cylindrical inflatables

The analysis indicates that the behaviour of such structures falls into one of three modes of deformation, Fig. 3:

- the 'first mode', during which there may exist large deflections and rotations in the structure but the membrane is not in contact with the ground nor are portions of the membrane in contact with one another,
- the 'second mode', during which portions of the membrane to either side of the line load are in contact, forming the so-called vertical contact zone of length  $L$ ,
- the 'third mode', during which the membrane is in contact with the horizontal ground surface adjacent to the support, forming the so-called horizontal contact zone of length  $a$ .

A similar analysis was presented by S. Lukasiewicz and P.G. Glockner [13] for the non-symmetrically loaded spherical membrane. This analysis clearly indicates a vertical and lateral instability at certain load levels, and the governing mode of failure are very much influenced by the initial geometry. The results also indicate that the onset of lateral instability is not identical to the configuration when the contact between the membrane and the horizontal surface is first established. Nor does the onset of vertical instability signify the existence or beginning of vertical contact. The extensive experimental data obtained from tests on a small-scale cylindrical inflatable model are presented and compared with analytical predictions in their investigation. They observed excellent agreement between the numerical and experimental results which confirm the validity of the theory and the assumptions used in its derivations.

A study of the free vibration of inextensible, air-inflated, cylindrical membrane structure was carried out by R.H. Plaut and T.D. Fagan [9]. In their work the weight of the membrane was included in the analysis. First, the equilibrium shape of the cross section was determined, and the small vibrations about this configuration were studied using linear approach. Free vibration frequencies and mode shapes were determined.

### **1.2.2 Review on the study of the large deflection behaviour of spherical inflatables**

The theoretical solution of problems of stability and large deformations of air inflated structures is difficult due to the strong non-linearity of the problem. Despite substantial theoretical achievements in the area of air supported structures the progress in developing a theory which will describe the behaviour of inflated spherical domes is slow and still limited to calculating the static deformations and wrinkling loads on the basis of classical methods of analysis.

A numerical analysis of the nonlinear behaviour of pneumatic structures was first presented by J.T. Oden and W.K. Kubitza [24]. They used the finite element representation of flexible pneumatic structures to describe the general kinematic properties of thin membranes. Using the first law of thermodynamics, a general relationship between the kinematic and kinetic variable associated with the behaviour of the finite elements of arbitrary pneumatic structures was obtained. This led to the general equation of the motion of the finite elements of thin membranes, and included such properties as anisotropy, nonlinear viscoelasticity, thermoviscoelasticity,

inhomogeneity, and plasticity, with no restrictions on the magnitudes of the deformations. Finally, the general formulation was modified and applied to a number of special cases, i.e. the stretching of square and circular rubber membranes.

Following the remarkable progress in the numerical computations, numerical methods, for instance, the finite element method [25] was also applied to the analysis of membrane structure. In membrane structures, wrinkled deformations are statically developed owing to their forms or kinds of loadings. Some investigations are reported on the analysis of wrinkled membranes. Tension field theory [26], which does not attach great importance to the normal deflection is not suitable to analyze the large deflection or the wrinkled deformations of membranes. Analytical investigation of the deformation due to wrinkles was published by M. Stein and J.M. Hedgepeth [27]. In their study, the basic idea was to assume an imaginary mean surface in the wrinkled region of the membrane and denote that the smaller principal stress vanishes in this region. This method assumes that the strains and deflections are small, and therefore were not applicable to the problems of large deflection.

An analytical study of large deflections of pneumatic membranes in the form of surface of revolution under symmetric loading was carried out by Y. Yoko *et al.* [10]. Large deflection of membrane inflatables are obtained in the close form using the nonlinear membrane shell theory. In their formulation, the wrinkled region of the membrane is considered in an Eulerian description satisfying the equation of equilibrium and the Gauss-Codazzi relation. The deformed shape of the inflatables at equilibrium is

defined by the boundary conditions and compatibility equation. The membrane extensibility is considered by solving the problems in specific models. Among them a hemispheric inflatable with a rigid plate at the top was studied in detail.

### 1.3 Objectives

The purpose of this thesis is to examine the large deformation and dynamic behaviour of air-inflated spherical domes with a vibrating mass at their apex. An attempt has been made to use available ANSYS software to study the pneumatic structures. It shows that ANSYS does not possess the capability to carry out both static and dynamic analysis of such structures. In order to study the forced vibration of the dome, static analysis of the membrane is first carried out to establish relationships between the load, the displacement and other parameters that describe the deformed membrane geometry. Based on these results, a dynamic equation of the plate is derived and solved with numerical methods.

A high profile spherical inflatable is defined as a spherical with its half central angle greater than  $90^\circ$ , Fig. 5a. A low profile spherical has the angle less than or equal to  $90^\circ$ . Both low and high profile spherical membranes are chosen to study as they are commonly used in practice. In view of the limited experience with and the relatively scarcity of information available concerning the dynamic behaviour of the spherical inflatables, designers of this type of structures face quite a challenge to design a safe spherical membrane. When the structure is subjected to load at the plate, very

large deflections and wrinkling occur in the vicinity of the loading point and also possibly near the support base in a high profile membrane as well. This type of membranes has a non-linear load-deflection relation. In particular configurations, it has a discontinuity in the load-deflection curve. Therefore, it is interesting to determine its large deformation dynamic behaviour over a range of profiles and configurations.

## 1.4 Assumptions

Throughout the formulation and evaluation process, it is assumed that:

- (1) A membrane with a small uniform thickness can resist only a tensile force, but not bending moments or compressive forces.
- (2) A wrinkled region is replaced by an imaginary, smooth, mean surface which is characterized by the circumferential force  $N_\theta = 0$ , and the meridional force  $N_\phi$  greater than zero.
- (3) A membrane is inextensible and weightless. Effect of the air or fluid inertia of the surrounding medium is neglected.
- (4) There is a horizontal surface next to and at the level of the support. The membrane near the support may come in contact with surface under a certain load at the plate. The membrane in contact with the surface deforms and lies flat on that surface.
- (5) The top of the inflatable can not deform below its support plane.

## Chapter 2 Formulation of the Theoretical Model

### 2.1 The differential geometry of revolutes

Axisymmetric inflatables are one common form of prestressed membranes. The membrane surfaces are generated by revolving an arc about a central axis in its plane, Fig. 4a. The surface of the deformed spherical dome under an axisymmetric load is also symmetrically formed by rotating a curve about the sphere axis. Such curve is to be determined by the force equilibrium and boundary conditions. The geometry of a surface of revolution is shown in Fig. 4a. The generating curve is called a meridian and lies in the so-called meridional plane. The cross sectional curve cut by a plane perpendicular to the axis of revolution is a circle of radius  $r$ . Two surface coordinates are selected: the azimuth angle  $\theta$  that the meridional plane makes with a reference plane, and the angle  $\phi$  between the principal normal to the meridian and the axis of revolution.

Consider a differential element taken from the deformed region subjected to stress resultants and surface loads as shown in Fig, (4b). In the deformed region, the equations of motion are derived as follows:

$$\frac{\partial (N_{\phi\theta} R_2)}{\partial \phi} + \frac{\partial (N_{\theta} R_1)}{\partial \theta} + N_{\phi\theta} \frac{\partial R_2}{\partial \theta} - N_{\theta} \frac{\partial R_1}{\partial \phi} + R_1 R_2 Q_2 = R_1 R_2 \rho t \ddot{v} \quad (1a)$$

$$\frac{\partial (N_{\phi} R_2)}{\partial \phi} + \frac{\partial (N_{\phi\theta} R_1)}{\partial \theta} + N_{\phi\theta} \frac{\partial R_1}{\partial \theta} - N_{\theta} \frac{\partial R_2}{\partial \phi} + R_1 R_2 Q_1 = R_1 R_2 \rho t \ddot{u} \quad (1b)$$

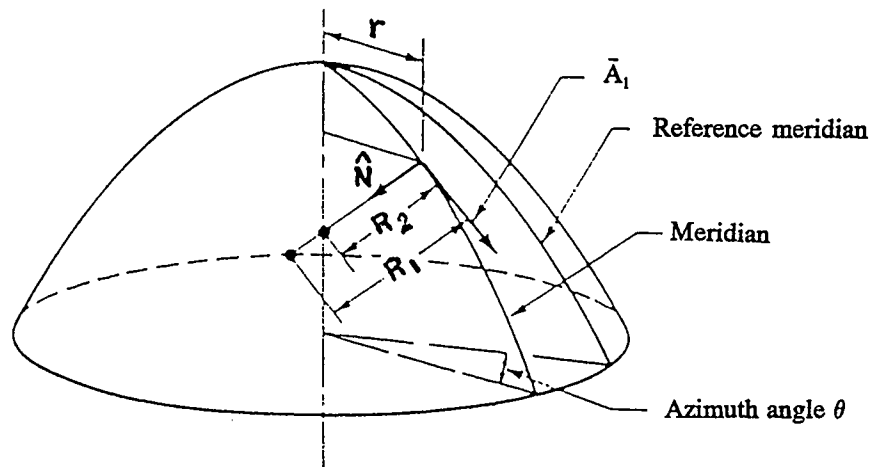


Figure 4a Geometry of membrane of revolution

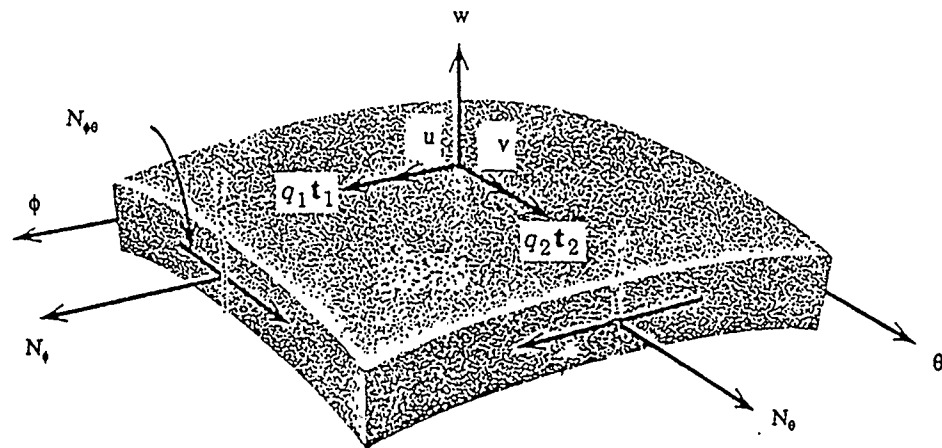


Figure 4b Stress resultants and surface load on a differential element

$$\frac{N_\phi}{R_1} + \frac{N_\theta}{R_2} + Q_n = -\rho t \ddot{w} \quad (1c)$$

For a detailed derivation, see ref. [38].

Noting the symmetry of load and deformation, it is obvious that  $N_{\phi\theta}=0$ ,  $q_2=0$ , and all the derivatives with respect to angle  $\theta$  are zero.

And since the mass of the membrane is neglected,  $\rho=0$ . Therefore, the equations are simplified to:

$$\frac{\partial (N_\phi R_2)}{\partial \phi} - N_\theta \frac{\partial R_2}{\partial \phi} + R_1 R_2 Q_1 = 0 \quad (2a)$$

$$\frac{N_\phi}{R_1} + \frac{N_\theta}{R_2} = P_1 \quad (2b)$$

Notice that in the above equations (2b),  $q_n$  is replaced by  $-P_1$  due to the sign convention. Eq. (2a) is the force equilibrium in the vertical direction. Under the symmetrical loading and deformation conditions, the equation of equilibrium can be expressed as:

$$2\pi N_\phi R_2 \sin \phi = Q \quad (3)$$

where  $Q$  is the resultant force in vertical direction.

The specific model under consideration in this thesis is a spherical dome with a built-in circular rigid plate at its top. The membrane is fastened along its base circumference. The un-deformed geometry of this model is depicted in two dimensions using the meridian curve as shown in Fig. 5a. Fig. 5b is the three dimensional picture of a spherical inflatable formed by revolving the meridian curve  $360^\circ$ . It is defined by a central half angle  $\Phi_0$ , spherical radius  $R$ , and radius  $r_0$  of the plate at the apex. The whole structure is under internal pressure  $P_1$ .

Due to the inextensible nature of the membrane, deformation can not occur as long as the membrane remains fully stretched by the internal pressure. In the another word, the membrane surface remains spherical as long as the two principal resultant forces,  $N_1$  and  $N_2$ , stay positive. Because deformation does not occur in the unwrinkled region, attention is focused only on the wrinkled region. Because the circumferential membrane force in the deformed region vanishes and the wrinkled surface is replaced by a smooth surface, the problem in defining the deformed configuration hinges on determining the meridian curve which revolves to form the wrinkled surface.

Another point to note in the dynamic analysis of this type of inflatables is the separation of static and dynamic formulation. Static formulation is required only for the no-mass membrane shell to establish the relations between the load and the deformed configuration parameters. The dynamic analysis is restricted to the plate at the apex. The membrane force around the plate edge and the internal pressure force can be derived from the relations determined in the static analysis.

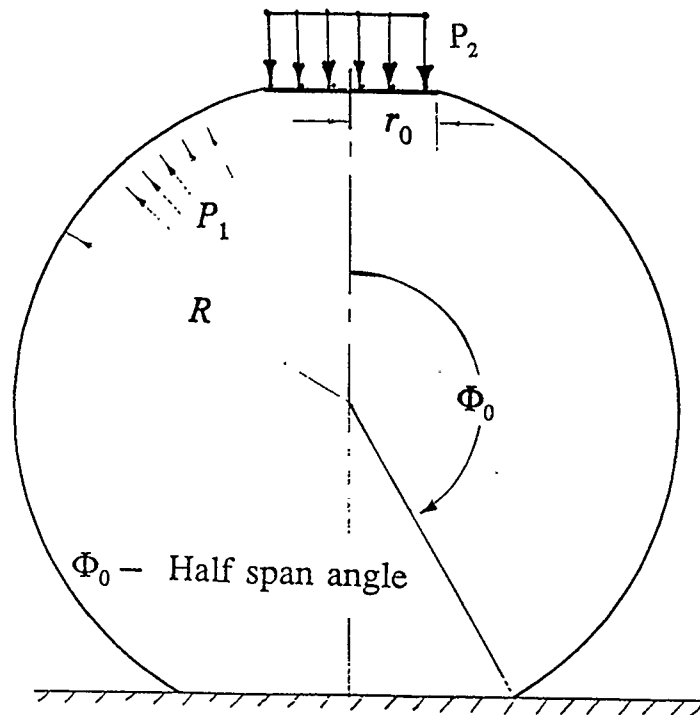


Figure 5a Initial cross-section of a spherical inflatable

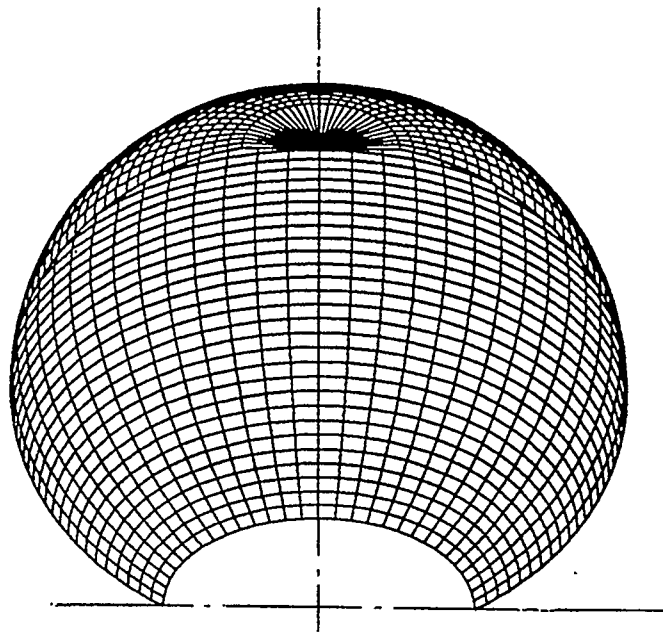


Figure 5b Spherical inflatable in 3-dimensional view

## 2.2 Static Analysis

Geometric relations of the axisymmetric membrane in Fig. 6 show:

$$\frac{dr}{d\varphi} = R_1 \cos \varphi \quad (4)$$

$$r = R_2 \sin \varphi \quad (5)$$

From Eq. (3) and Eq. (2b), the equilibrium equations in normal and vertical direction are respectively expressed as:

$$\frac{N_\varphi}{R_1} + \frac{N_\theta}{R_2} = P_1 \quad (6a)$$

$$2\pi r N_\varphi \sin \varphi = Q \quad (6b)$$

where  $Q$  is the total vertical force exerting on the section,

$P_1$  is the internal pressure(absolute) of the deformed structure,

$P_2$  is the external pressure applied at the rigid plate,

$N_\theta$  is the zero in wrinkled region.

Thus the force  $Q$  in this specific case can be written as:

$$Q = \pi r_o^2 (P_1 - P_2) + \int_0^s 2\pi r P_1 ds \cos \varphi \quad (7)$$

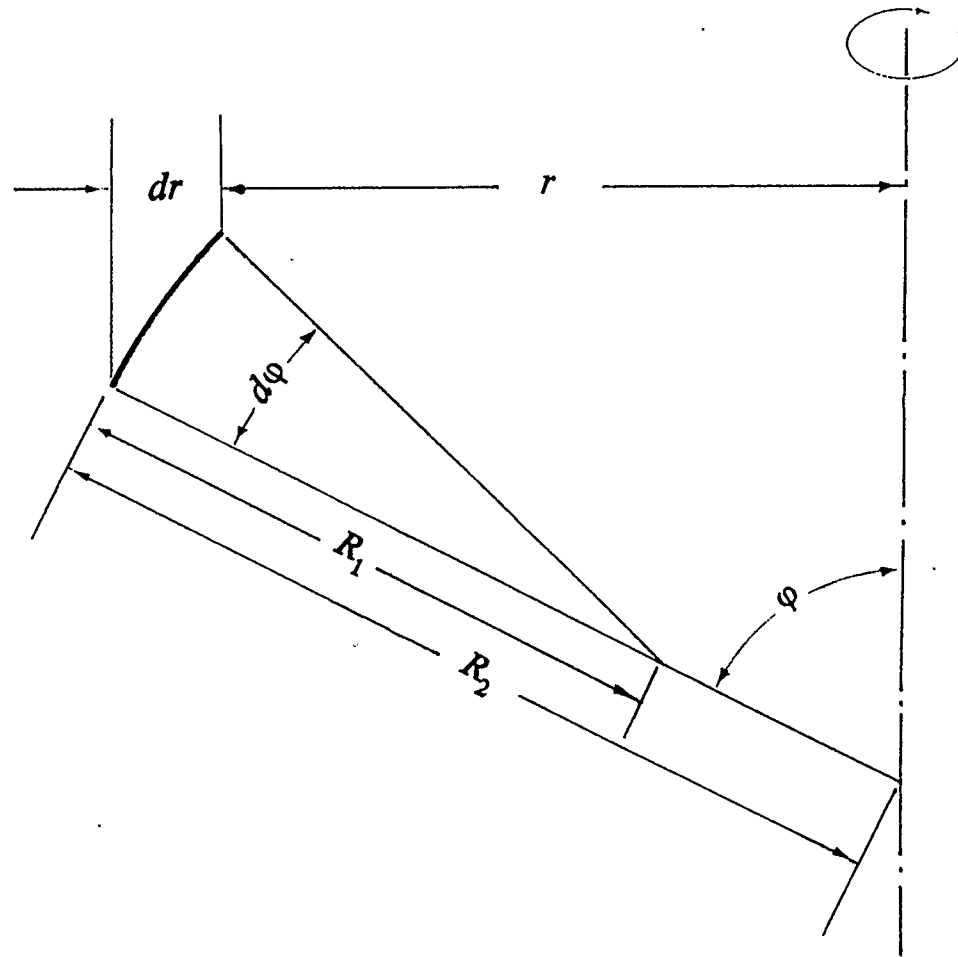


Figure 6 A membrane segment in its meridian plane

where  $ds$  is the differential length on the meridian curve. With the geometric relations of Eq. (4) and (5), the length is expressed as:

$$\begin{aligned}
 ds &= R_1 d\varphi \\
 &= \left[ \frac{1}{\cos\varphi} \frac{dr}{d\varphi} \right] d\varphi \\
 &= \frac{1}{\cos\varphi} dr
 \end{aligned} \tag{8}$$

Meanwhile Eq. (7) can be rewritten as:

$$\begin{aligned}
 Q &= \pi r_o^2 (P_1 - P_2) + \int_{r_o}^r 2\pi r P_1 \left[ \frac{dr}{\cos\varphi} \right] \cos\varphi \\
 &= \pi r_o^2 (P_1 - P_2) + \int_{r_o}^r 2\pi P_1 r dr \\
 &= \pi r^2 P_1 - \pi r_o^2 P_2
 \end{aligned} \tag{9}$$

With the circumferential force vanishing in the wrinkled region, Eq. (6a) becomes:

$$N_\varphi = P_1 R_1 \tag{10}$$

Substituting expression (9) into (6b) gives:

$$N_\varphi = \frac{\pi r^2 P_1 - \pi r_o^2 P_2}{2\pi r \sin\varphi}$$

Therefore,

$$N_{\varphi} = \frac{r^2 P_1 - r_o^2 P_2}{2r \sin \varphi} \quad (11)$$

Recall Eq.(4):

$$R_1 = \frac{1}{\cos \varphi} \frac{dr}{d\varphi} \quad (12)$$

Substitute the above  $R_1$  into Eq. (10) yields:

$$N_{\varphi} = P_1 \frac{1}{\cos \varphi} \frac{dr}{d\varphi} \quad (13)$$

Eliminating  $N_{\varphi}$  in Eq. (11) and (13) arrives at:

$$P_1 \frac{1}{\cos \varphi} \frac{dr}{d\varphi} = \frac{r^2 P_1 - r_o^2 P_2}{2r \sin \varphi} \quad (14)$$

The above equation can be rearranged as:

$$\frac{dr}{d\varphi} = \frac{1}{2 \tan \varphi} \left( r - \frac{r_o^2 P_2}{r P_1} \right) \quad (15)$$

Equation (15) is referred to as the fundamental differential equation in wrinkled regions and is integrable to yield a closed form as

$$r = \sqrt{\frac{P_2}{P_1} r_o^2 + C \sin\varphi} \quad (16)$$

where  $C$  is an integration constant to be determined by boundary conditions which, according to geometrical continuity over boundaries, are defined by the following boundary conditions. Two modes of wrinkled membranes are necessary to be described before writing the boundary conditions. By examining the deformed geometries of a meridian curve, one may there are two possible wrinkling formation. The first mode is partial wrinkling. The wrinkled region appears only around the plate; away from the plate membrane remains unchanged. The second mode is fully wrinkling where the entire membrane surface is covered by wrinkles. Fig. 11 illustrates the two wrinkling modes.

for a partially wrinkled case:

$$\begin{aligned} r(\varphi=\phi_1) &= r_o \\ r(\varphi=\phi_2) &= R \sin\phi_2 \end{aligned}$$

where  $\phi_2$  is the angle dividing the wrinkled and unwrinkled regions.

for a fully wrinkled case:

$$\begin{aligned} r(\varphi=\phi_1) &= r_o \\ r(\varphi=\phi_2) &= R\sin\Phi_0 \end{aligned}$$

where  $\phi_0$  is the half central angle in the undeformed configuration.

The compatibility equation is derived in the following way. A curve length before deformation in meridional direction is:

$$dS = R d\alpha \quad (17)$$

where  $\alpha$  is an angle in the meridian plane of the undeformed reference frame. After deformation, in the new frame, the arc length is:

$$ds = R_1 d\varphi \quad (18)$$

Because the membrane is inextensible, to enforce inextensibility of the membrane, the curve length in meridian plane must remain unchanged before and after deformation:

$$ds = dS \quad (19)$$

where the lower case letter s stands for length in the deformed system and the upper case letter S stands for the length in the initial state where no deformation has occurred yet. From Eq. (12), (16), (17), (18) and (19), one arrives at an equation:

$$\frac{C}{2 \sqrt{\frac{P_2}{P_1} r_o^2 + C \sin \varphi}} d\varphi = R d\alpha \quad (20)$$

Therefore, an integral form of compatibility equation for the partially wrinkled membrane shell is:

$$\int_{\phi_1}^{\phi_2} \frac{C}{2 \sqrt{\frac{P_2}{P_1} r_o^2 + C \sin \varphi}} d\varphi = R (\phi_2 - \phi^o) \quad (21a)$$

For the fully wrinkled membrane the integral form of the compatibility equation is:

$$\int_{\phi_1}^{\phi_2} \frac{C}{2 \sqrt{\frac{P_2}{P_1} r_o^2 + C \sin \varphi}} d\varphi = R (\Phi - \phi^o) \quad (21b)$$

To have a physical interpretation of the above two equations one may perceive the left-hand-side of the equations as the meridian curve length of the wrinkled region, and the right hand side as the original length.

For a dome sealed at its base without any air leakage, the internal pressure obeys the isothermal law, ie. the pressure  $P_1$  is inversely proportional to the total deformed volume. The total volume after deformation is:

$$V = V_w + V_{uw} \quad (22)$$

where  $V_w$  is the volume enclosed by the wrinkled membrane, and  $V_{uw}$  is the volume enclosed by the unwrinkled membrane. In the case of a fully wrinkled membrane,  $V_{uw} = 0$ .

$$\begin{aligned} V_w &= \pi \int_{\phi_1}^{\phi_2} r^2 R_\varphi d\varphi \sin\varphi \\ &= \frac{\pi}{2} \int_{\phi_1}^{\phi_2} C \sqrt{\frac{P_2}{P_1} r_o^2 + C \sin\varphi} d\varphi \end{aligned} \quad (23)$$

$$\begin{aligned} V_{uw} &= \pi \int_{\phi_2}^{\Phi} R^2 \sin^2\varphi (R \sin\varphi d\varphi) \\ &= \pi R^3 \left( \cos\varphi - \frac{1}{3} \cos^3\varphi \right) \Big|_{\phi_2}^{\Phi} \end{aligned} \quad (24)$$

Then the internal pressure after deformation is determined by

$$P = \frac{P_o V_o}{V} \quad (25)$$

where  $P_o$  is the initial internal pressure and  $V_o$  is the volume of the dome without deformation.

In summary, if the dome is partially deformed and wrinkled either by pushing down or pulling up, the deformed configuration can be defined by solving a set of equations:

$$\sqrt{\frac{P_2}{P_1} r_o^2 + C \sin \phi_1} = r_o \quad (26a)$$

$$\sqrt{\frac{P_2}{P_1} r_o^2 + C \sin \phi_2} = R \sin \phi_2 \quad (26b)$$

$$\int_{\phi_1}^{\phi_2} \frac{C}{2 \sqrt{\frac{P_2}{P_1} r_o^2 + C \sin \phi}} d\phi = R(\phi_2 - \phi_o) \quad (26c)$$

$$P_1 = \frac{P_o V_o}{V} \quad (26d)$$

$$V = \frac{\pi}{2} \int_{\phi_1}^{\phi_2} \sin \varphi C \sqrt{\frac{P_2}{P_1} r_o^2 + C \sin \varphi} d\varphi + \pi R^3 \left( \cos \varphi - \frac{1}{3} \cos^3 \varphi \right) \Big|_{\phi_1}^{\phi_2} \quad (26e)$$

If the dome is fully wrinkled, the above set of equations becomes:

$$\sqrt{\frac{P_2}{P_1} r_o^2 + C \sin \phi_1} = r_o \quad (27a)$$

$$\sqrt{\frac{P_2}{P_1} r_o^2 + C \sin \phi_2} = R \sin \Phi \quad (27b)$$

$$P_1 = \frac{P_o V_o}{V} \quad (27c)$$

$$\int_{\phi_1}^{\phi_2} \frac{C}{2 \sqrt{\frac{P_2}{P_1} r_o^2 + C \sin \varphi}} d\varphi = R (\Phi - \phi_o) \quad (27d)$$

In the case that  $P_1$  stays constant at  $P_o$ , Eq.(26d), (26e), (27c), and (27d) can be removed from the above two sets of equations.

Calculation results indicate that although  $P_1$  does not change over a great range, it considerably influences the results when large volume change is involved. In order to study the role of influence of the changing internal pressure, two cases are studied. In one case  $P_1$  stays constant and in the other  $P_1$  varies according to the isothermal gas law. The results are presented and compared in the Numerical Results and Analysis chapter.

After solving for  $C$ ,  $\phi_1$ ,  $\phi_2$  and  $P_1$ , the deformed configurations of the membrane are determined from the following equations:

$$r = \sqrt{\frac{P_2}{P_1} r_o^2 + C \sin \phi} \quad (28)$$

$$h = \int_{\phi}^{\phi_2} R_1 \sin \phi \, d\phi$$

i.e.

$$h = \int_{\phi}^{\phi_2} \frac{C \cos \phi \sin \phi}{2 \sqrt{\frac{P_2}{P_1} r_o^2 + C \sin \phi}} \, d\phi \quad (29)$$

Each set of  $(r, h)$  values defines a point on a deformed meridian curve as shown in Fig. 7. The complete deformed curve is determined by connecting the finite number of points as angle  $\phi$  sweeps from  $\phi_2$  to  $\phi_1$ .

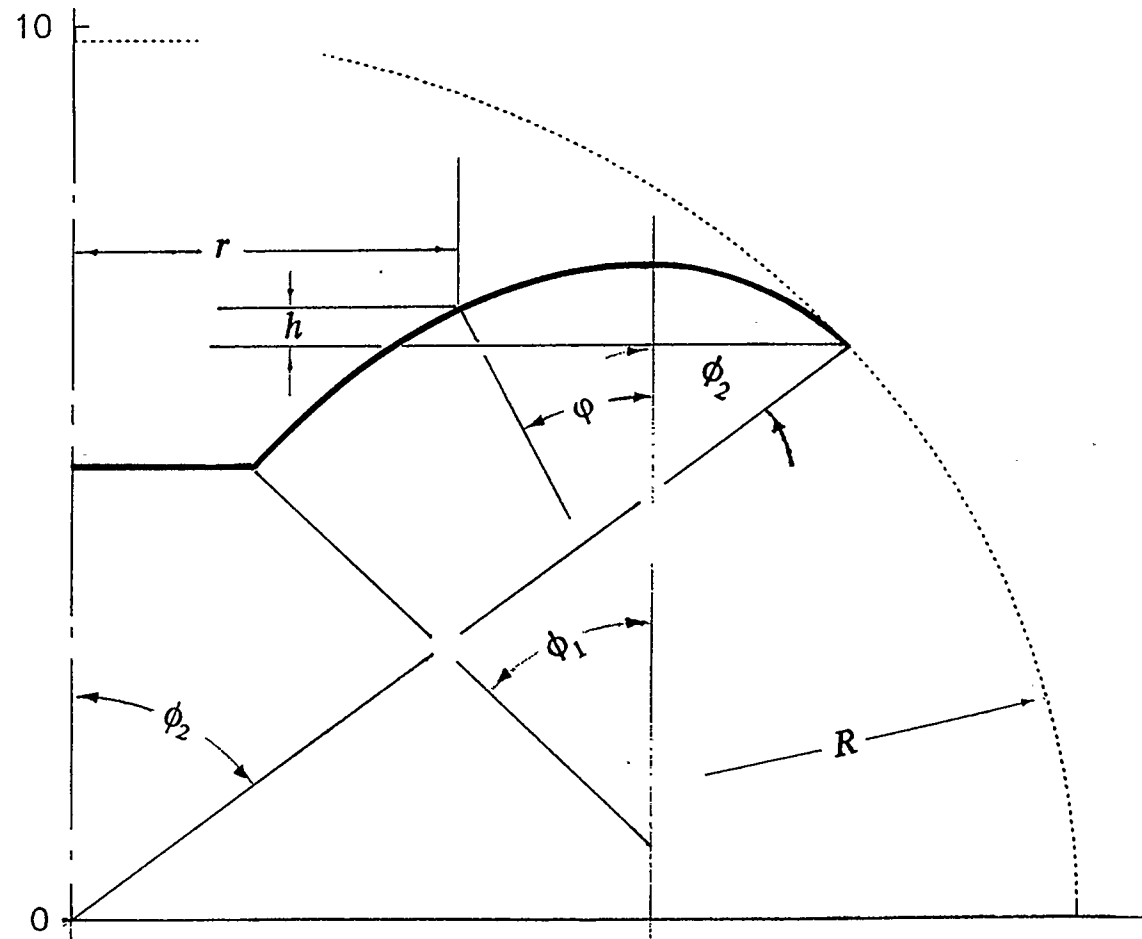


Figure 7 A point on a deformed membrane surface

### 2.3 Dynamic Response of the Plate

Apply Newton's Second Law to the plate shown in the free body diagram of Fig. 8:

$$-m\ddot{y} - 2\pi r_o N_{\varphi(\varphi=\phi_1)} \sin\phi_1 + \pi r_o^2 P_1 - F - mg = 0 \quad (30)$$

Eq. (13) states:

$$N_{\varphi(\varphi=\phi_1)} = \frac{P_1 C}{2r_o}$$

Substitution of this expression into Eq. (30) gives:

$$m\ddot{y} + \pi P_1 C \sin\phi_1 - \pi r_o^2 P_1 + F + mg = 0$$

Acceleration is then determined from:

$$\ddot{y} = -\frac{F(t)}{m} - g + \frac{\pi P_1}{m} (r_o^2 - C \sin\phi_1)$$

where  $P_1$ ,  $\phi_1$  and  $C$  are functions of  $y$ . To be explicit, the above equation is written as:

$$\ddot{y} = -\frac{F(t)}{m} - g + \frac{\pi P_1(y)}{m} [ r_o^2 - C(y) \sin\phi_1(y) ] \quad (31)$$

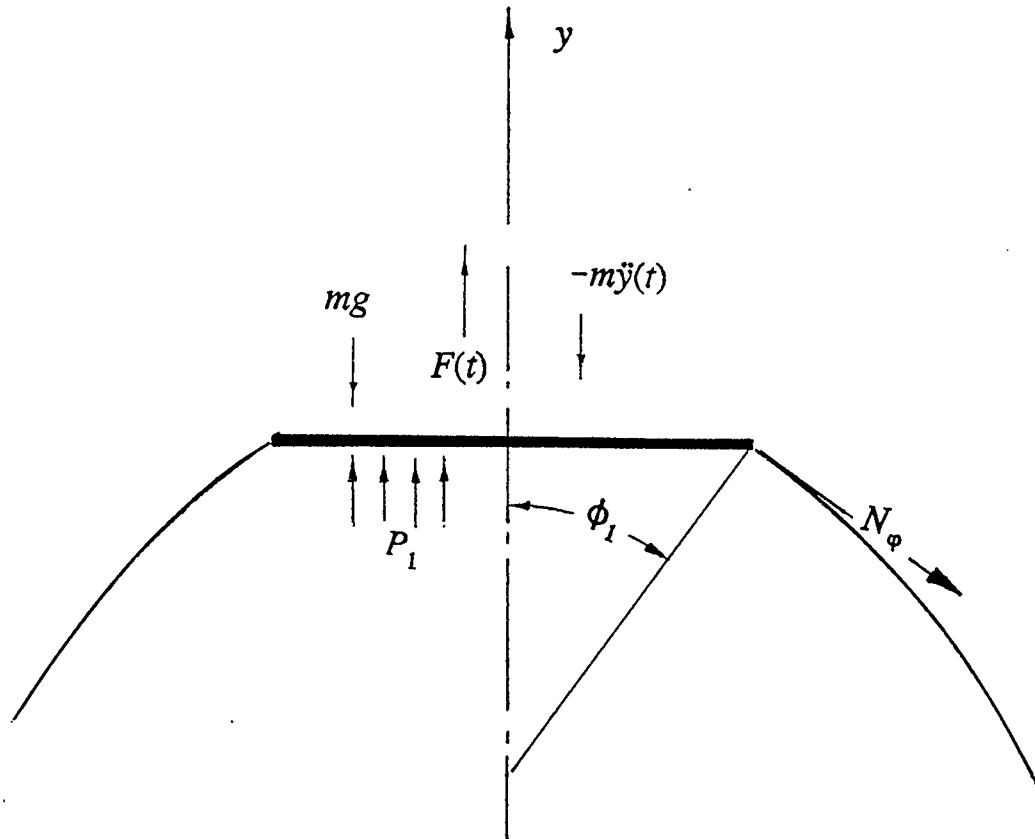


Figure 8 Free body diagram of the plate in vibration

Eq. (31) is the governing dynamic equation to be solved for the displacement-time relationship of the plate. This is a nonlinear equation which can not be solved in a closed form.  $P_1$ ,  $\phi_1$  and  $C$  are discontinuous functions of the displacement  $y$ . Numerical approach must be applied to define the time history of the vibrating plate. Runge-Kutta method is used in the solution process with prescribed initial velocity and deflection of the plate.

The main task becomes to find piece wise functions of  $P_1$ ,  $\phi_1$  and  $C$  and incorporate them into the governing equation. It is accomplished in the following way.

From the previous static analysis of the spherical inflatables, parameters  $P_1$ ,  $\phi_1$  and  $C$  for a given initial configuration are defined at each applied external load  $P_2$ , so is the corresponding plate deflection. As an example, Table 1 is a list of relevant data to define a deformed membrane. It is possible to express  $P_1$ ,  $\phi_1$  and  $C$  as functions of the deflection instead of  $P_2$ . When the plate moves between the lowest and the highest possible position the structure undergoes more than one abrupt change in the deformation configurations. These changes make it necessary to describe the parameters  $P_1$ ,  $\phi_1$  and  $C$  with sections of continuous function. Polynomial regression is applied to process the calculated results to find the functions in polynomial forms. The order of polynomial is affected by the shape of the data curve. Fig. 9 illustrates the functions obtained from the processing, which models the relationship between angle  $\phi_1$  and the plate deflection with initial shape shown. This step is required for each given initial shape.

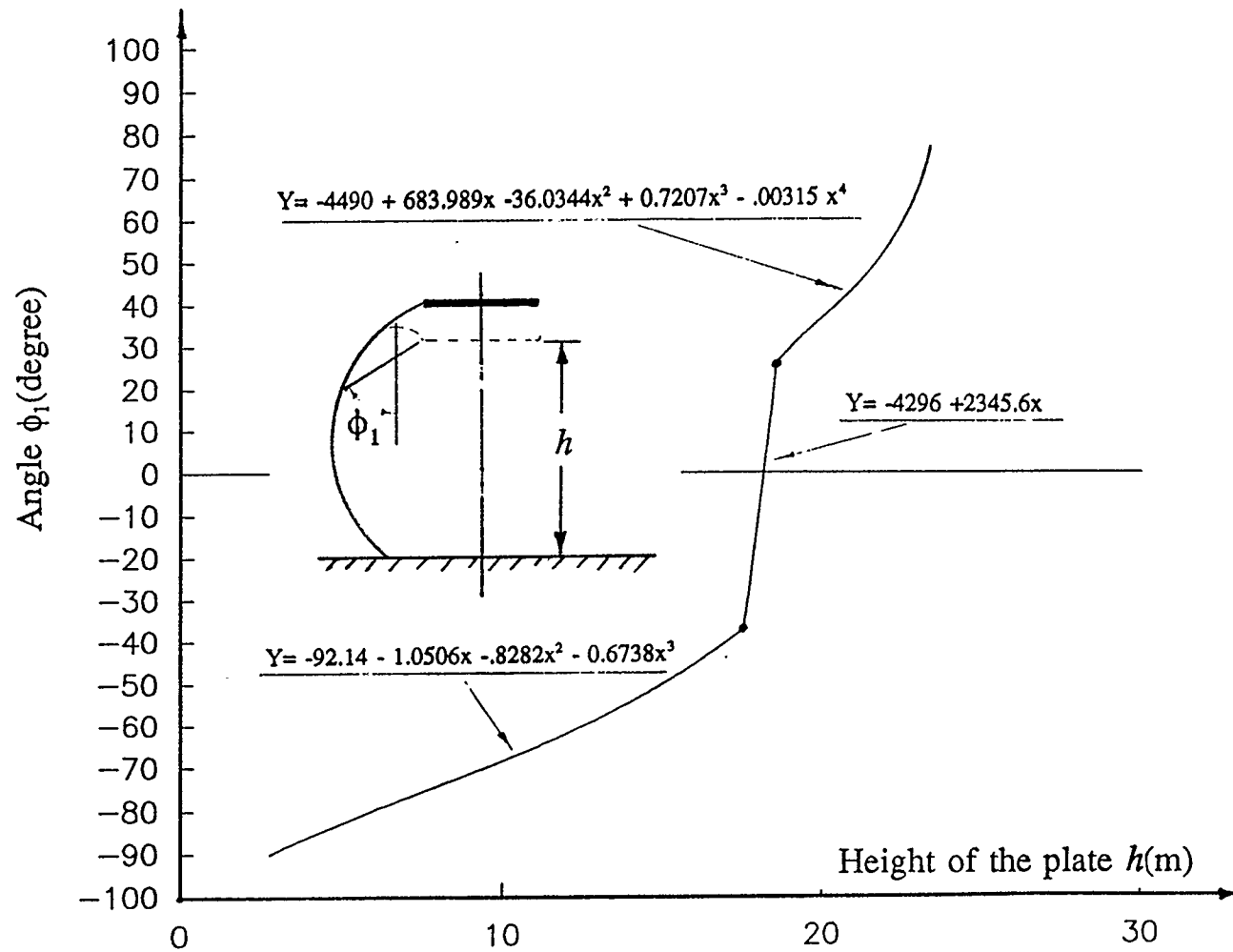


Figure 9 Angle  $\phi_1$  as function of the height of the plate

Table 1 Parameters to define a deformed configuration of semi-spherical dome

$P_2$	$\phi_1$ (degree)	$\phi_2$ (degree)	C	$P_1$	h
-700	46.975	67.028	494.369	12.318	10.7168
-250	36.958	79.646	245.102	11.073	10.422
-180	32.76	84.44	206.42	10.669	10.232
-100	25.058	73.893	160.184	10.147	9.844

## Chapter 3 Numerical Solutions and Techniques

### 3.1 Static Analysis

When the membrane inflatables are subjected to an uniform load at the apex, very large deflections and wrinkling can occur and change the initial geometry of the structure significantly, at least in the vicinity of the load application zone. Such large deflections and highly nonlinear behaviour require a geometrically nonlinear analysis. The governing equation that describes the deformed membrane contain multi-valued functions leading to multiple solutions with accompanying convergence problems and difficulties in the physical interpretation of the results. One must solve two sets of equations: (26a, 26b, 26c, 26d, 26e) and (27a, 27b, 27c, 27d) in order to analyze the full range of possible deformed membrane shapes from a partially to a fully wrinkled configuration. Certain difficulties must be overcome in the solution process. Although a closed form solution is obtained for differential equation (15), and only one constant of integration  $C$  is to be determined, other unknowns  $\phi_1$ ,  $\phi_2$  and  $P_1$  are involved and must be found simultaneously so that deformed part of a spherical membrane under external pressure  $P_2$  can be defined. These unknowns appear in the two sets of equations as variables of trigonometric functions and also in integral forms. Closed forms for any one of these unknowns are not possible. Numerical methods must be applied to determine these parameters.

By assuming the internal pressure  $P_1$  to remain constant, the numerical analysis can be greatly simplified. Much of the previously published research work in this area used this assumption, see ref. [9], and [11] through [23]. As large membrane deformation is induced by the load, such assumption is no longer valid. In this study the differences in the behaviour of the two inflatables of the same geometry is compared. One of them has constant internal pressure and the other has its internal pressure obey the isothermal gas law.

The solution technique is complicated by the fact that there are domains of integration with upper and lower bounds as functions of unknown deflection. A further complication arises when large deflection internal pressure of a sealed dome is a function of an unknown deformed shape. Moreover the functions in the two sets of equations must be evaluated using numerical techniques and an iteration approach because no closed form solution is possible.

When one attempts to solve the two sets of equations using a numerical approach, it is very important to understand thoroughly the varying range of the unknowns, their physical meanings in the deformed configuration and the mutual relations between the unknown parameters. As iteration is employed in the solution process, one corrupted and/or divergent step in evaluating the singular equations may result in a complete failure in the process.

After numerous trials and careful result analysis,  $\phi_2$  is chosen as the single dependent variable in the solution process. All other parameters such as  $\phi_1$  and  $C$  could

be used in the trial process. But they do not provide good control in step by step iteration process because of the forms they appear in the equations. For example,  $\phi_1$  and  $C$  are associated with square root functions. Whether to take the positive or negative part is not clear until the whole calculation process is finished for that iteration. And a failed calculation, such as taking a square root of a negative value, or the variable of an anti-sinusoidal function turns out to be greater than 1, will terminate the next iteration. Unfortunately, all these irregularities are unavoidable if choosing  $\phi_1$  or  $C$  as the independent variables.

Unless otherwise specified, it is assumed in the following numerical analysis that the initial internal pressure in all spherical inflatables is 10 Pa., the radius of the rigid plate at the top of the dome is 2.5 m., and the radius of the spherical membrane is 10 m. For the purposes of comparison and data analysis of the membranes of different profiles and internal pressure configuration, the behaviour of three typical spherical inflatables are thoroughly investigated. These inflatables are: a semi-spherical with constant internal pressure, a semi-spherical with its internal pressure obeying gas law  $P_1 = P_0 V_0 / V$ , and a high profiled spherical dome with its half central angle as  $150^\circ$ .

In the case when the membrane is partially wrinkled,  $\phi_2$  is incremented from  $\Phi$  to  $\phi^\circ$ . According to Eq. (26b),  $C$  is evaluated at each given  $\phi_2$  from

$$C = R^2 \sin \phi_2 - \frac{P_2 r_o^2}{P_1 \sin \phi_2} \quad (32a)$$

where  $P_1$  assumes a marginally greater than initial internal pressure  $P_0$ . This value will be verified and updated in later trials.

Angle  $\phi_1$  is then calculated from Eq. (26a) :

$$\sin\phi_1 = \frac{r_o^2(1-\frac{P_2}{P_1})}{C} \quad (32b)$$

and from Eq. (26e). Total volume is evaluated with:

$$V = \frac{\pi}{2} \int_{\phi_1}^{\phi_2} C \sin\varphi \sqrt{\frac{P_2}{P_1} r_o^2 + C \sin\varphi} d\varphi + [\pi R^3 (\cos\varphi - \frac{\cos^3\varphi}{3})]_{\phi_2}^{\phi_1} \quad (32c)$$

Next,  $P_1$  can be verified using Eq. (26d) :

$$P_1 = \frac{P_o V_o}{V} \quad (32d)$$

If this  $P_1$  value differs from the assumed value in evaluating  $C$  in Eq. (32a) over a prescribed tolerance,  $P_1$  is updated by the new value and the process has to be restarted with Eq. (32a). If  $P_1$  falls within the tolerance, evaluation proceeds to the next step to calculate the wrinkled meridian curve length to check if the compatibility equation Eq. (26c), is satisfied. It is accomplished by checking if a specially introduced function  $Y$  is near zero. This function is the difference between the exact meridian curve length before deformation and the numerically integrated curve length after deformation. A perfect satisfaction of the compatibility is indicated by  $Y=0$ .

As  $\phi_2$  is incremented from  $\phi^o$  to  $\Phi_0$  with a fixed step, a root bound is found when function  $Y$  changes its sign. Within the root bound, the root is found with the prescribed

accuracy by applying Newton-Raphson's method or the bisection method. Simpson's rule is employed to achieve a satisfactory accuracy in evaluating the enclosed volume by the deformed membrane and the deformed meridian curve length. Each time when  $\phi_2$  is incremented,  $P_1$  is first assumed to be the value from previous trial before  $\phi_2$  is incremented. If this first assumed  $P_1$  value differs from the later calculated value beyond the prescribed tolerance, the later calculated  $P_1$  value replaces the assumed value and the process from (32a) to (32d) will be repeated until the difference in value  $P_1$  falls within the prescribed range.

Fortran computer programs of more than 1300 lines were written to perform the iteration process with the bisection scheme used in the root finding routine. Fig. 12 is the simplified flow chart of the program.

Relations of  $\phi_1$ ,  $C$ , and  $\phi_2$  to the applied pressure were established by adding the exerted pressure  $P_2$  step by step over an allowable range. The lower bound of  $P_2$  is negative infinity where the inflatable is pulled straight to form a truncated cone surface. The maximum  $P_2$  is the pressure applied at the plate to push it down to touch the bottom of the dome. Each  $P_2$  yields one set of the values of  $P_1$ ,  $C$ ,  $\phi_1$  and  $\phi_2$ . Thus one can determine the height of the displaced plate measured from the supporting base of the dome. It should be pointed out that all these relations are bounded since the lower and upper limits of plate displacement are known. The bottom plane of the undeformed inflatable is the lowest position that the plate can descend. The highest position the plate would reach is the point where the ratio of external load  $P_2$  to the internal pressure

approaches an infinity in the outward direction, causing the membrane to be pulled straight to form a truncated cone shown in Fig. 13. The parameters describing the deformed configuration parameters are listed in the following table.

Table 2 Parameters At  $P_2$  Approaches Negative Infinity

$P_2$	$\phi_1$	$\phi_2$	C	$H_{\max}$
$-\infty$	$\sin^{-1} \frac{R \sin \Phi_0 - r_0}{R(\Phi_0 - \phi^0)}$	$\sin^{-1} \frac{R \sin \Phi_0 - r_0}{R(\Phi_0 - \phi^0)}$	$\infty$	$\sqrt{R(\Phi_0 - \phi^0)^2 - (R \sin \Phi_0)^2}$

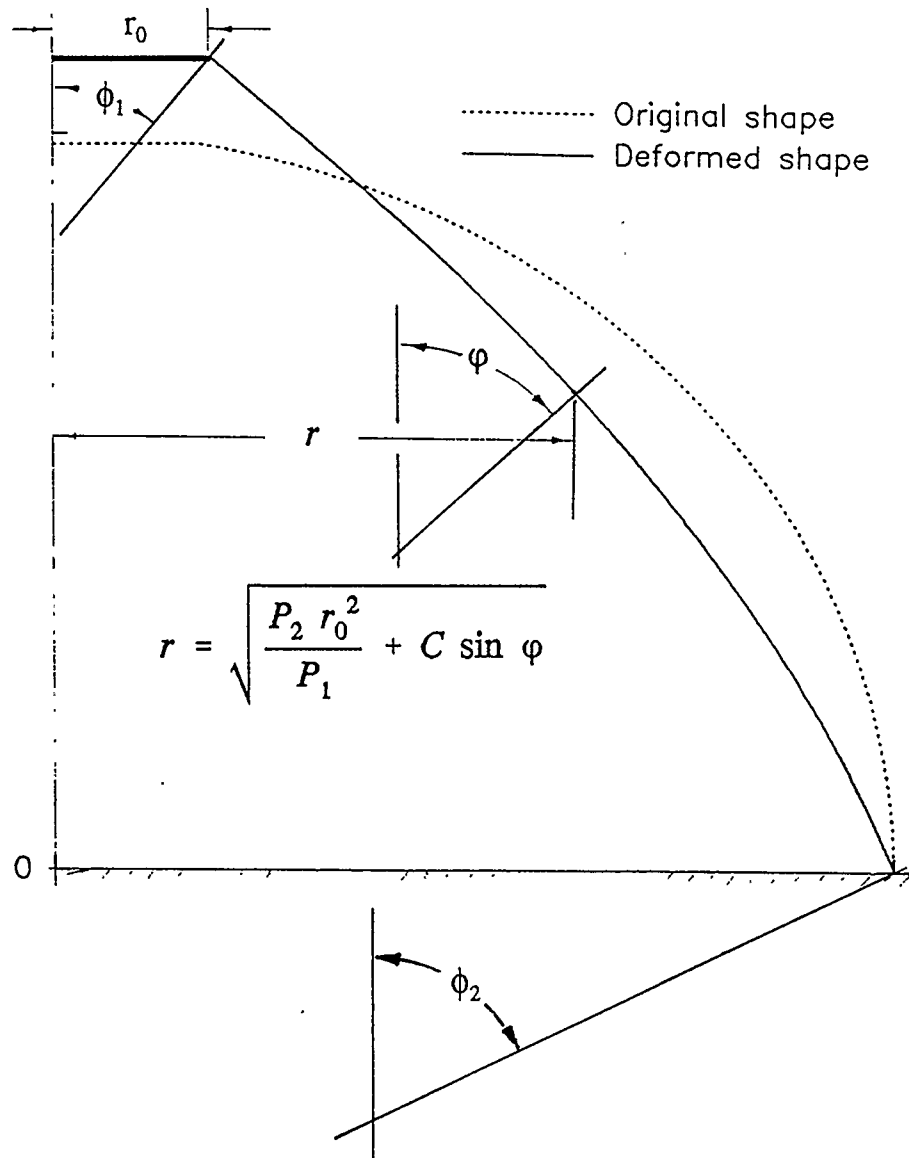


Figure 10 Parameters defining a deformed spherical inflatable

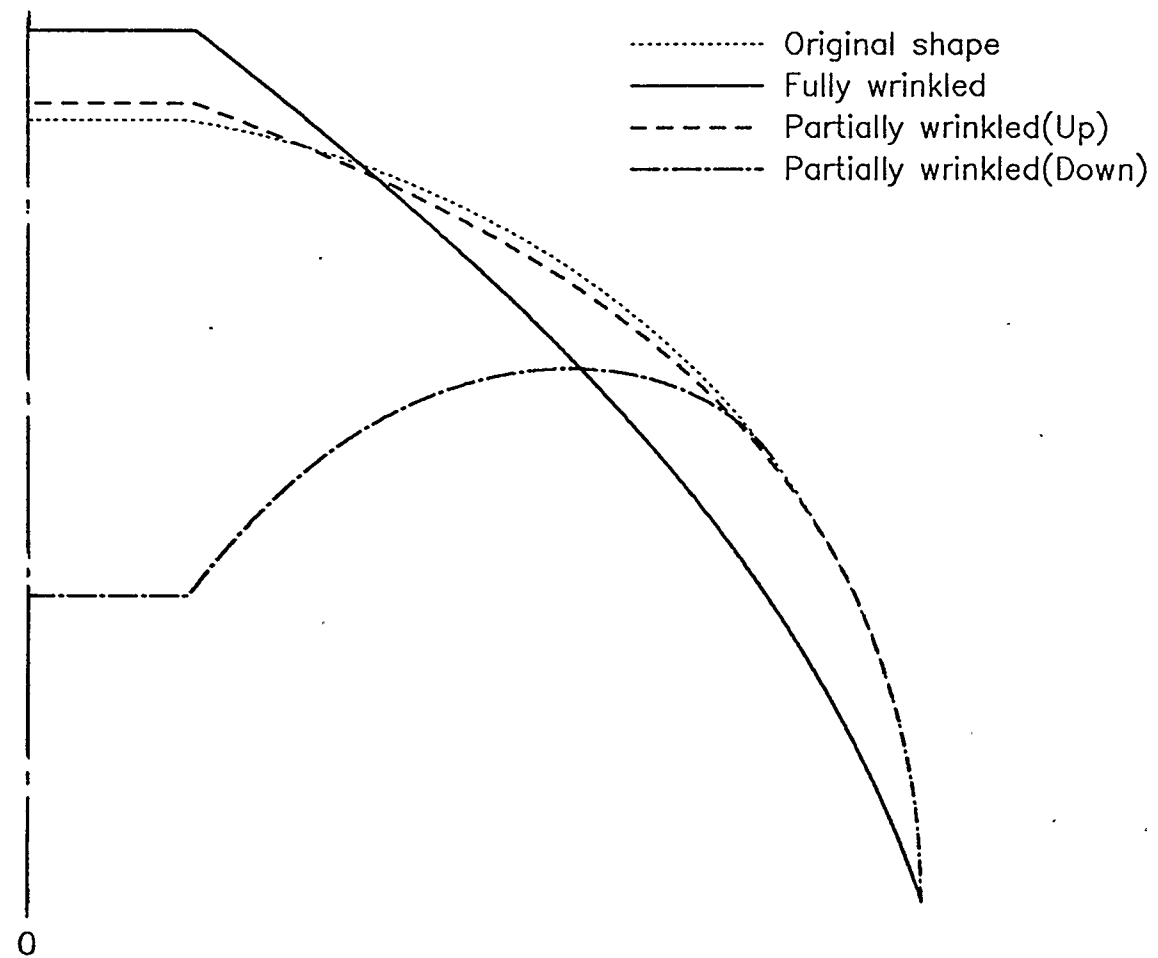
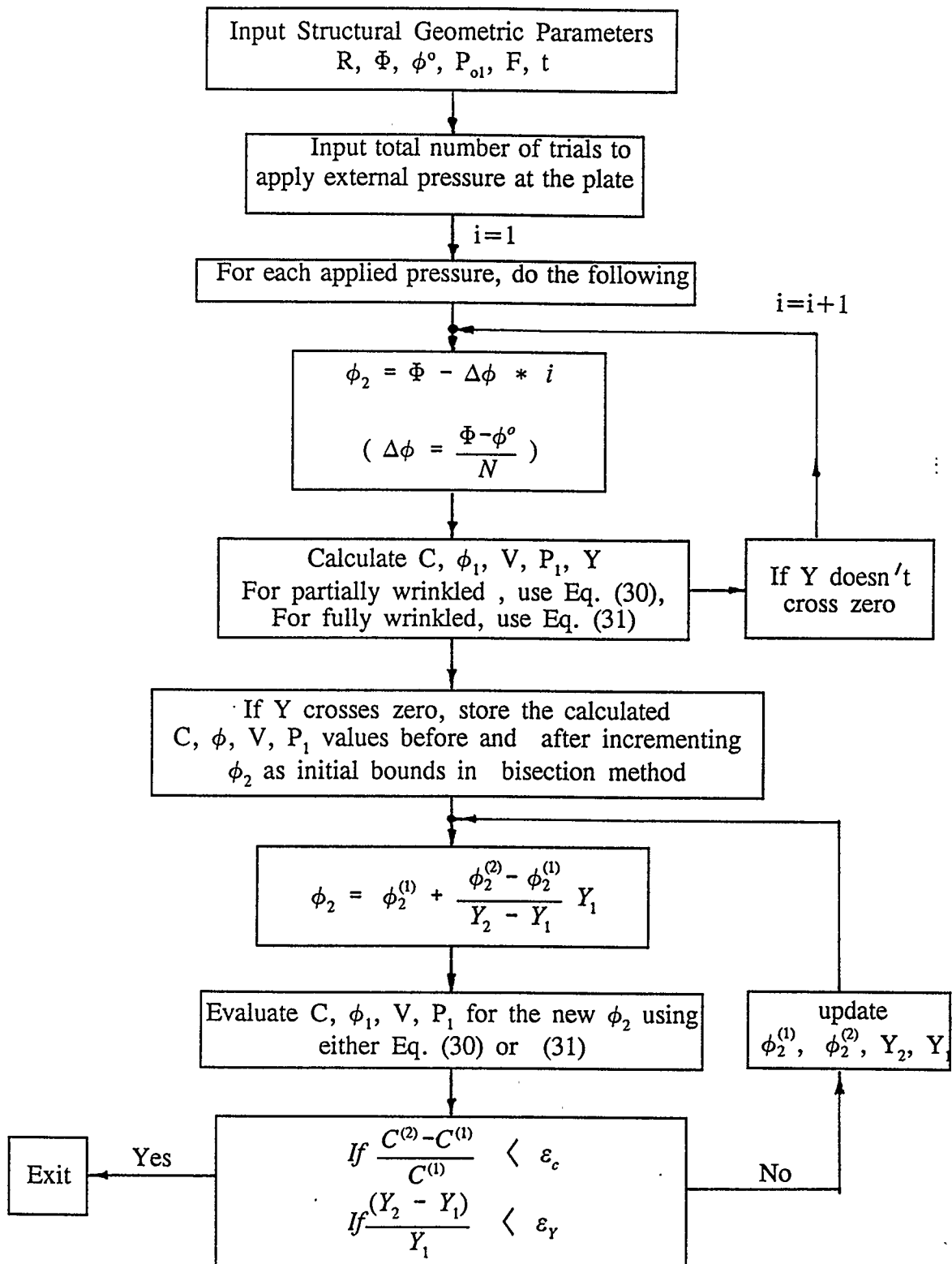


Figure 11 Three modes of deformation of a low profile spherical membrane

Figure 12 Flow Chart of Root Finding Routine



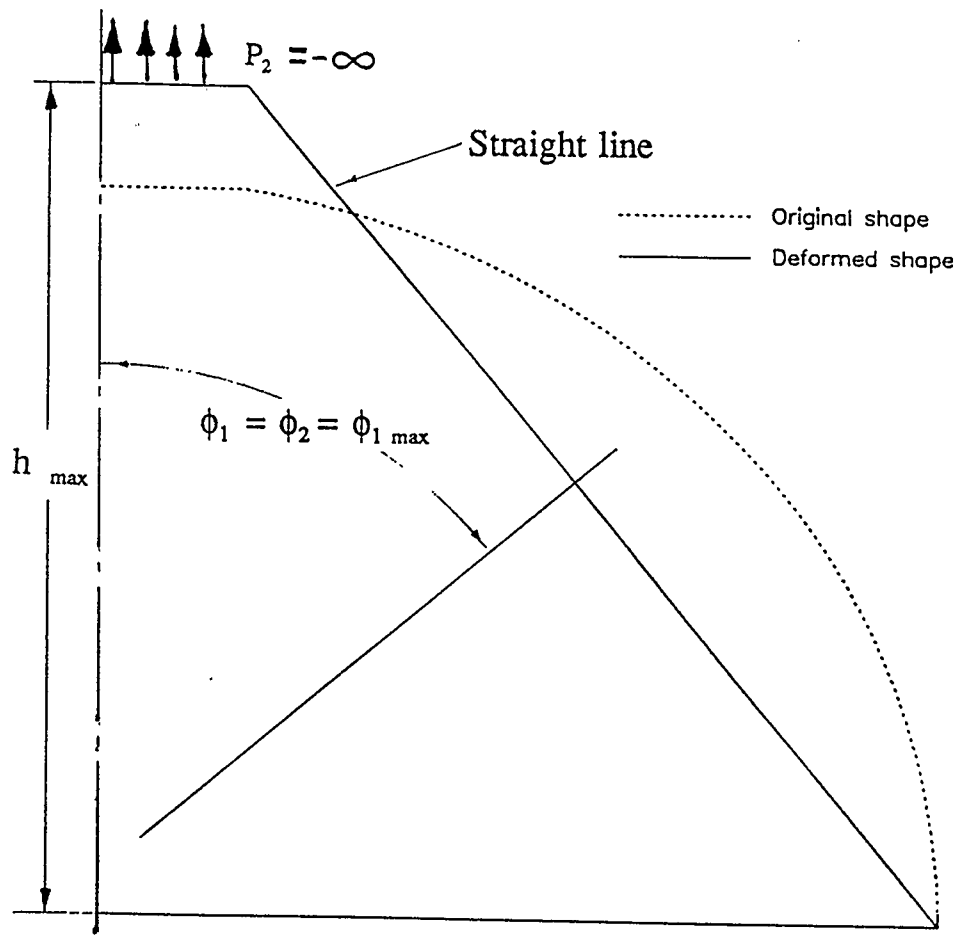


Figure 13 Deformed membrane by infinite suction at the plate

### 3.2 Dynamic Analysis

The time-displacement relationship of the plate at the top can be found by solving Eq. (32) with Runge-Kutta Scheme. Fourth order integration scheme is employed. To apply this scheme, the equation is modified into two first order simultaneous differential equations:

$$\dot{y} = V \quad (33a)$$

$$\begin{aligned} \dot{V} &= \frac{dV}{dt} \\ &= -\frac{F(t)}{m} - g + \frac{\pi P_1(y)}{m} (r_o^2 - C(y) \sin \phi_1(y)) \end{aligned} \quad (33b)$$

where  $P_1(y)$ ,  $C(y)$  and  $\phi_1(y)$  are non-linear functions in sectioned, polynomial forms with deflection  $y$  as the variable. One set of the initial conditions states that

$$y(t=t_o) = y_o \quad (34a)$$

$$\frac{dy}{dt}(t=t_o) = \dot{y}_o \quad (34b)$$

Positive velocity means that the velocity direction points upward.

Starting with the initial condition and integrating from the initial time point with a small integration step, numerical values of time histories of displacement and velocity of the plate are obtained over a time span. Fortran programs of 800 lines were written to execute this integration.

Both free and forced vibrations of the structure are analyzed. In free vibrations, ie.,  $F=0$ , the vibration frequency also varies with its oscillation amplitude. Thus it also is valid to state that the free vibration frequency is dependent not only on its initial conditions, but also on its geometric configuration. Spherical inflatables with a sealed interior have a higher stiffness and thus higher free vibration frequency as compared to the domes of the same geometric configuration but constant internal pressure. The inward vibration magnitude is larger than the outward value because inflatables have lower stiffness in responding to inward loads.

The resonance occurs when the forcing frequency is close to that of free vibration with the same initial condition. These inflated structures show non-periodic and chaotic response to all harmonic excitations because of the variable and discontinuous structural stiffness.

Phase planes are plotted to display how vibrating velocity and displacement relates to each other. In free vibrations, the phase planes are like egg shells as in Fig. 14. The rough and superimposed lines are due to numerical computation error. The symmetrical image of the phase plane with respect to its central horizontal axis ( $V=0$ ) indicates that free vibrations are periodical. The maximum velocity points are the lowest and the highest points on the plot. If one draws a line between the two points the phase plane are divided into 2 parts by the maximum width line. The intersection of this vertical line and the horizontal axis give the static equilibrium position of the plate because  $V_{\max}$  corresponds to zero acceleration, which is the point where the resultant force becomes

zero. Coming back to the two divided parts of the maps, one may see that the velocity changes much more rapidly in the upward motion than it does in the downward motion. This can be well explained by the fact that the structure is much stiffer when being pulled outward than it is pushed inward. The same reason makes the phase planes of forced vibration have a flattened right half side portion and an elongated left half portion as shown in Fig. 15. Velocity and displacement relationship does not show any bound at a resonant state. As time goes by, the curve becomes divergent (see Fig. 16 and Fig. 17) until the plate touches the dome bottom.

Spectrum analysis is carried out to examine the structural dynamic response to periodic loads of various frequency. This is accomplished by monitoring the magnitude of the system response while varying the forcing frequency of a low magnitude force step by step over a range. Even though the system response to periodic load is chaotic, away from the resonance zone, a maximum plate displacement is always possible to be recorded over a sufficiently long span of time. The time history of meridian force around the plate is calculated using Eq. 11. The results are presented and analyzed in detail in the next chapter.

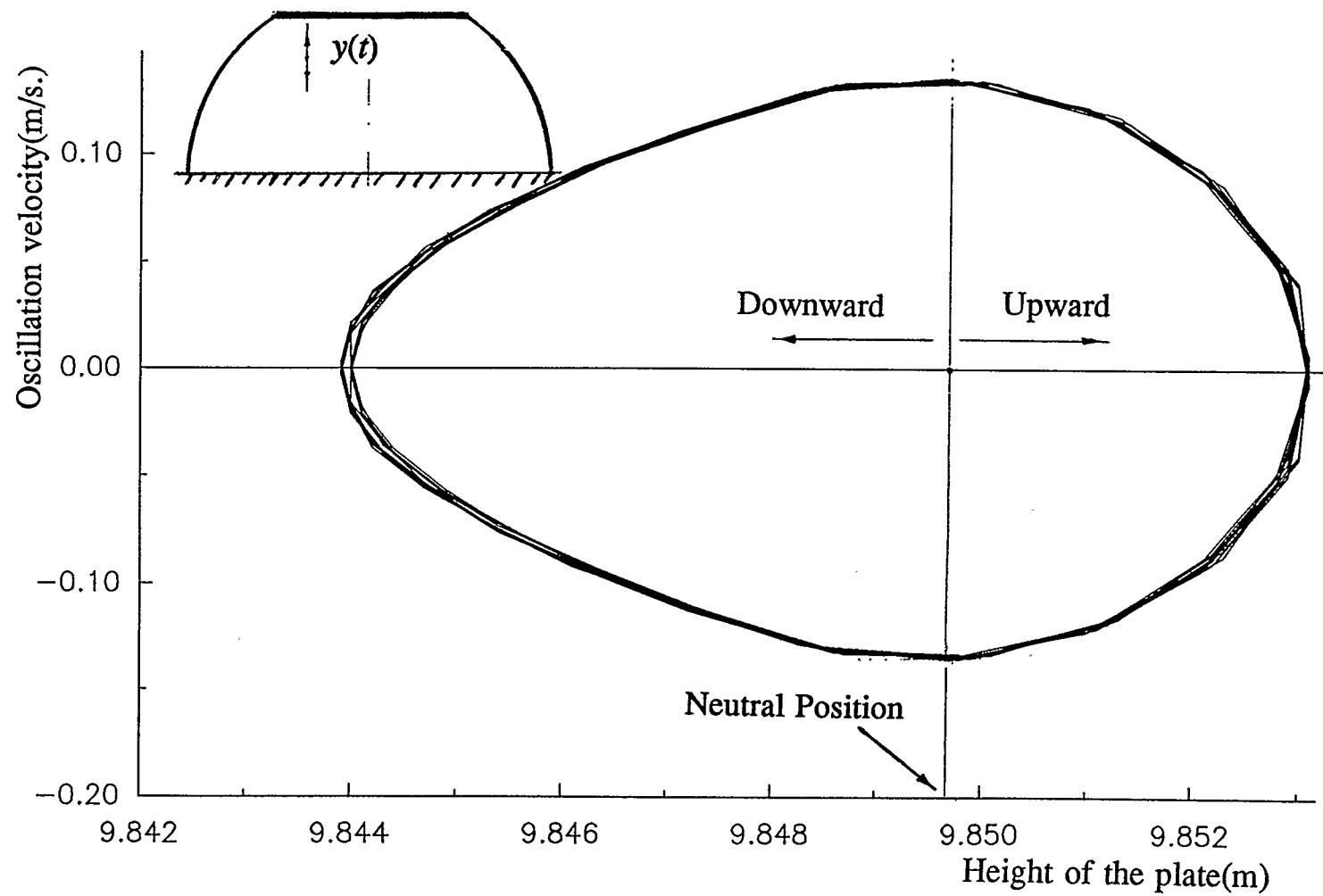


Figure 14 Phase plane of the plate in free vibration

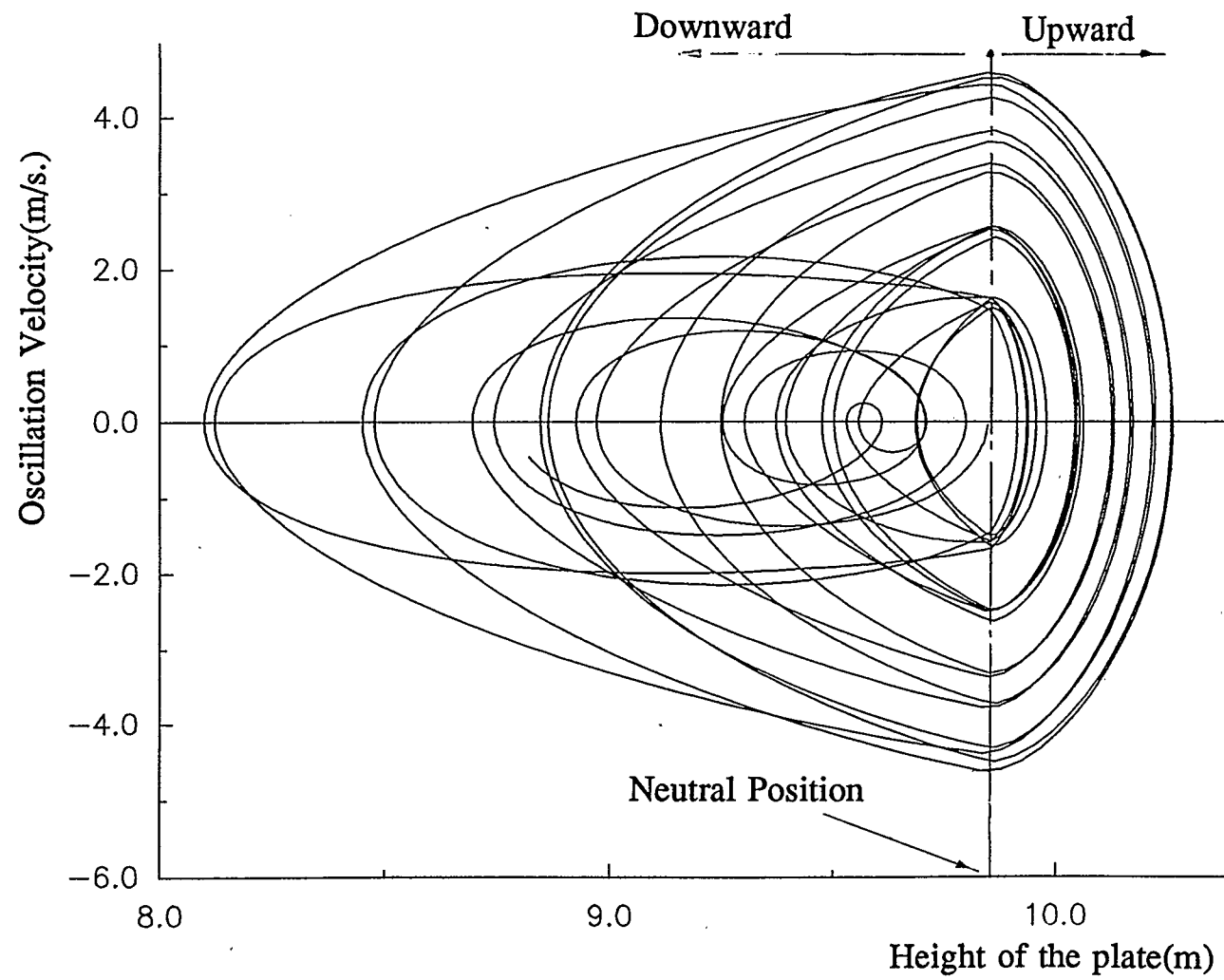


Figure 15 Phase plane of the plate in forced vibration

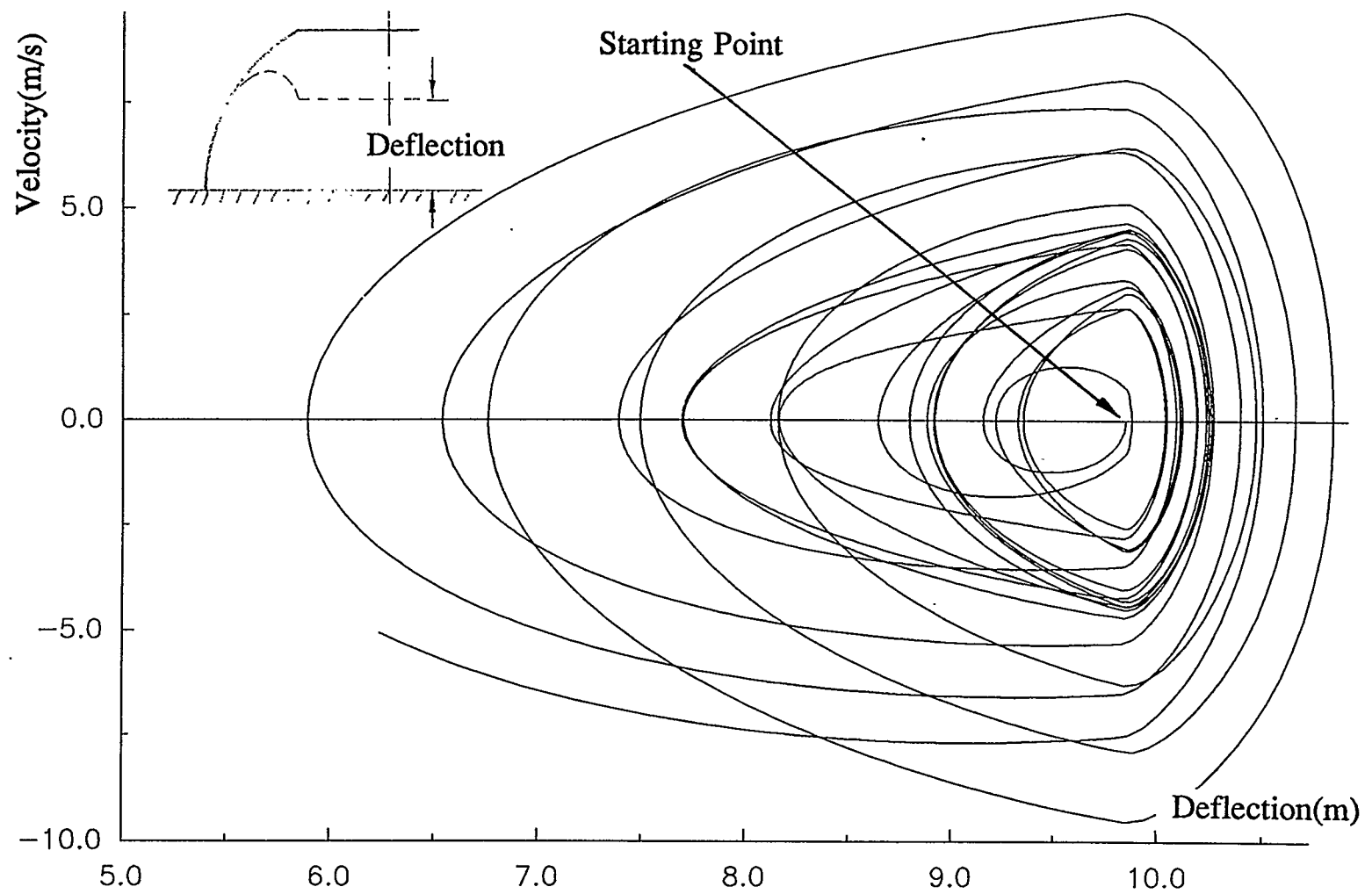


Figure 16 Phase plane at the resonant state

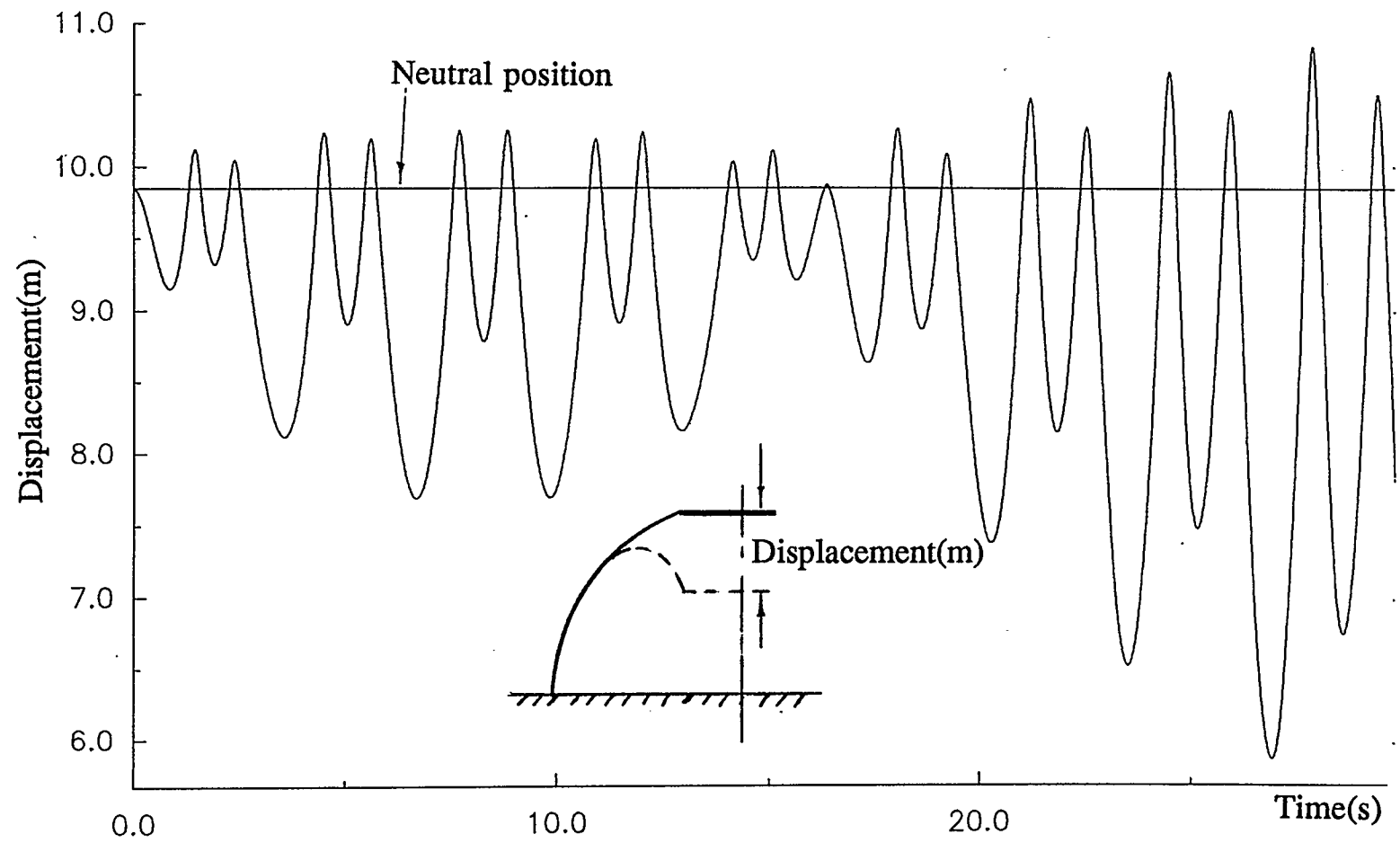


Figure 17 Vibration of the plate at the resonant state

## Chapter 4 Numerical Results and Analysis

### 4.1 Static Loading and Deformation

Fig. 18 and Fig. 19 illustrate the difference in load-deformation of the plate on top of a spherical inflatable with two types of internal pressure patterns. One of the membranes has its internal pressure regulated so that it stays at the initial internal pressure value. The other is a sealed inflated structure with its internal pressure obeys the isothermal gas law, ie. the pressure is inversely proportional to the total volume of a deformed dome. The calculation results indicate that the constant inner pressure dome is softer than the sealed dome, especially under the push-down load. In a sealed spherical dome, large volume reduction can be induced by the inward load so that the compressed air inside the dome may significantly stiffens the membrane in turn to support the applied loads. This is why in Fig. 18 the slope of the load versus displacement curve of the sealed membrane increases much faster than the other two structures as the increasing inward load causes significant air compression inside the sealed dome. It is thus inaccurate to assume that the internal pressure remains the same if large volume reduction is induced by the inward load. However, such assumption is valid in the case when the dome is subjected the suction load because the volume reduction by the load is insignificant comparing to the original volume. Fig. 19 shows that the sealed and regulated low profile domes have almost the same load-displacement relation under suction load. The following table lists the significant difference in large deformation

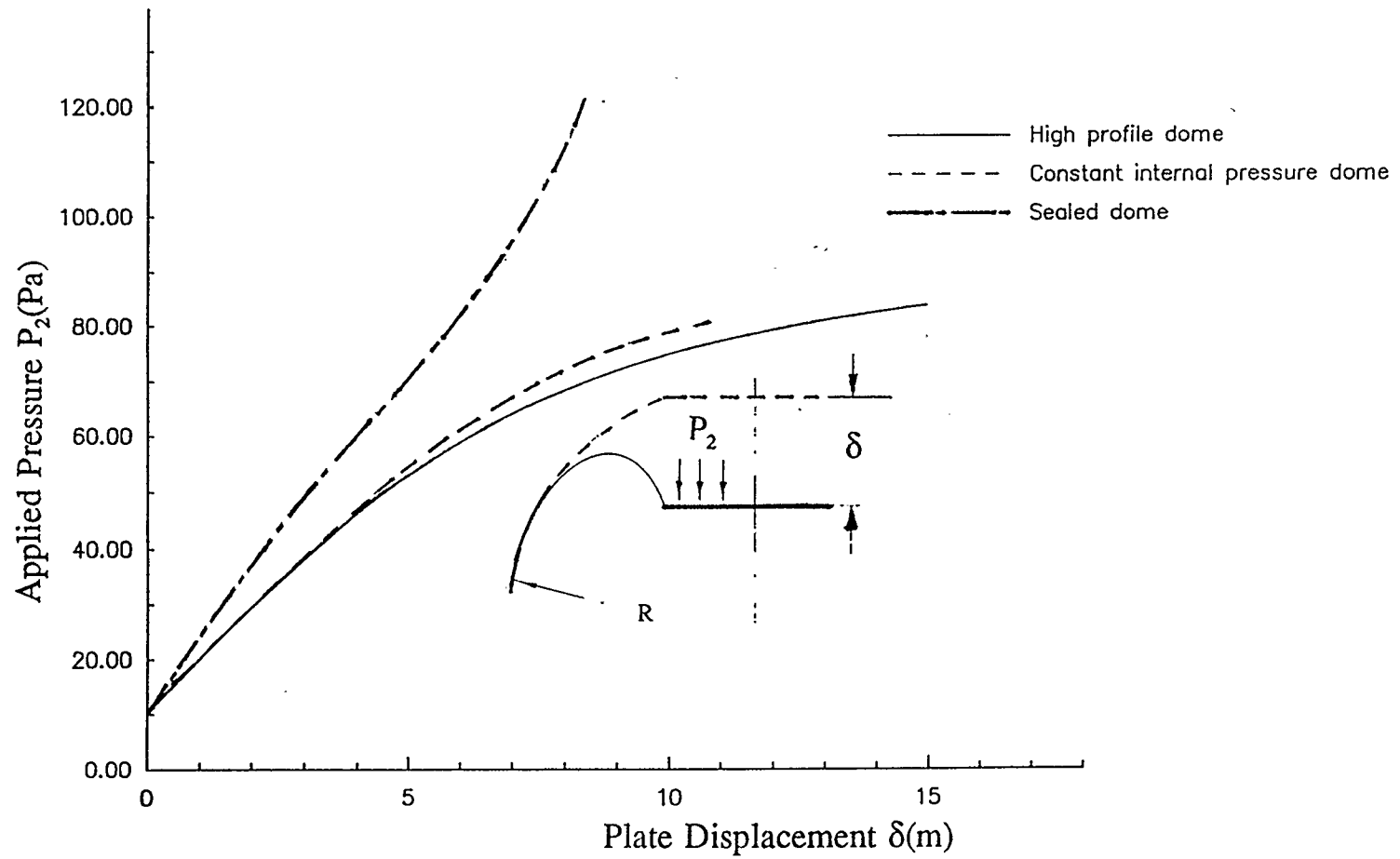


Figure 18 Load-displacement relations in 3 different configurations  
(Downward displacement: Domes subjected to push-in load at the plate)

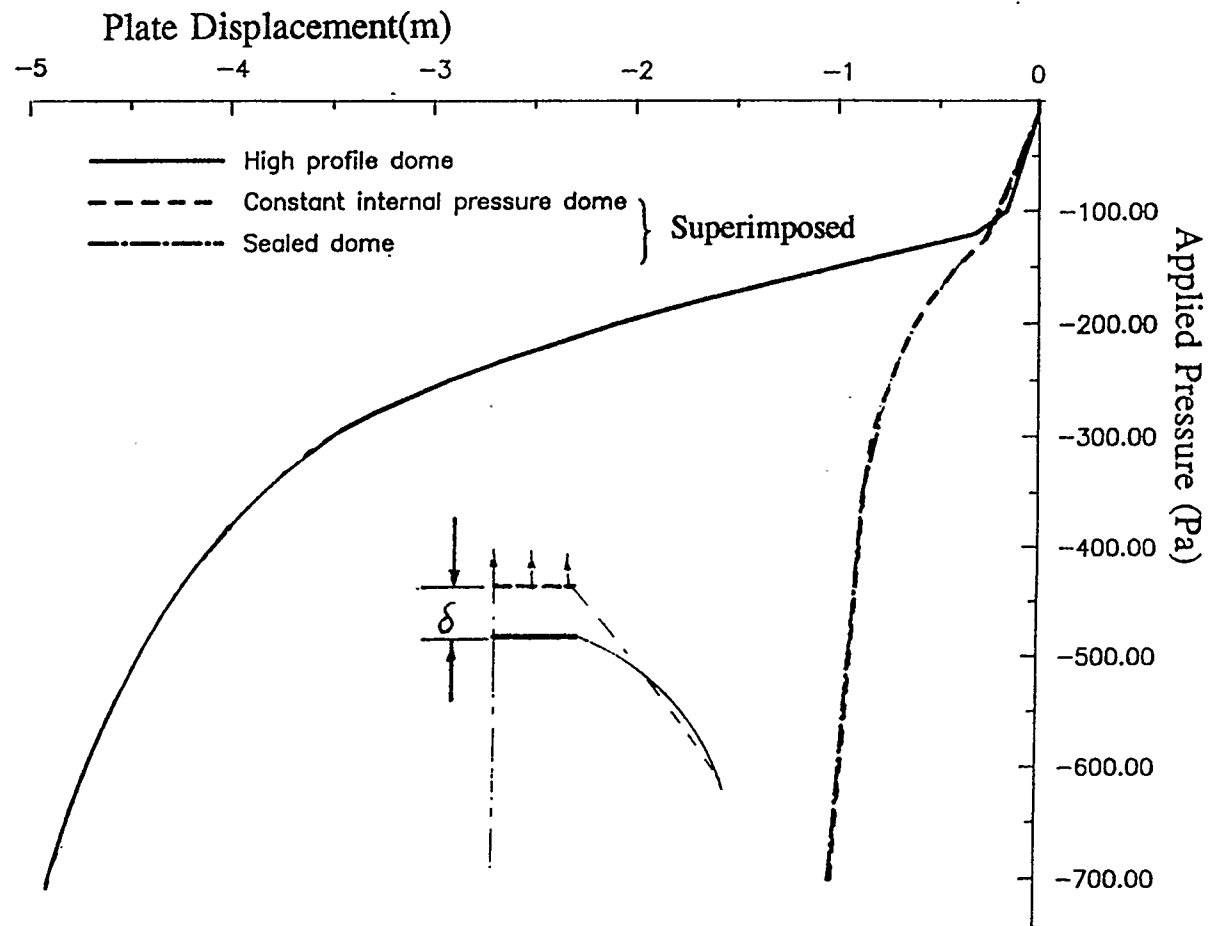


Figure 19 Load-displacement relations in 3 different configurations  
(Upward displacement: Domes subjected to pull-up load at the plate)

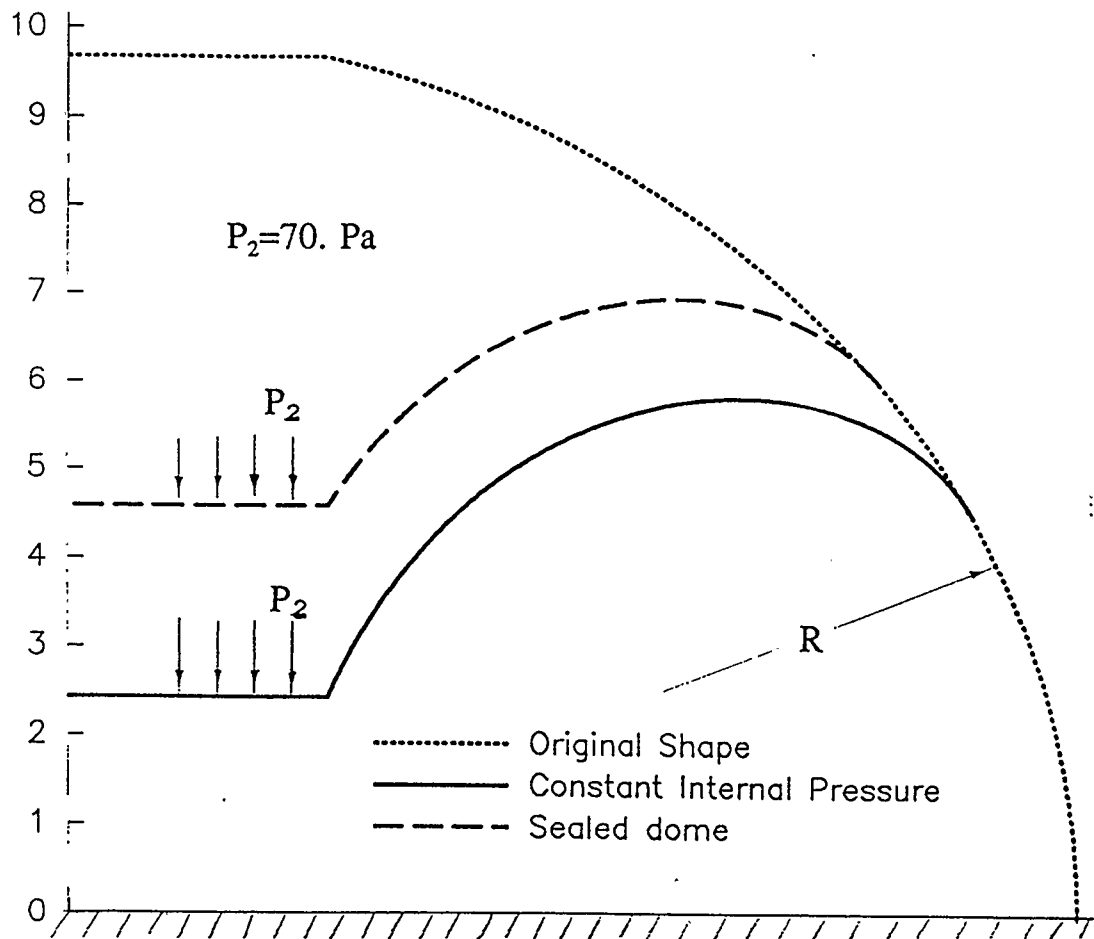
behaviour; and Fig. 20 presents the significant differences in the deformed geometric shapes of a low profile dome in large deformation under the same external load but with two types of inner pressure regulation as listed in Table 3.

Table 3 The effect of inner pressure on the membrane deformation

Applied Pressure $P_2$ and Inner Pressure Assumption	Plate Displacement (meter)	% of Total Vol./Original Vol.	Inner Pressure (Pa)	% of Wrinkled
$P_2=70$ , Const. $P_1$	7.2853	69.29	10.0	64.65
$P_2=70$ , $P_1=V_0P_0/V$	5.1170	82.43	12.123	50.837

Fig. 21 is the load-displacement curve of a high profile spherical inflatable. Several distinctive stages of deflection development are presented in this graph. Five deformed shapes of the pneumatic structure are schematically shown in Fig. 22a and Fig. 22b, with all corresponding loading states labelled in Fig. 21. Looking closely at the load-deflection curve in Fig. 27, one notices big slope variation in two curve sections, an inflection point E which separates full wrinkle and partial wrinkle of the membrane by a suction force. The discussion of the four regions is as follows.

Region C-D in Fig. 21 is an area where no deflection is induced by applied pressure even though its magnitude increases from zero to the inflation pressure. Applying pressure at the plate does not result in immediate deflection as long as the circumferential stress in the membrane stays positive. Because the wrinkle starts first in



Constant Internal pressure dome:  $P_1 = 10. \text{ Pa}$

Sealed dome:  $P_1 = 10V_0/V \text{ Pa}$

Figure 20 Deformed semi-spherical membranes

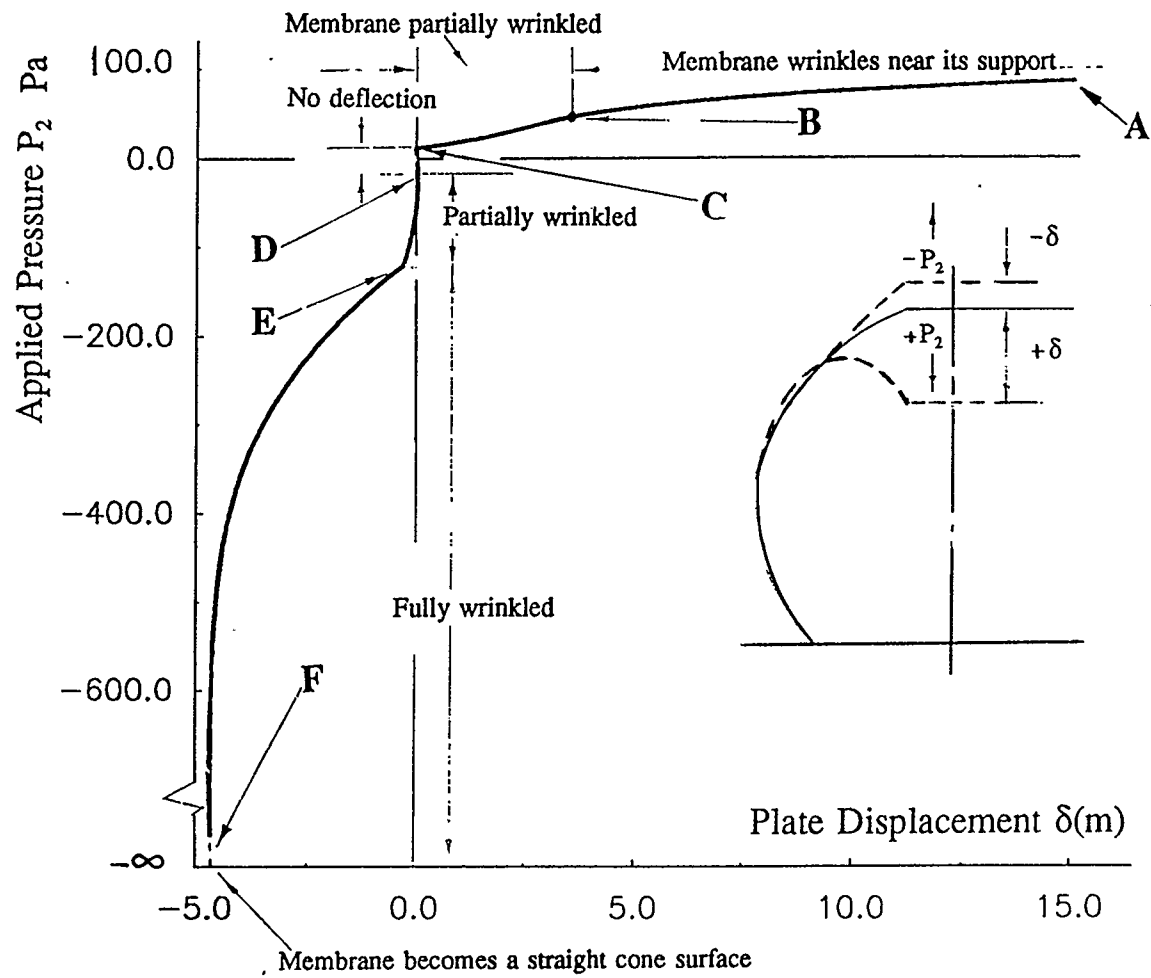
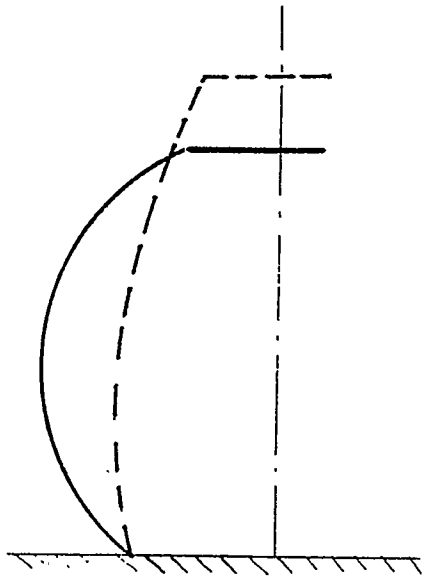
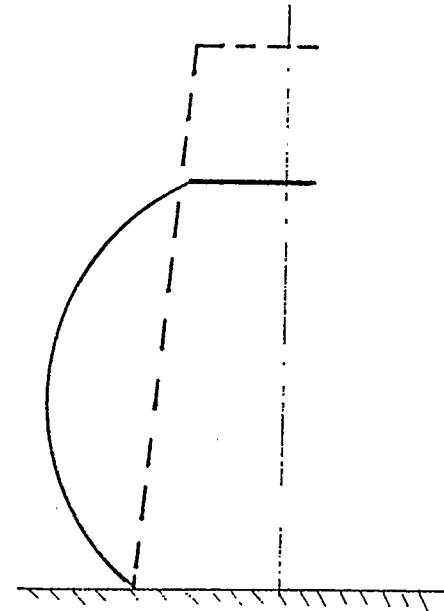


Figure 21 Distinct load-deflection curve of a high profile dome

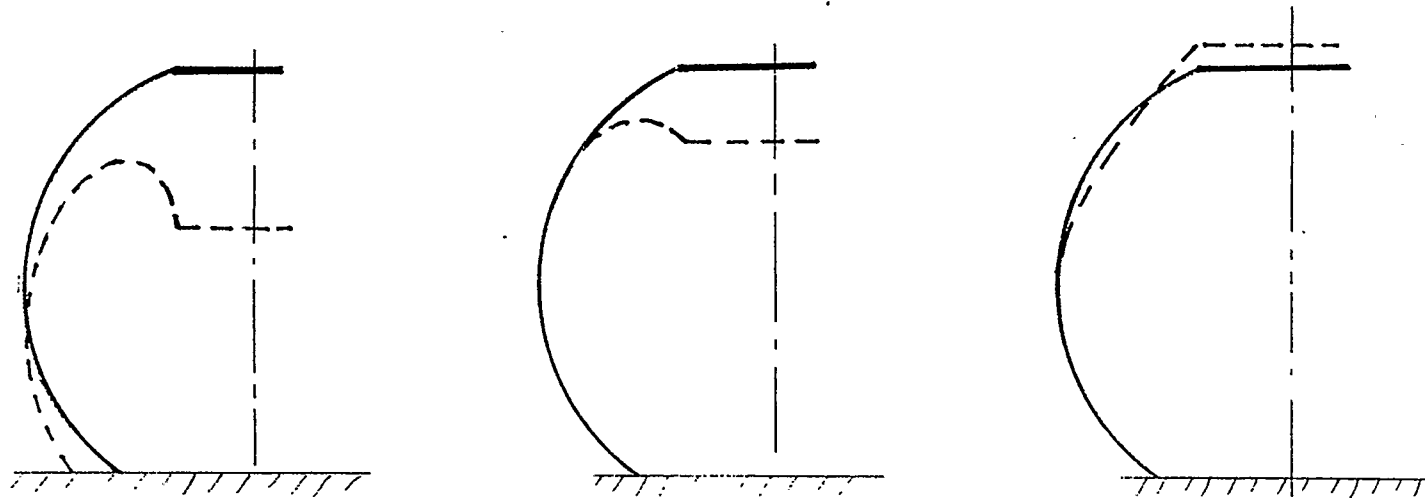


State E-F Membrane is Fully wrinkled



State F Membrane is stressed to form a cone surface  
( $P_2/P_1 = -\infty$ )

Figure 22a Schematic diagram of a deformed spherical membrane in high profile



State A-B Membrane is deformed  
with base settlement

State B-C Wrinkles form only near  
the plate edge by pressure

State D-E Wrinkles form only near  
the plate edge by suction

Figure 22b Schematic diagram of a deformed spherical membrane in high profile

this vicinity to understand how deflection is induced by the external pressure  $P_2$ . Before any wrinkle appears around the plate edge, the two principle forces  $N_\phi$  and  $N_\theta$  around the plate edge are expressed as follows:

$$\begin{aligned} N_\phi &= \frac{1}{2r\sin\phi}(P_1 r^2 - P_2 r_o^2) \\ &= \frac{R}{2}(P_1 - P_2) \end{aligned} \quad (35a)$$

$$\begin{aligned} N_\theta &= P_1 R - \frac{1}{2r\sin\phi}(P_1 r^2 - P_2 r_o^2) \\ &= \frac{R}{2}(P_1 + P_2) \end{aligned} \quad (35b)$$

In Eq. (35a), one can notice that as  $P_2$  increases from 0 to  $P_1$ , the meridional force  $N_\phi$  decreases from the value of  $P_1 R/2$  to zero, while the circumferential force  $N_\theta$  is increased by the applied pressure. When the force in meridional direction approaches zero from positive values, the membrane in this region is at a critical point to buckle in that direction. At a larger load  $P_2$ , part of the membrane next to the plate buckles first, allowing the plate to move inward to an equilibrium position. The formation of circumferential wrinkles caused by the inward deflection in the deformed region around the plate is illustrated in Fig. 23a. The plate comes to an equilibrium position in the deformed configuration where load is balanced by internal pressure and meridional force around the plate edge.

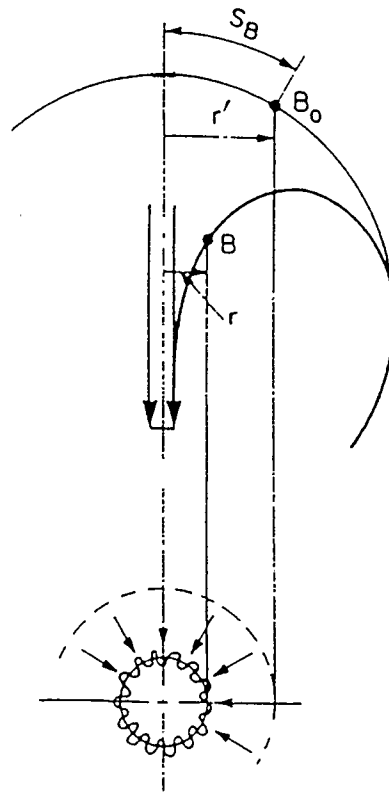


Figure 23a Formation of wrinkles near the plate

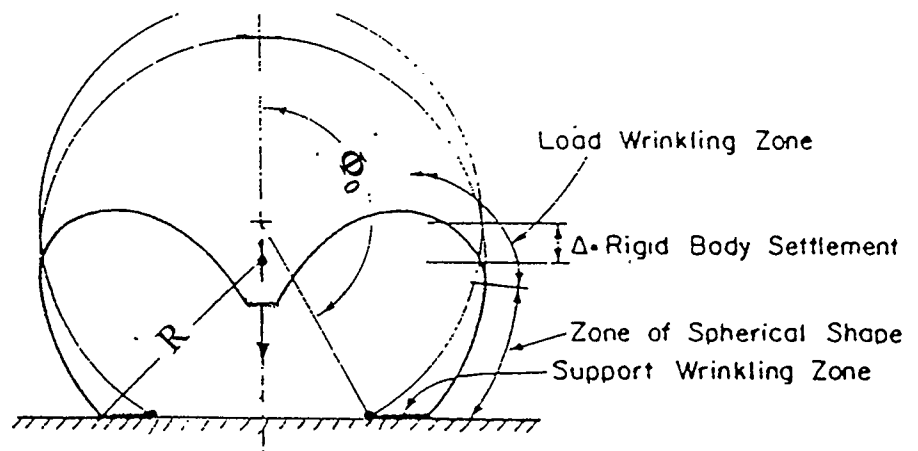


Figure 23b Formation of wrinkles near the support

In the case that suction force is applied at the top plate, value of  $P_2$  is negative. As  $P_2$  decreases from zero to negative  $P_1$ , the state of two principal membrane forces around the plate undergoes a different changing process. The initially stretched membrane will not be buckled in the meridian direction. Instead, it is the circumferential force to be reduced from  $P_1 R/2$  to zero under this loading condition, with the meridian force steadily increased by the applied load  $P_2$ .

Another point which should be emphasized is the continuity of the two principal membrane forces at the boundary between the wrinkled and unwrinkled region. In the partial wrinkled membrane case, the meridional principal force is continuous across the boundary ( $\phi = \phi_2$ ) while the circumferential force is not. The boundary separating the wrinkled and unwrinkled membrane can not be determined using the spherical membrane shell theory simply by setting  $N_\theta$  to zero because this force undergoes a sudden jump across the boundary.

In region A-C of Fig. 21, as the applied pressure rises from  $P_1$  to  $P_2$  (maximum), the plate is pushed inward until it touches the dome bottom, see Fig. 23b.

Region D-E in Fig. 21 shows the outward displacement induced by the upward load (suction) applied at the plate when the load magnitude is greater than internal pressure. In this region membrane is partially wrinkled in the meridian direction. Since the load straightens the inextensible membrane of small curvature, the applied suction does not yield large displacement in this case. The structure becomes very stiff to the upward load. Most part of the deflection in this region results from straightening the

meridian curve in neighbouring area of the plate. At a critical load, in the case of low profile domes, wrinkles extend down to the support. Such a state is indicated by the boundary conditions:

$$r(\varphi=\phi_1) = r_0$$

$$r(\varphi=\phi_2) = R \sin \Phi_0$$

The partial wrinkling of the membrane in the high profile inflatables is a different sequence. For the practical housing application purposes the diameter of the bottom edge circle is usually designed to be larger than that of the rigid plate at the top. Because of this configuration, membrane wrinkle first occurs in the vicinity of the plate. As the suction  $P_2$  increases, at one point, the circumferential force  $N_\theta$  vanishes at the bottom region. A secondary wrinkle region starts to grow from the support toward the equator with the increase in the suction. At the critical load, both wrinkle regions meet at the equator. The critical state of the high profile dome is calculated with the following boundary conditions:

$$r(\varphi=\phi_1) = r_0$$

$$r(\varphi=\phi_2) = R$$

Further increase in suction will deform the inflatable into a fully wrinkled membrane in region E-F of Fig. 21. This region covers the area where membrane is totally wrinkled. Further increase in load tends to straighten the meridian curve more.

This explains why structures have the highest stiffness in this full wrinkle region. And if suction becomes infinitively large, the dome surface will be pulled straight to form a truncated cone.

Fig. 24 presents results obtained by Yoshitsura Yoko [10] for the case with the following conditions:

$$P_1 = 980 \text{ Pa} , \quad R = 10 \text{ m}, \quad r_o = 1.736 \text{ m}, \quad t = 1 \text{ mm}$$

As a comparison, results calculated in this study are also plotted in the published graphs. The results obtained in this study, represented by the dots and stars, show a good agreement with those previously published in ref.[10].

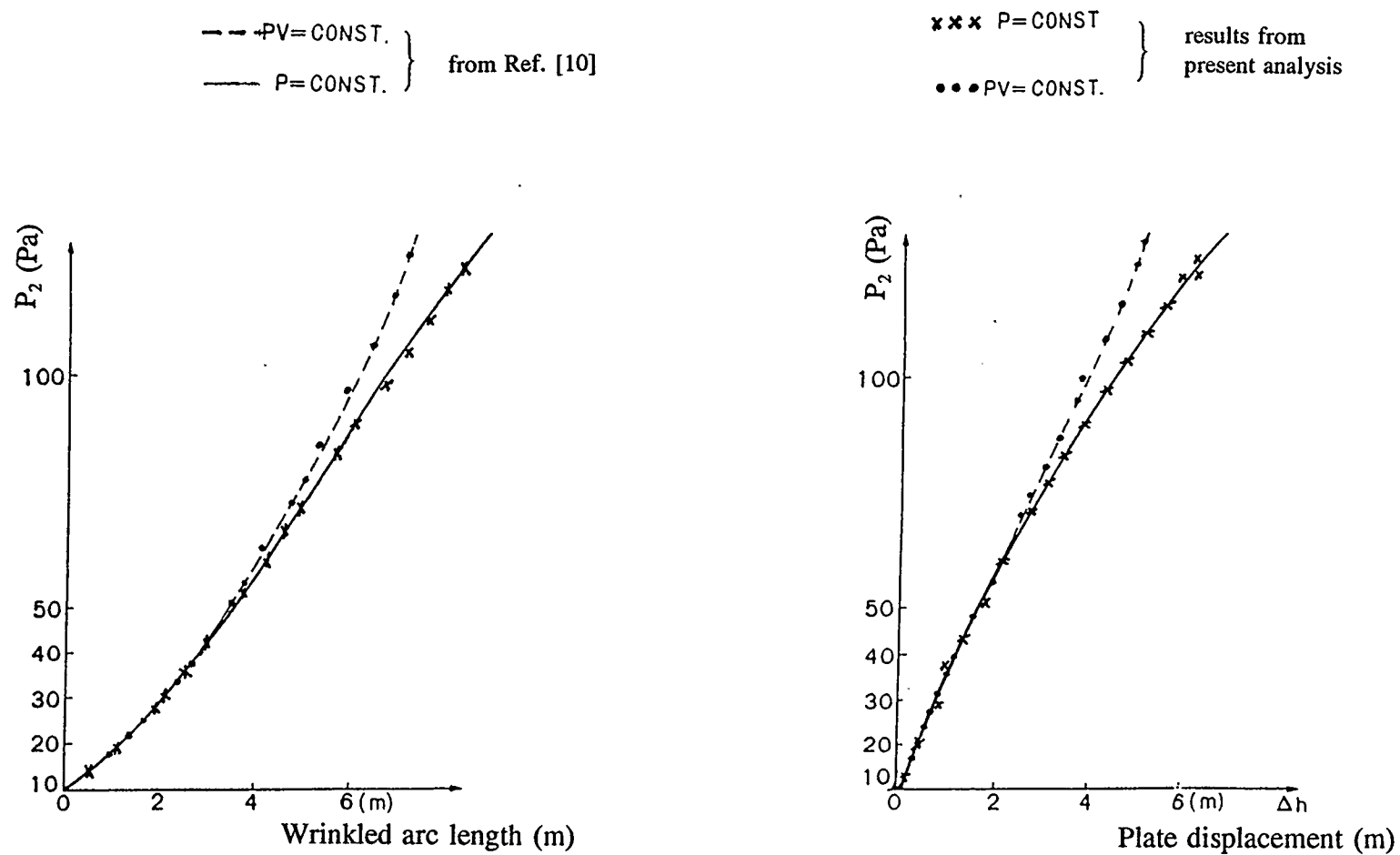


Figure 24 Comparison of the results to the earlier data curves from ref. [10]

## 4.2 Dynamic Behaviour

When the plate is in free or forced vibration, it is legitimate to observe the plate making larger downward motion than outward since the structure is stiffer in the outward direction. Because the structure is stiffer in outward motion and there exists a discontinuity in stiffness between  $P_2/P_0 = -1$  and  $P_2/P_0 = 1$ , an interesting vibration pattern appears in all small amplitude oscillations around the neutral position by choosing proper parameters.

In a free vibration system without gravity, the no load position is the plate's equilibrium point in oscillation. In order to start the oscillation, a sufficiently large external force must be applied to move the plate out of the equilibrium position. Such external force must have the magnitude greater than that applied by the internal pressure. The plate will not start to vibrate if the external force magnitude is lower than that of the internal force.

Once free vibration is initiated, such stiffness discontinuity does not affect the motion since the plate always carries sufficient momentum force to move the plate across the no-load point. Fig. 25 depicts the large and small amplitude free vibration patterns induced by different initial conditions. The system in small oscillations without gravity effect can be an analogy to a spring-mass system as in Fig. 26. The stiffness of the two springs is the linearized value of the membrane stiffness in the vicinity of no load position. The spring stiffness values are calculated using energy conservation law and are based on the vibration magnitude and the maximum velocity of the plate.

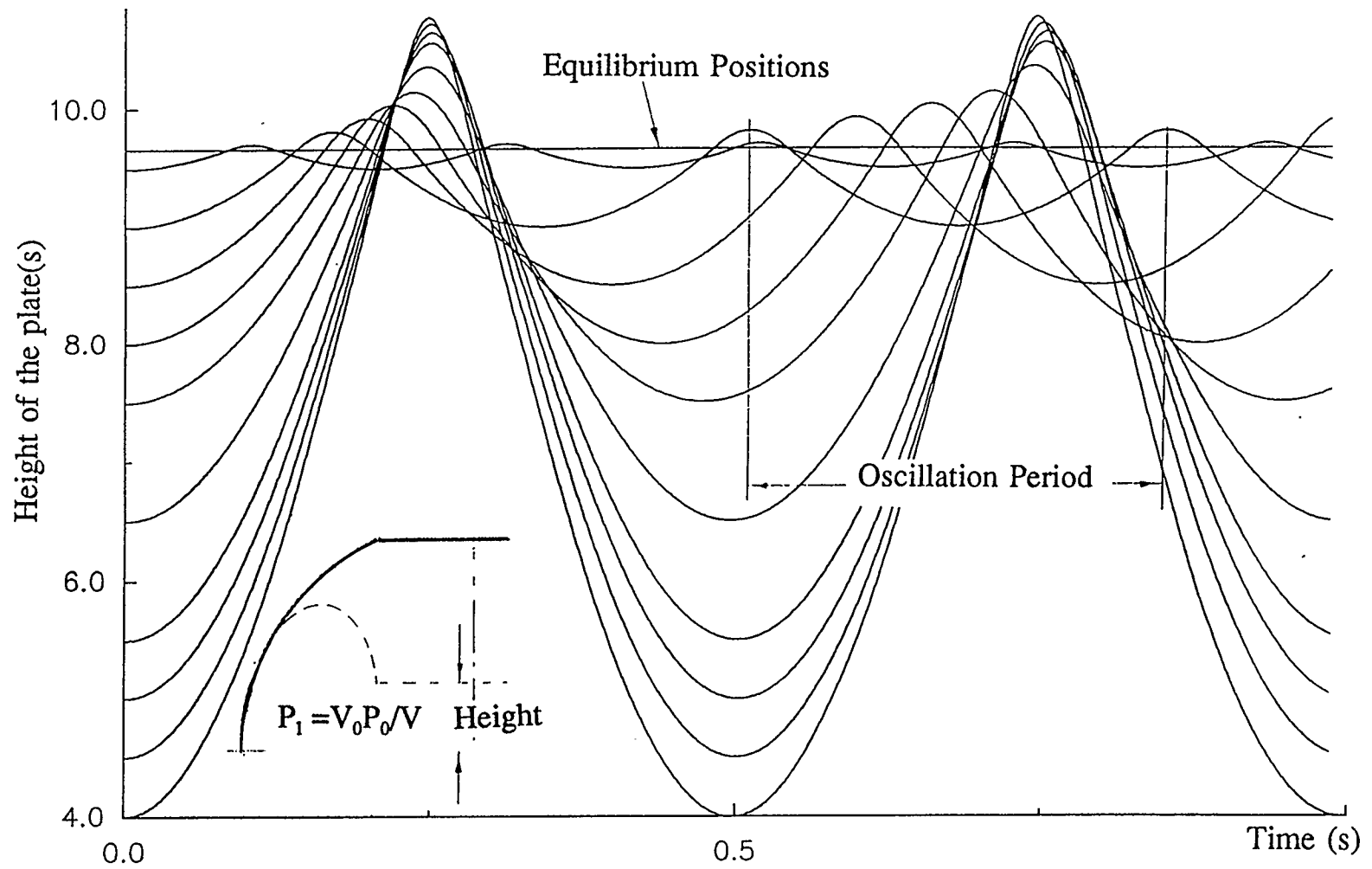


Figure 25 Free oscillation patterns with different magnitudes

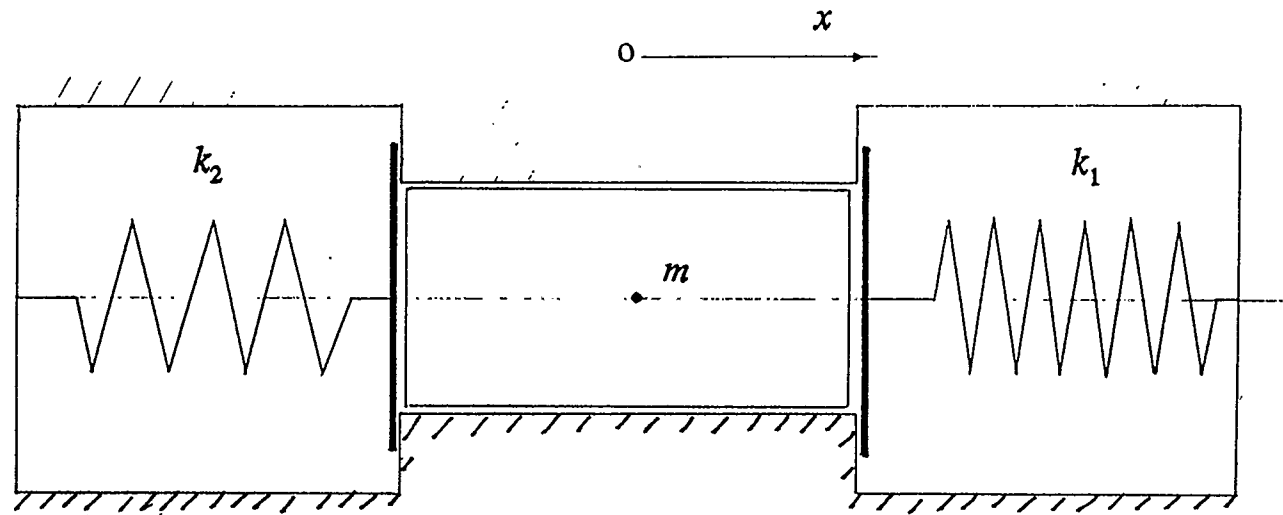
A numerical solution of the time-displacement relation of this mass-spring system is graphically shown below; a graphic expression of the time-displacement relation is displayed in Fig. 27. Similarities between the two systems are obvious when comparing Fig. 27 to free oscillation patterns in Fig. 30, and keeping in mind that Fig. 27 represents a constant spring stiffness system with the stiffness values linearized in the vicinity of the neutral position of the plate. The linearized model gives an very close oscillation period of 0.22 sec., comparing to the value of the nonlinear model as 0.24 second.

Unlike the cases of a linear system where free vibration frequency is independent of oscillation magnitude, the free oscillation frequency of inflatables are related to the magnitude. The configuration of this type of spherical dome makes the structural stiffness resemble a very special spring. Its stiffness is lower in the downward motion than in the upward motion. Moreover, the stiffness diminishes with the inward displacement while the stiffness increases to infinity as the outward displacement reaches the maximum value. In all free vibrations the downward motion dominates. Therefore, the overall system stiffness decreases as the vibration magnitude is set bigger and bigger, causing the free oscillation period to become longer as shown in Fig. 25. However, as the upward motion amplitude approaches the maximum height, the increasing stiffness in this direction becomes dominant, meaning the overall structural stiffness increases and the free vibration period becomes shorter. An inflection point in relation between oscillation frequency and amplitude is visible in Fig. 28. Table 3 shows the change in frequency as the mass is doubled and quadrupled. It is once again that because of the high nonlinearity

in stiffness so that no simple relationship exists between the plate mass and its oscillating frequency.

Table 4 Oscillation Frequency Affected By The Plate Mass

Mass(kg)	5	10	20
Frequency (Hz)	4.85	3.16	1.08



Governing equation of motion:

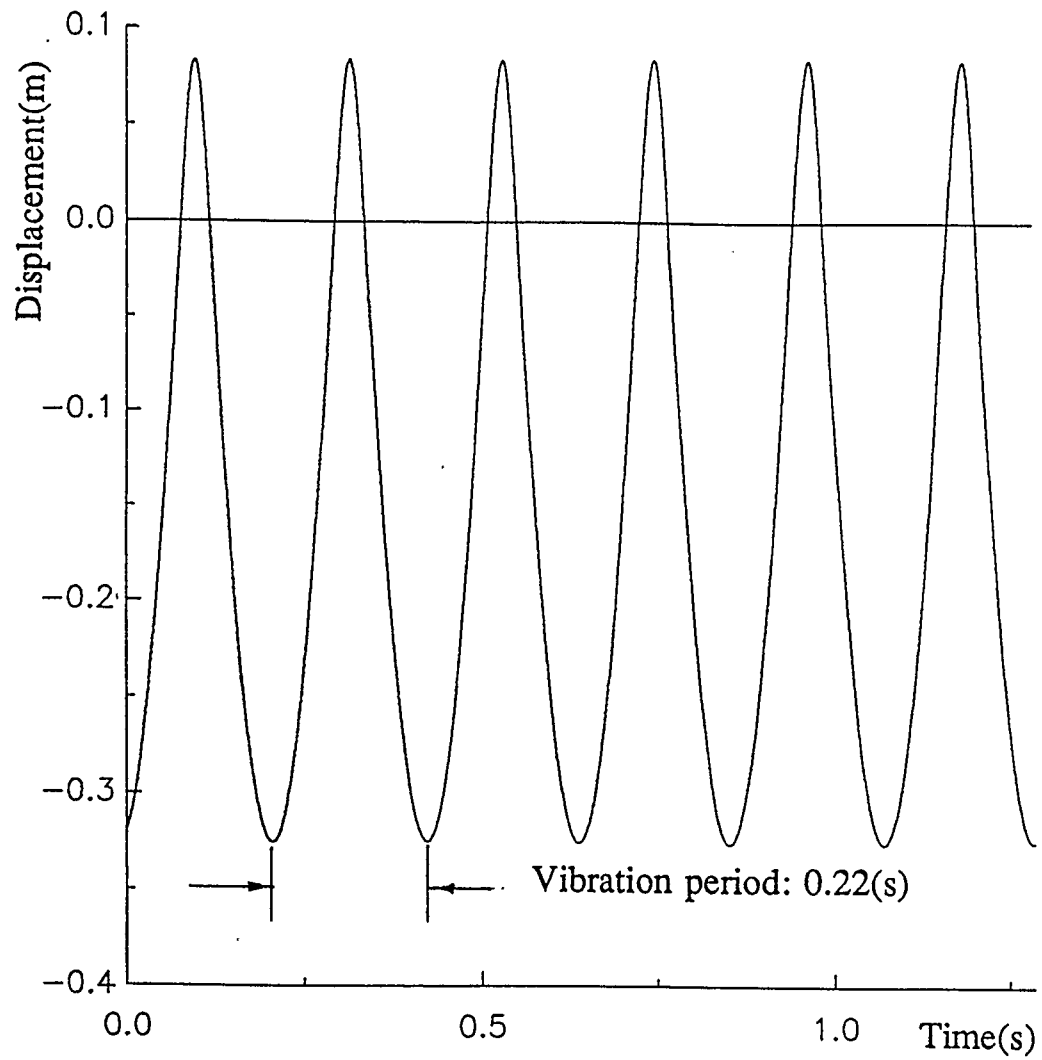
$$\ddot{x} + \frac{k}{m}x + f^0 = f(t)$$

$$k = \begin{cases} k_1 & x > 0 \\ k_2 & x < 0 \end{cases} \quad f^0 = \begin{cases} f^1 & x > 0 \\ f^2 & x < 0 \end{cases}$$

The graph shows the force  $F$  as a function of displacement  $x$ . It consists of two linear segments. For  $x > 0$ , the force is  $F = k_1 x + f^1$ . For  $x < 0$ , the force is  $F = k_2 x + f^2$ . The segments meet at the origin  $(0,0)$ .

where  $k_1$  and  $k_2$  are linearized in the vicinity of the neutral position;  $f^1$  and  $f^2$  are the minimum force to displace the plate.

Figure 26 An approximated spring-mass model of the dome



$$x_0 = -0.32(\text{m}) \quad v_0 = 1.0 (\text{m/s}) \quad g = 0 \quad m = 5 \text{ kg.}$$

$$k = \begin{cases} k_1 = 26810 \text{ N/m} & x > 0 \\ k_2 = 855.4 \text{ N/m} & x < 0 \end{cases} \quad f^0 = \begin{cases} f^1 = 196. \text{ N} & x > 0 \\ f_2 = -196. \text{ N} & x < 0 \end{cases}$$

Figure 27 Time - displacement curve from the approx. mass-spring model

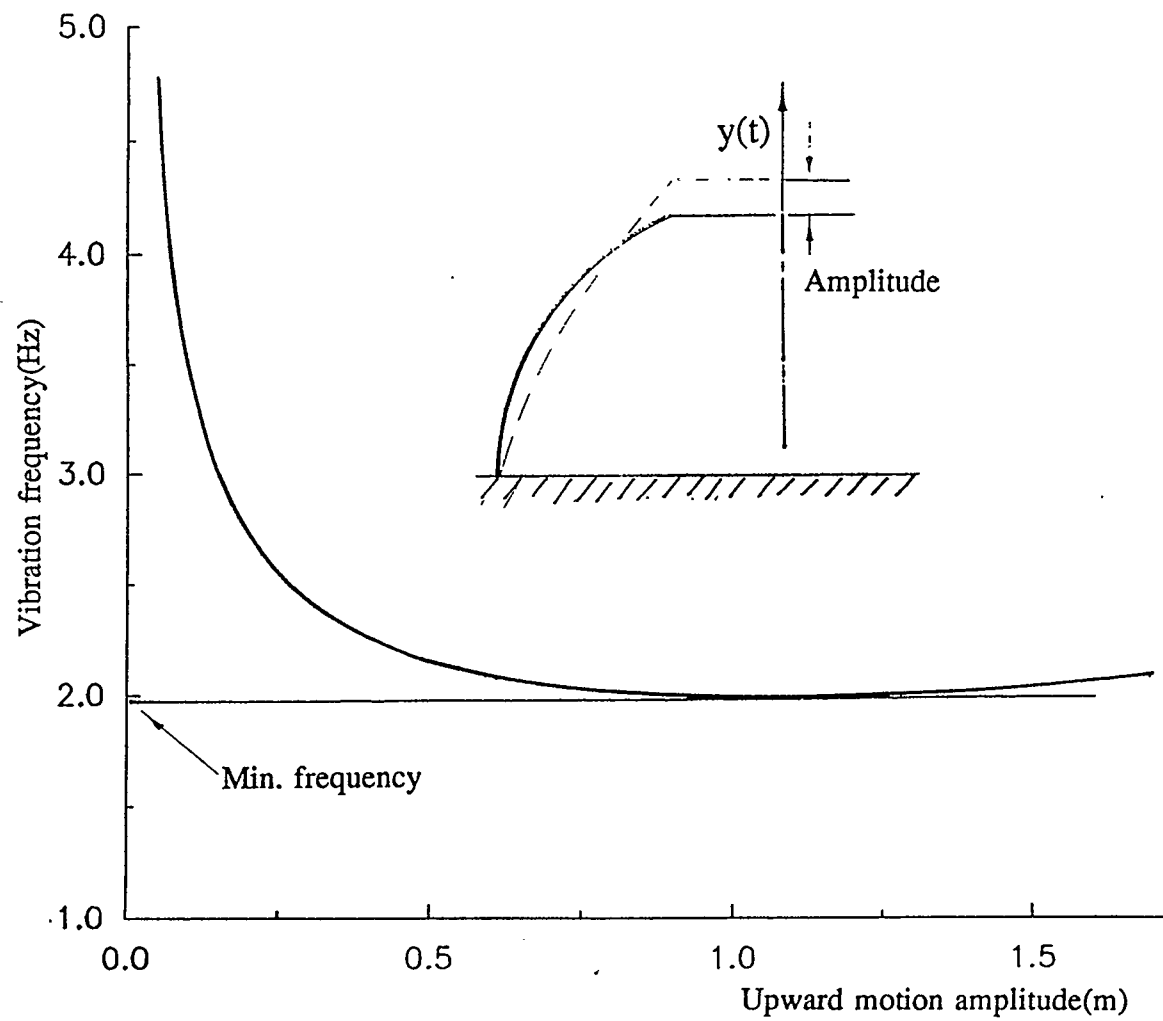


Figure 28 Free vibration frequency as function of vibration amplitude

The resonance occurs when the forcing frequencies are close to the free oscillating frequencies as shown in Fig. 17 in page 54. In the phase plane of Fig. 16 the curve initiates at the zero velocity and near the no-load position point, and then expands until the plate touches the bottom of the dome. Away from the resonance zone, the inflatable system responds to all periodic excitations in a bounded, chaotic, and non-periodic way as shown in Fig. 15. Both Fig. 29 and Fig. 33 show the random behaviour resulting from system's nonlinearity in load-displacement relationship. The investigation in forced vibration indicates that conventional methods such as perturbation scheme and averaging technique to find the steady state solution to the non-linear differential equation must be abandoned or modified since they assume periodic output solutions. Fig. 30 displays that a totally sealed dome has higher free oscillation frequency because it has higher over all stiffness when comparing to a dome with the same geometry but of constant inner pressure.

Fig. 31 and Fig. 32 are the results of a spectrum analysis of a high profile dome. The frequency of the excitation force with the low amplitude is sweeping from 5(Rad/s.) to 200. (Rad/s.). The maximum vibration amplitude is recorded at each forcing frequency as shown in Fig. 33. By plotting the maximum magnitude of vibration response against the excitation frequency, ie. a spectrum chart, one can locate the membrane structural resonance frequency at the peak maximum response. In Fig. 31, resonance is indicated to occur when forcing frequency is approximately 18 (Rad/s). Unlike a single-degree freedom linear vibration system where a natural frequency is a constant value and is determined by the system's stiffness and the vibrating mass, the membrane structures

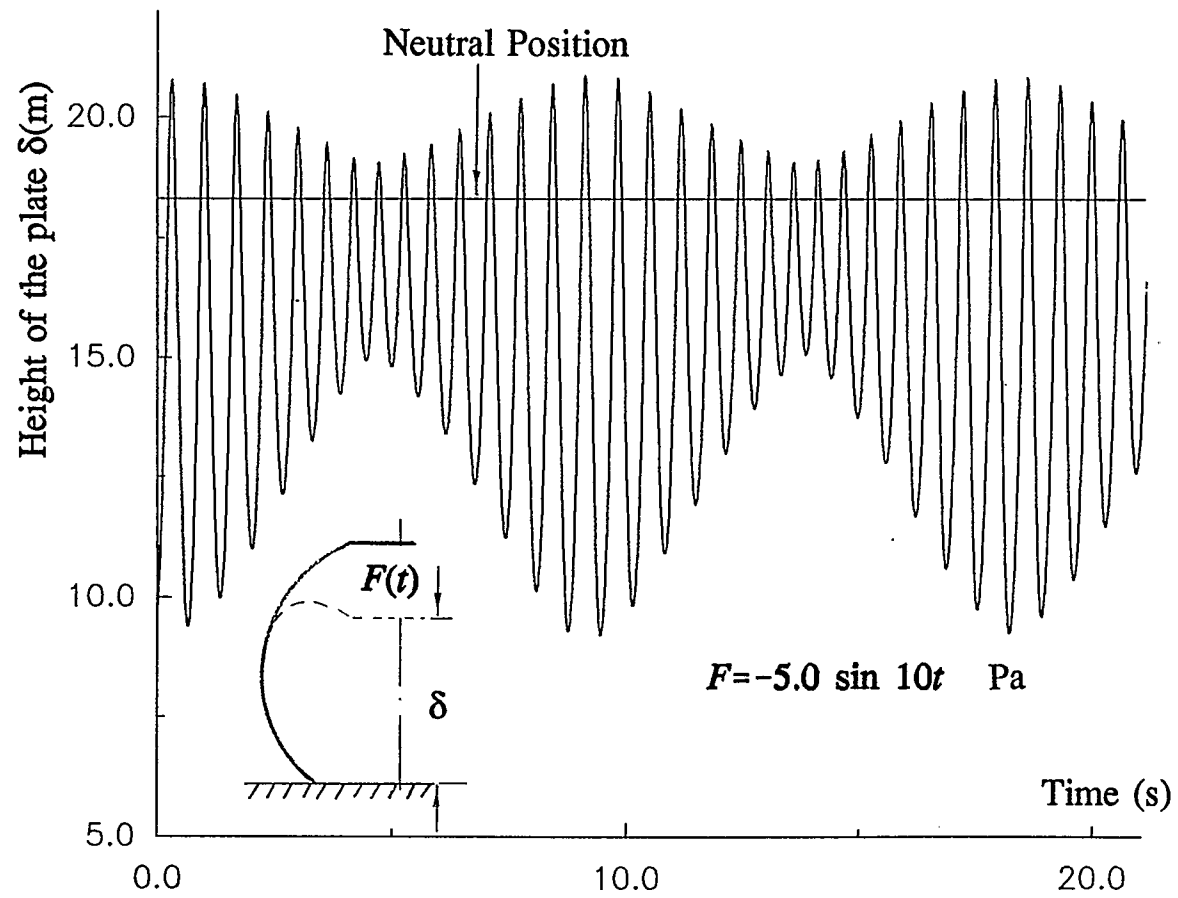


Figure 29 Forced vibration of the plate

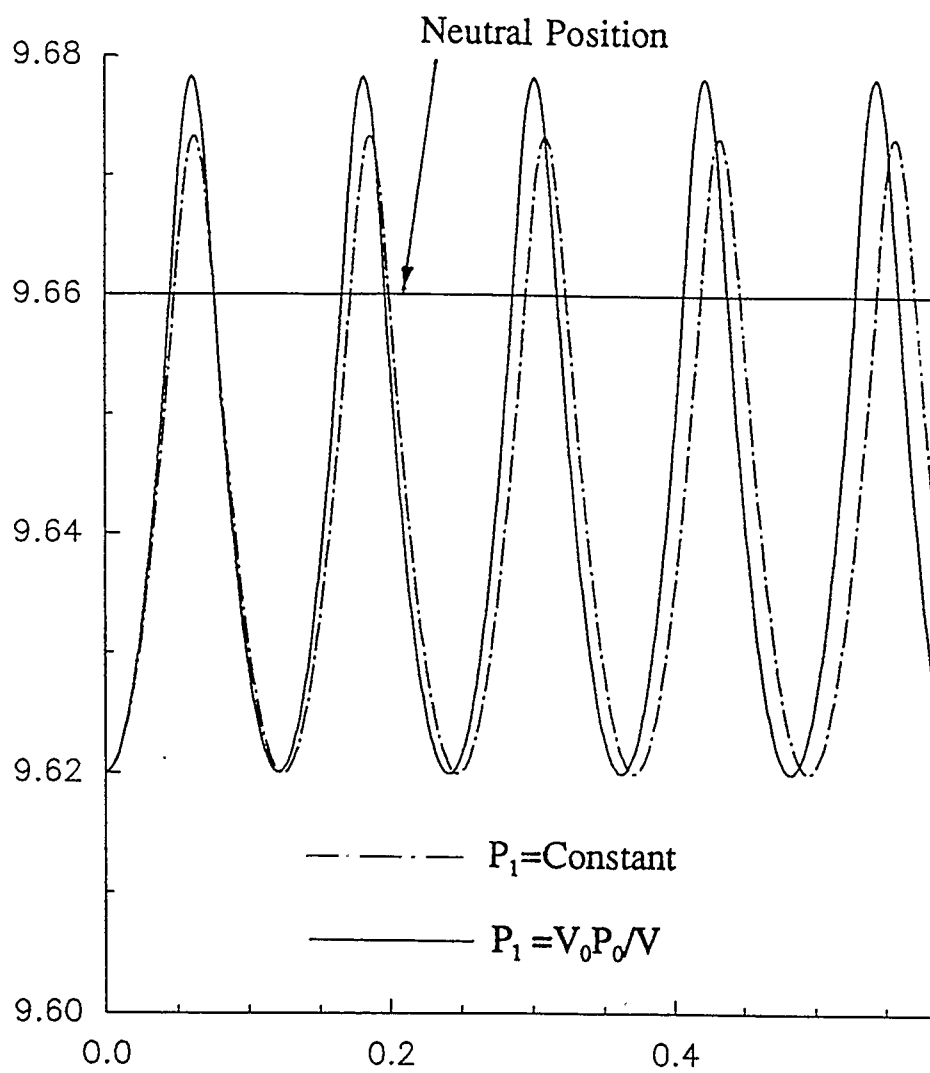


Figure 30 Free oscillation of a plate with different internal pressure assumptions

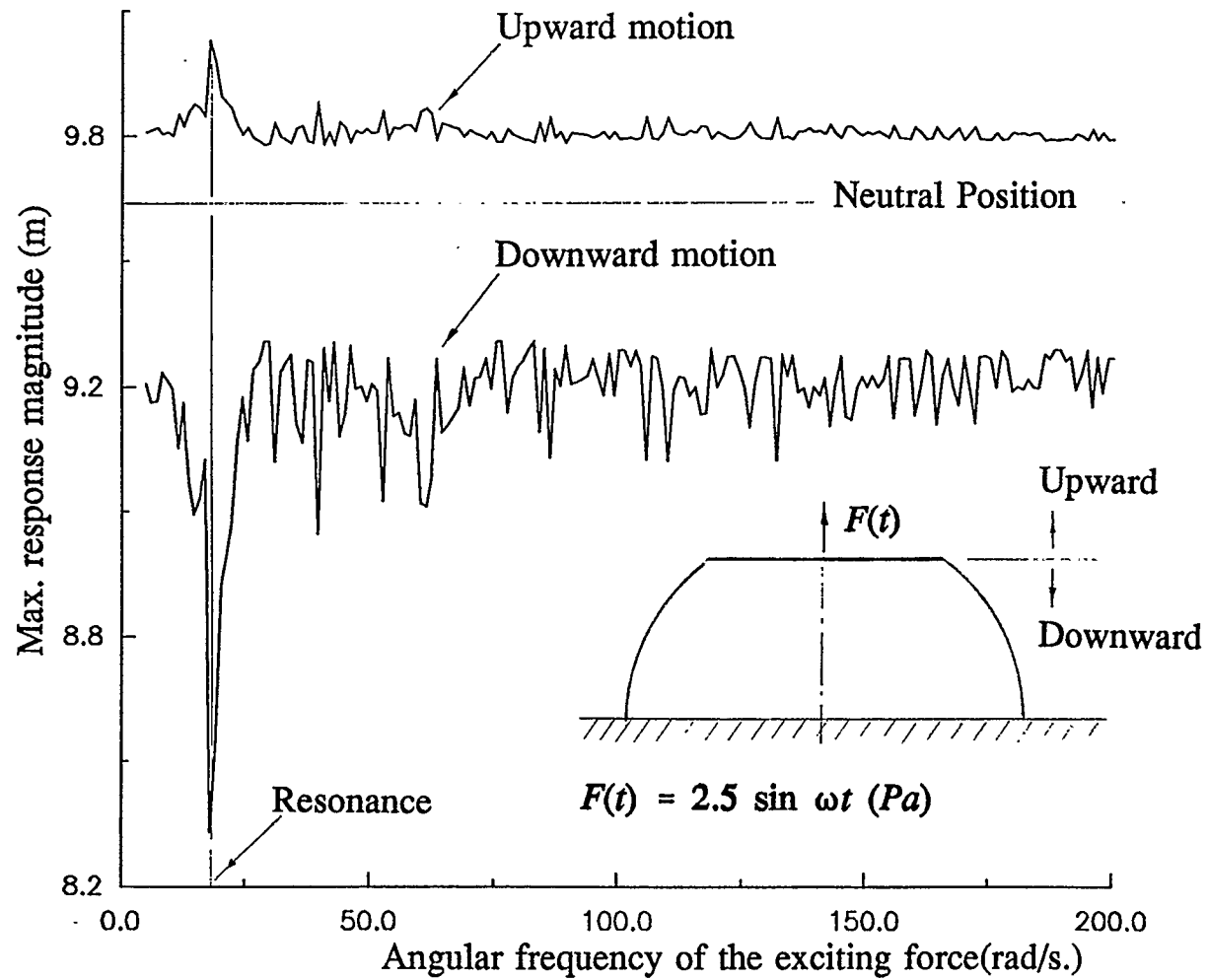


Figure 31 Spectrum analysis of a spherical dome

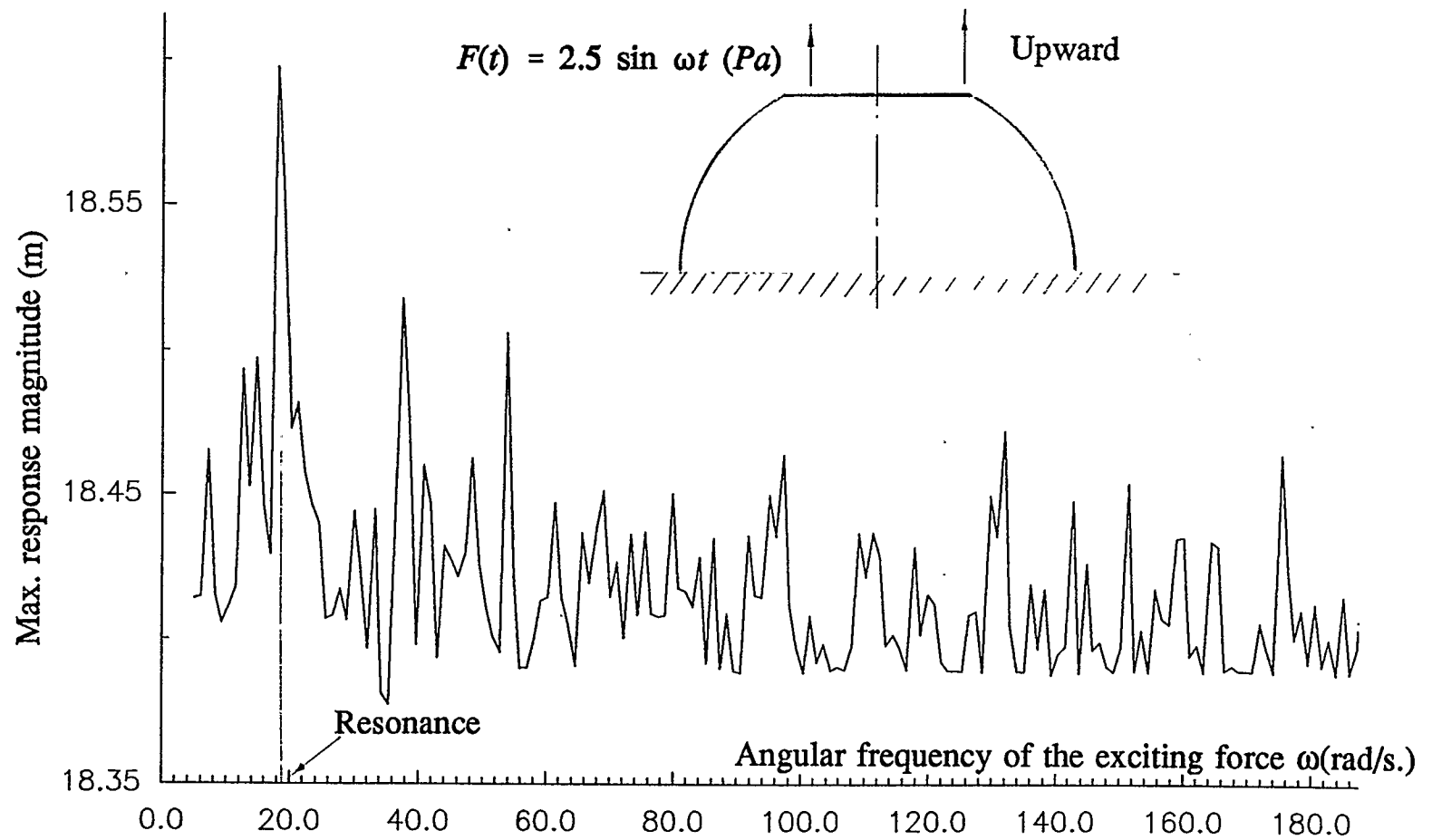


Figure 32 Spectrum analysis of a spherical dome: upward motion

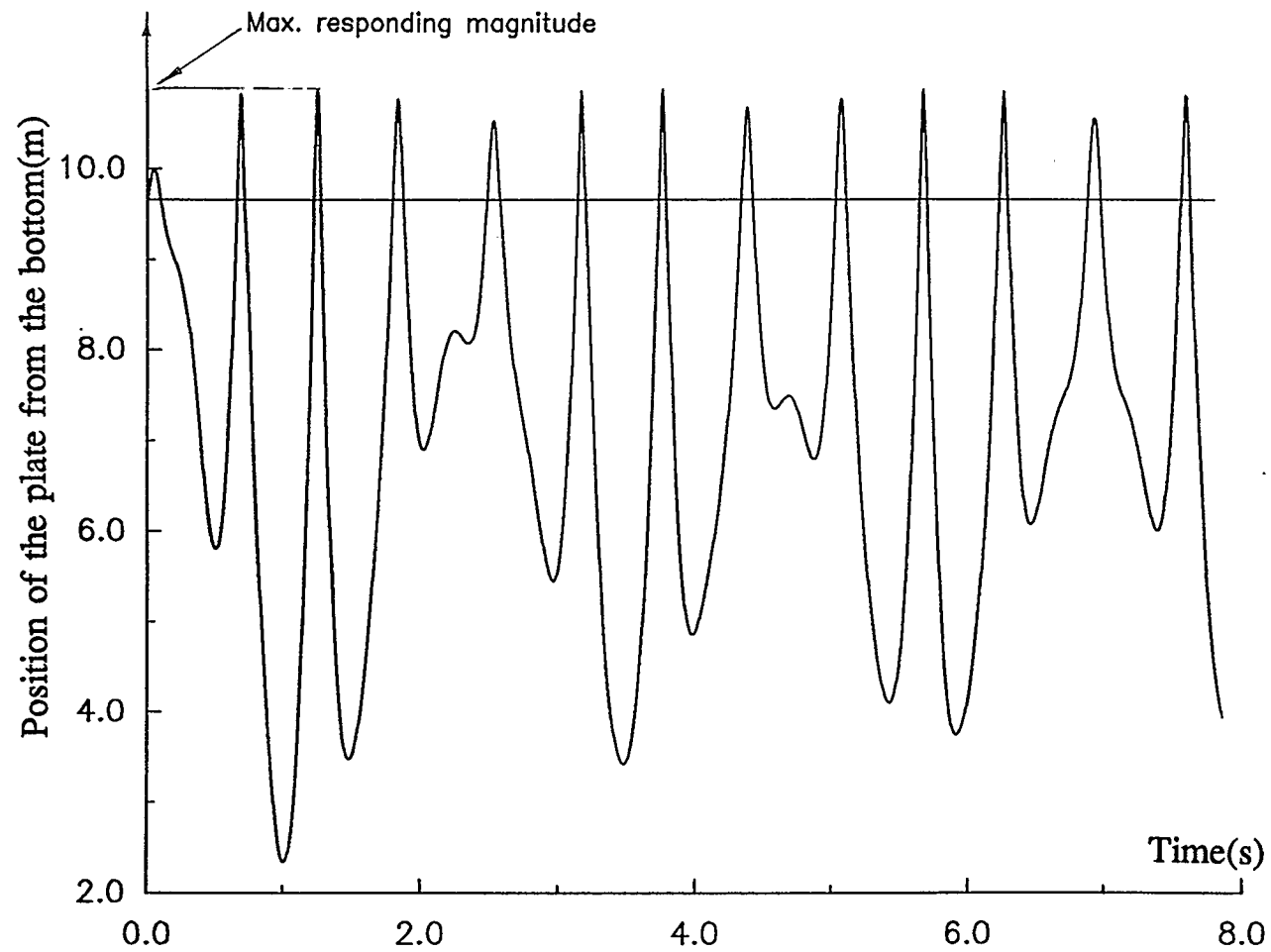


Figure 33 The max. upward motion amplitude in forced vibration  
away from the resonance

analyzed in the present study do not have such fixed valued free vibration frequency. As is just analyzed and shown in Fig. 25 and Fig. 28, the free vibration frequency strongly depends on the oscillation magnitude because of the discontinuous structural stiffness. Thus the term 'natural frequency' in a linear system does not apply in this type of membranes. Therefore, there does not exist a frequency ratio between the forced vibration and the free vibration states. This analysis also shows that, unless the spectrum analysis has been carried out, it is uncertain that at what forcing frequency the resonance would occur because the membrane structure has no fixed valued natural frequency that can be equated to the forcing frequency to estimate the resonance zone.

The time history of the meridian force around the plate edge is shown in Fig. 34 and Fig. 35. Fig. 34 is a zoom-in picture of the meridian force around the plate which is in free vibration. The two lower humps are the changing meridian force in inward motion. And the three big spikes are the force in outward motion. The sudden change in the three spikes is explained by the transition states between a fully wrinkled and partially wrinkled membrane. The minimum value of this force is zero. It occurs when the equivalent external force at the plate is just balanced by the internal pressure force. Such equivalent force is the vector sum of the inertia force, gravity force and an externally applied force.

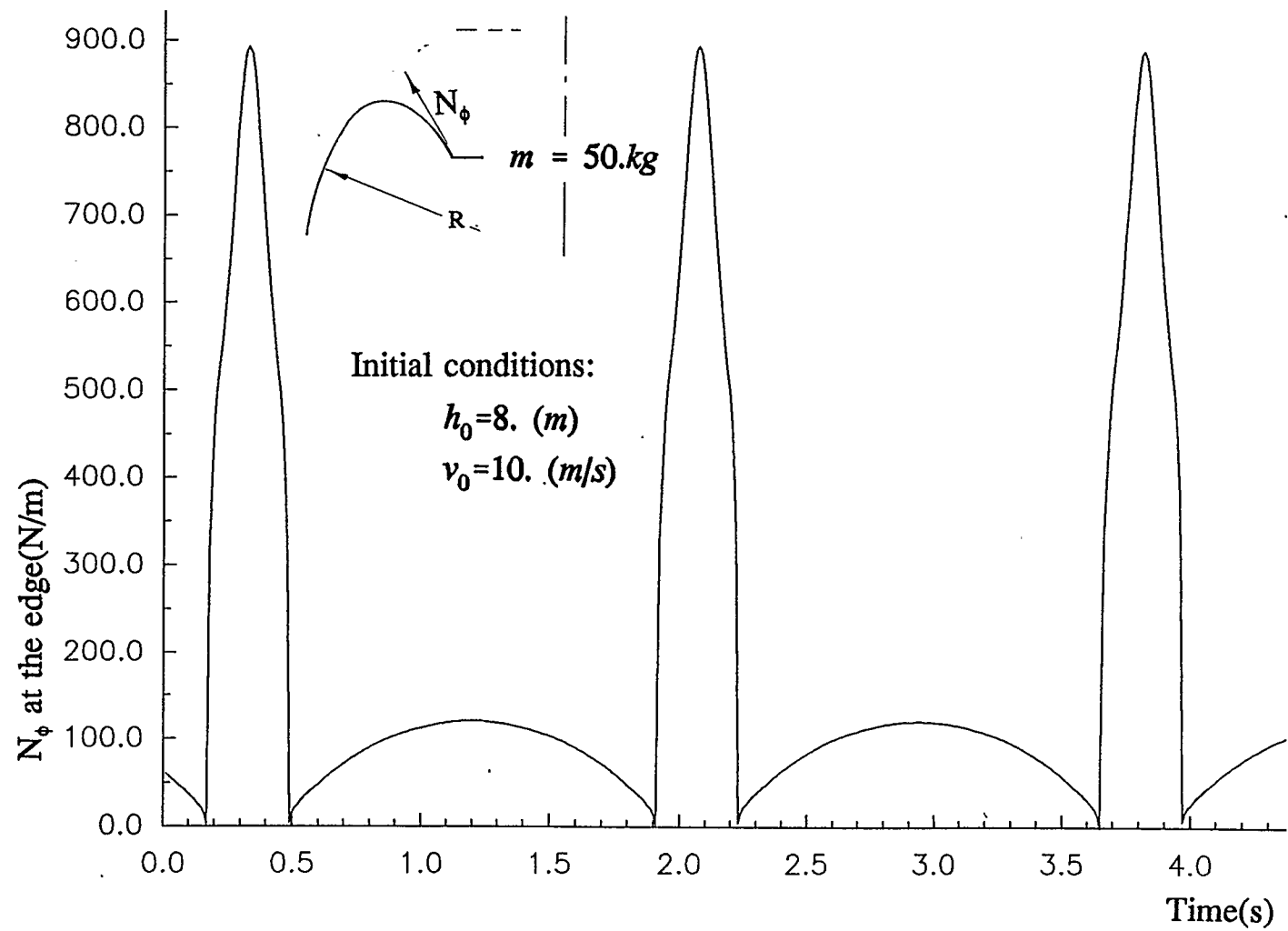


Figure 34 Meridian force  $N_\phi$  around the plate edge in free vibration

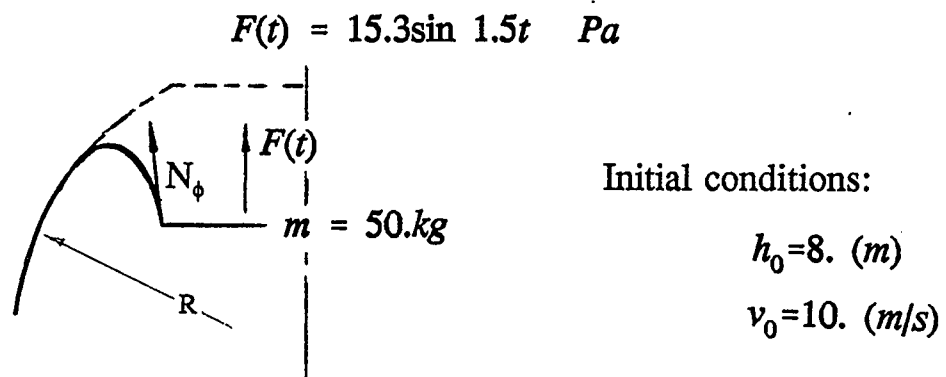
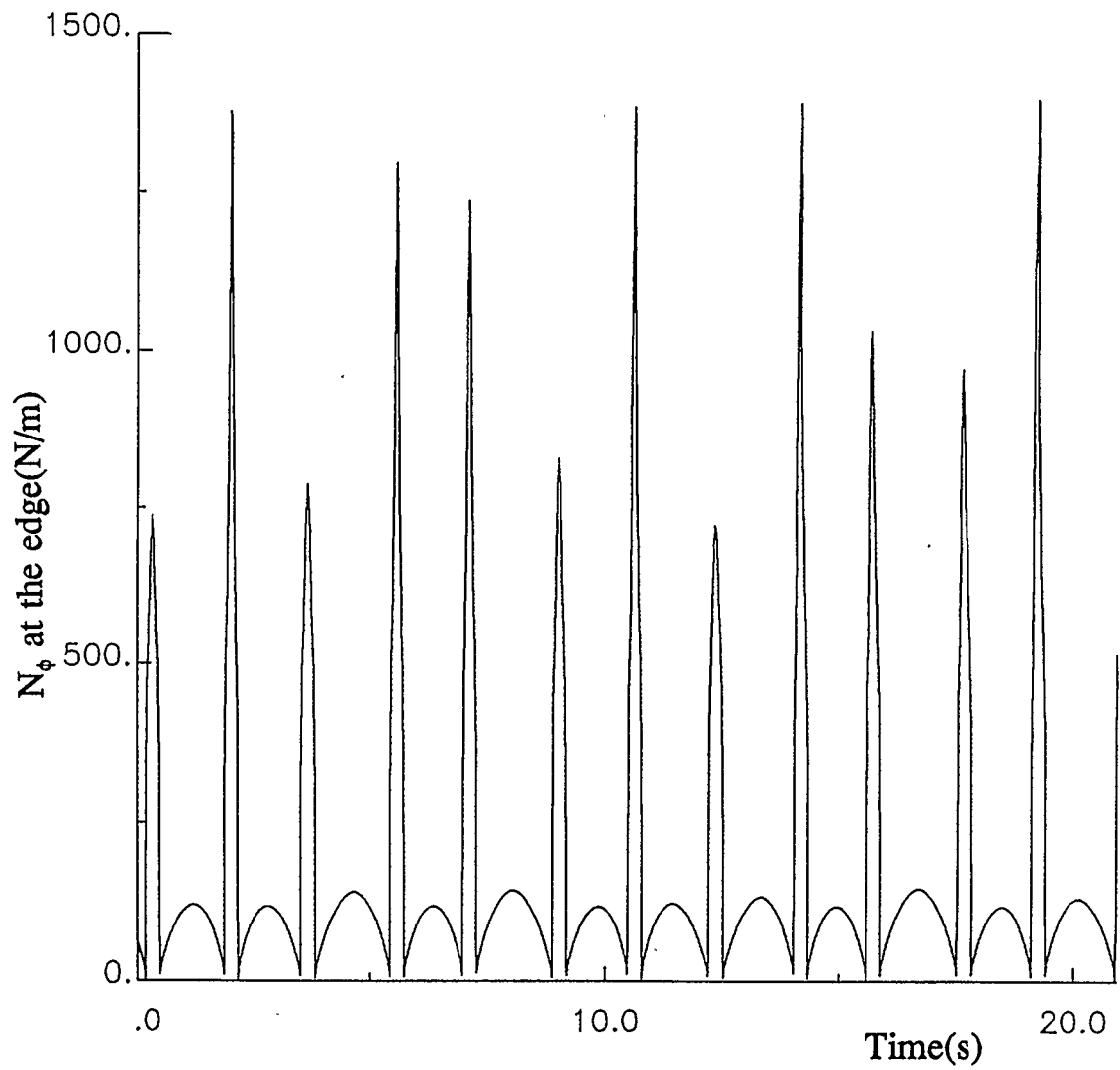


Figure 35 Meridian force  $N_\phi$  around the plate edge in forced vibration

## Chapter 5 Concluding Remarks and Summary

### 5.1 Summary and Limitations

This thesis has presented a non-linear analysis of the large deflection dynamic behaviour of inflated spherical membrane structures with a heavy rigid plate at the top. The effect of the interaction between the structure and the surrounding medium is neglected. Focus is on weightless and inextensible membranes. A significant change in the initial geometry of the structure is caused by large deflections and wrinkling under loading. Such large deflections and highly nonlinear behaviour require a geometrically non-linear analysis of the equations in defining the deformed configurations. These equations may be relatively simple in appearance and can be reduced to one first order differential equation as the governing differential equation. However, they contain multi-valued functions leading to multiple solutions with accompanying convergence problems in the numerical solutions. The solutions of the equations are also difficult to interpret. A simple closed form solution which describes the deformed and wrinkled membrane is obtained from the governing differential equation. However, the determination of the constant of integration satisfying both the boundary conditions and the compatibility equation is a very complex and challenging task. This task must be carried out in numerical approaches. Singularity and divergence problems must be overcome in numerical analysis to define the deformed configurations over a range of loading cases. More than 2000 lines of computer programs have been written in Fortran language to carry out the static and dynamic analysis and

to process output results. The dynamic behaviour of the structure was thoroughly studied based on the static analysis results.

In the high profile spherical inflatables, where the half central angle  $\Phi_0$  is greater than  $90^\circ$ , wrinkles not only exist around the loading point, but also possibly near the support region. Under push-in load at the high profile inflatables, wrinkling in the support region is the result of vanishing meridional tension, ie.,  $N_\phi=0$ . In the case of pull-out loads, the wrinkling in the same support area is caused by vanishing of the circumferential tension. In both loading cases, the wrinkling near the support region results in a vertical overall rigid body motions, thereby producing a discontinuity in the load-displacement relation curve. Such unique discontinuity does not occur in the low profile spherical pneumatics.

If the reduction in the spherical membrane is not large, the internal pressure has negligible influence on the deformed configuration. As the volume reduction exceeds 20% of the initial volume, the increasing internal pressure due to compression significantly stiffens the inflatable. Comparing to a spherical dome of the same geometry but with a constant internal pressure, a sealed dome is much stronger when deflection is in the order of the initial height or the radius of the inflatable.

No analytical form of expression can be obtained to define the relations between parameters that define the deformed configurations and the load. Numerical analysis is necessary to determine the relations.

It is found that the behaviour of the plate in free vibration is non-symmetric about its equilibrium position. The amplitude of inward motion is larger than that of the outward motion. Free vibration frequency is also affected by the vibration magnitudes. Because of the increasing structural stiffness with the plate displacement, the free oscillation frequency of the plate diminishes as the vibration amplitude becomes higher. Another interesting feature of the vibrating system is that the free oscillation frequency has a minimum value as the magnitude becomes large. At the maximum height, the inflatable is deformed to a truncated cone with infinitively large structural stiffness.

In the case when a periodic external force is applied to the plate, it responds in a bounded chaotic pattern. The maximum height position of the plate is fixed by the condition when the inextensible membrane is stretched straight, while the lowest point of the plate is at the bottom of the inflatable. Resonance occurs when the forcing frequency is close to the free vibration of the same initial conditions.

It was assumed that the membrane is inextensible. When a large deformation is produced by a heavy inward load, this assumption may lead to a stiffer inflatable. The calculated deflection would be less than the actual deflection because in reality great reduction in volume raises inflation pressure and causes the unwrinkled membrane to be expanded and stretched thinner, thus reducing the total structural stiffness. In the case when the membrane is stretched longer, there is also wrinkling near the support due the material extensibility. The overall effect is a reduction in the structural stiffness in large deflection.

In the dynamic analysis, the self-weight of the membrane must be considered when the surface density of the membrane is comparable to the that of the vibrating plate. If the magnitude of the membrane inertia force is high and the inflation pressure of the dome is low, the effect of the inertia force from the vibrating membrane may not be neglected. Large internal pressure can create high tension membrane since the two principal forces  $N_\phi$  and  $N_\theta$  are proportional to the internal pressure of the dome. And high tension and internal pressure can act together to weaken the influence of dynamic inertia force of the membrane.

As it was assumed that the wrinkled surface is replaced by a smooth imaginary mean surface, care must be taken when using this assumption in the large deflection analysis. In reality it may not be true if the wrinkled surface becomes rough and unevenly divided by deep grooves, formed by the membranes where the extremely low bending resistance and compressive stiffness of the material becomes significant within the wrinkle region. These rough surfaces are dominated by a few large wrinkles, which were observed by W. Szyszkowski and P.G. Glockner[20] in their laboratory experiment.

## 5.2 Concluding Remarks

This thesis has presented a thorough numerical analysis of large deflection dynamic behaviour of spherical membranes with a heavy rigid plate at its top. Attention is focused on the weightless and inextensible membrane. It is shown that the behaviour of such structure is nonlinear and its response to the applied dynamic force is random and chaotic.

The work presented in this thesis is an initial part of a study on the dynamic behaviour of spherical inflatables. It is the author's hope that this work will pave the ground for later study where the effects of membrane weight on both the static equilibrium and vibration frequency are considered. It is also hoped that, by applying the principle of Lagrange minimum total potential energy, the experimentally found uneven wrinkled surface in the deformed region can be treated. Such wrinkles resulting from the finite bending stiffness and compression rigidity of the membrane become significant in a very large deflection mode. It is anticipated to establish the natural frequency and the associated modes of the membrane in the future, taking into account the weight and the extensibility of the material and the interaction between the dynamic structure and the surrounding medium.

## References

1. Clark, G., "The History of Airships", Jenkins, London, 1961.
2. Dollfus, C., "Balloons", Prentice-Hall, London, 1962.
3. Kamrass, M., "Pneumatic Buildings", Scientific American, Vol. 194, No. 6, June 1965.
4. Allison, D., "Those Ballooning Air Buildings", Architectural Forum, Vol. 111, July 1959.
5. Otto, F., "Tensile Structures", Vols. 1 and 2, MIT Press Cambridge, 1967, 1969.
6. Bird, W.W., "The Development of Pneumatic Structures, Past, Present, and Future", Proceedings, 1st International Colloquium on Pneumatic Structures, ASS, Stuttgart, West Germany, 1967.
7. Bucholdt, H.A., "Tension Structures", Structural Engineer, Vol. 48, No. 2, Feb. 1970.
8. Subcommittee on Air-Supported Structures, "Air-Supported Structures", ASCE Spec. Publ., 1979.

9. Plaut, R.H. and Fagan, T.D. , "Vibration of An Inextensional, Air-Inflated, Cylindrical Membrane", J. Applied Mechanics, Trans. ASME, Vol. 55, Sept. 1988, 672-675.
10. Yoko, Y., Matsunaga, H., and Yokoyama, Y., "On the Behaviour of Wrinkled Regions Of Pneumatic Membrane in Forms of Surface Revolution Under Symmetric Loading", Proceedings ASS Pacific Symposium (Pt. 2), Tension Structures and Space Frames, 1971, pp.499-460.
11. Lukasiewicz, S.A. and Glockner, P. G. , "Collapse by Ponding of Air-Supported membranes", J. Structural Div., 1525-1532(1978).
12. Lukasiewicz, S.A. and Glockner, P.G. , "Lateral Stability of Lofty Air-Supported Spherical Membranes", Int. J. Non-linear Mechanics. Vol. 18, No. 6, 491-499.
13. Lukasiewicz, S.A. and Glockner, P.G. , "Ponding Instability of Air-Supported Spherical Membranes With Initial Imperfections", Int. J. Non-linear Mechanics, vol. 18, No. 1, pp. 1-9, 1983.
14. Szyszkowski, W. and Glockner, P.G. , "Finite Deformation and Stability Behaviour of Spherical Inflatables under Axisymmetric concentrated Loads", Int. J. Nonlinear Mech. 19, 489-496(1984).

15. Dacko, A.K. and Glockner, P.G. , "On the Large-deflection and Stability behaviour of Spherical Inflatables under Symmetric Plate and Cylindrical Loads", Engineering Struct. 11, No. 2, 97-111(1989).
16. Glockner, P. G. , "Recent Developments on the Large Deflection and Stability Behaviour of Pneumatics", Studies in Applied Mechanics, Vol. 16, 261-283, Elsevier, Amsterdam(1987).
17. Malcolm, D.J., and Glockner, P.G., "Collapse by Ponding of Air-supported Membranes", ASCE, Vol. 104, No. ST9, Proc. Paper 14002, Sept., 1978, 1525-1532.
18. Glockner, P.G. and Szyszkowski, W. , "Some Stability Considerations of Inflatable Structures", Proceedings I.A.S.S. Symposium on Shell and Spatial Structures in Engineering, Rio de Janeiro, Sept. 1983, 116-134(1984).
19. Glockner, P.G., Szyszkowski, W. and Dacko, A.K. , "Key Response Characteristics of Spherical Pneumatics Under Axisymmetric loading", Proceeding Int. Colloquium on Space Struct. for Sports Buildings (Edited by Tien T. Lan and Y. Zhilian) 556-573. Elsevier Applied Science Press, Amsterdam (1987).
20. Szyszkowski, W. and Glockner, P.G. , "Spherical Membranes Subjected to Vertical Concentrated Loads: an experimental study", Engineering Struct. 9, 183-192 (1987).

21. Szyszkowski, W. and Glockner, P.G. , "Geometrically Non-linear Problems for Membrane Structures", CSCE Annual Conference, Saskatoon, Sask.,1985, 213-232.
22. Dacko, A.K. and Glockner, P. G. , "Spherical Inflatables under Axisymmetric Loads: another look", Int. J. Non-linear Mech. 23 393-407(1988).
23. Glockner, P.G. , Dacko, A.K. , Szyszkowski , W. and Swisterski, W. , "Response of Spherical Pneumatics to Symmetric loads: an overview", Proceedings ASS-MSU Symposium on Domes from antiquity to the percent, Mimer Sinan University, Istanbul, 1988, 685-694.
24. Oden, J.T., and Kubitza, W.K., "Numerical Analysis of Nonlinear Pneumatic Structures", ASS 1st International Colloquium on Pneumatic Structures, Stuttgart, May 1967, 87-107.
25. Oden, J.T. and Sato, T., "Finite Strains and Displacements of Elastic Membranes by the Finite Element Method", Int. J. Solids Structures, 1967, vol. 3, 471-488.
26. Mansfield, E.H., "Load Transfer via a Wrinkled Membrane", Proc. Roy. London. A. 316, 1970, 269-289.
27. Stein, M. and Hedgepeth, "Analysis of Partially Wrinkled Membranes", NASA Tech. Note, D-813, July, 1961, 1-32.

28. Feng, W.W. and Yang, W.H. , "On Contact Problems of an Inflated Spherical Non-linear Membrane", Journal of Applied Mechanics, Trans. of ASME, Mar. 1973, 209-214.
29. Horvay, G. and Clausen, I. M. , "Membrane and Bending Analysis of Axisymmetrically Loaded Axisymmetrical Shells", J. Applied Mechanics, Trans. ASME, Mar. 1955, 25-30.
30. Royles, R. and Llambias, J.M. , "Point Loading Effects On The Ethinodome", Technical Note, Computers and Structures, Vol. 29, No. 3, 527-530, 1988.
31. Avinoam Libai, "The Transition Zone Near Wrinkles in Pulled Spherical Membranes", Int. J. Solids Structures, Vol. 26, No.8, 927-939.
32. Moon, F.C., "Experiments on Chaotic Motions of a Forced Nonlinear Oscillator: Strange Attractors", ASME Journal of Applied Mechanics, Vol. 47, 1980, 638-644.
33. Holmes, P. J. and Moon, F. C. , "Strange Attractors and Chaos in Nonlinear Mechanics", Journal of Applied Mechanics, Trans. ASME, Vol. 50, 1021-1032, Dec. 1983.
34. Wu, C.H., "Nonlinear Wrinkling of Nonlinear Membranes of Revolution", J. Appl. Mech. 45, 1978, 533-538.
35. Zak, M., "Statics of Wrinkling Films", J. Elasticity 12, 1982, 51-63

36. Timoshenko, S. and Young, D. H., Advanced Dynamics, New York: McGraw-Hill, 1948.
37. Timoshenko, S. and Woinowsky-Krieger, S., Theory of Plates and Shells, 2nd Ed., New York: McGraw-Hill, 1959.
38. Harry Kraus, Thin Elastic Shells, John Wiley & Sons, Inc., 1967. 37-55.

## **Appendix**

### **Computer Programs**

1. Determination of Parameters to Describe Deformed Configurations Under Static Load
2. Calculation of Time History of Deflection and Velocity of the Vibrating Plate, Spectrum Analysis of the Spherical Membrane for Forcing Frequency at Resonance
3. Sample Output of Static Deformation Results

```

*****
*
*      This program determines the geometric parameters to define
*      the deformed spherical membrane inflatables under static load
*      Trapezoidal rule and bisection method are employed
*      in the numerical calculation process
*
*****
c
      Parameter (IP2max=40)
c  For double precision, Active the Following:
      Implicit real*8(A-H,O-Z)
      Real PP2(IP2max)
c
      common /Pres2/PP2(IP2max)
      common /Const/Pi,Cov,Ra,r0,Phi1,Ang0,N1,N2,V1,P01,Angm
      common /Var/P1,P2,Ang1,Ang2,Sl,Sv1,Vd1,Vd2,Pbert,Phi,ht
      common /Crt/P2crt,P1crt,C2crt,hert,Vert,An1crt,Vmax
      common /Crtb/Pb2crt,C1crt,hbert,Vbert,Ab1crt,Ab2crt
      common /Crt9/P2crt9,P1crt9,C2crt9,hert9,Vert9,An2crt9
      common /Tape/NT20,NT30
      common /IconP1/ICP1,Itact
      common /Prevvs/Ang2Ls,Ang1Ls,Sv1Ls,ItowrkLs,P2Ls,C2Ls
      common /Prevbs/Anb2Ls,Anb1Ls,Pb2Ls,C1Ls
      common /paramb/Anb2,Anb1,Slb,Pb2,rb,Svb,hb
c
      NT20=20
      NT30=30
c
      open(unit=NT20,file='modison2.in')
      open(unit=NT30,file='modison2.out')
c  File NT40 is specified for Graftool software
      open(unit=NT40,file='modison2.grt')
c
      write(NT40,*) '/Height,P2,Ang1,Ang2,C2,P1,(h0-ht),% wrinkle'
      write(NT40,*) '/Delete Zero Height Row'
      write(NT40,*) '/Re-arrange Data Sequence according so that'
      write(NT40,*) '/P2 is in ascending order'
      write(NT40,*) '*****'
      Pi=3.14159
c
c  NT— Total no. of externally applied pressure to exam
c  E — Young's modulus
c  t — Shell thickness
      read(NT20,*) NT
      If(NT .gt. IP2max) then
        write(6,*) 'Increase Array size PP2!'
        write(NT30,*) 'Increase Array size PP2!'
        go to 1111
      End if
      read(NT20,*) Ra,r0,Phi1,P01
      read(NT20,*) ICP1,Itact
c  ICP1 eq. 1 means const. internal pressure
      If(Phi1 .gt. .5*Pi .and. ICP1 .eq. 0) then
        write(6,*) 'High Profile Dome Must Have Const. Int. Pres.'
        go to 1111
      End if
c
c  There are NT+2 rows by 8 columns of data, additional 2 comes from
c  two critical cases.
      write(NT40,*) NT+2,8
      read(NT20,*) (PP2(I),I=1,NT)

```

```

write(NT30,*) ' '
write(NT30,*) '*****'
write(NT30,*) ' '
write(NT30,*) 'No. of Pressure Trials          : ',NT
write(NT30,*) ' '
write(NT30,*) 'Applied Pressure as factors of Initial Internal'
write(NT30,*) 'Pressure: '
write(NT30,*) (PF2(I),I=1,NT)
write(NT30,*) ' '
write(NT30,*) '*****'
c
c PF2(i) in input file are factors of P01
  Do 2 I=1,NT
    PF2(I)=PF2(I)*P01
    If(I .gt. 2 .and. I .lt. NT)then
      If(PF2(I)-PF2(I-1) .lt. 0.)then
        write(6,*)
        &      'Input Pressue Must Be in Ascending Order'
        write(NT30,*)
        &      'Input Pressue Must Be in Ascending Order'
        stop
      End if
    End if
  2 Continue
c
  Cov=180./Pi
  read(NT20,*) N1,N2
  read(NT20,*) Xacc,Facc
  write(NT30,*) 'Radius of sphere          : ',Ra
  write(NT30,*) 'Radius of rigid plate      : ',r0
  write(NT30,*) 'Meridional Angle at the root(deg.) : ',Cov*Phil
  write(NT30,*) 'Initial internal pressure    : ',P01
  write(NT30,*) 'Curve divisions In The Wrinkled'
  write(NT30,*) 'Region for Numerical Integration : ',N1
  write(NT30,*) 'Max allowable # of trials    : ',N2
  write(NT30,*) 'Tolerance of C2 (root)       : ',Xacc
  write(NT30,*) 'Tolerance of Length Summation : ',Facc
c
c Critical load to cause membrane to wrinkle at its base:
  Pbcrt=(Ra*sin(Phil)/r0)**2*P01
  Ang0=asin(r0/Ra)
  Da=(Phil-Ang0)/N1
  h0=0.
  Do 1000 i=1,N1
    Ang=Ang0+Da*(i-1)/N1
    h0=h0+Ra*Da*sin(Ang)
  1000 Continue
  h01=Ra*(cos(Ang0)-cos(Phil))
c Original volume before deformation:
  V1=Ra**3*Pi*(cos(Phil)*(cos(Phil)**2/3.-1.)-cos(Ang0)*
  & (cos(Ang0)**2/3.-1.))
c
c Calculate the most upward position:
  Hmax=((Ra*(Phil-Ang0))**2-(Ra*(sin(Phil))-r0)**2)**.5
  Ht=r0*Hmax/(Ra*sin(Phil)+r0)
  Vmax=((Ra*sin(Phil))**2*(Hmax+Ht)-r0**2*Ht)*Pi/3.
c
c Angle to which both Ang1 and Ang2 approach as P2 goes to negative
c infinity
  Angm=acos((Ra*sin(Phil)-r0)/(Ra*(Phil-Ang0)))
c
  write(NT30,*) ' '

```

```

write(NT30,*) 'Original Enclosed Volume      :',V1
write(NT30,*) 'Original Height Of The Plate   :',H01
write(NT30,*) 'Maximun Height Of The Plate    :',Hmax
write(NT30,*) 'Volume at the Maximun Height   :',Vmax
write(NT30,*) 'Ang(1) and Ang(2) at This Max. Height :',
& Angm*Cov
c
read(NT20,*) NY
If(NY .eq. 1)then
  write(NT30,*) 'Input critical pressure values from file'
  read(NT20,*) P2crt,P1crt,C2crt,hcrt,An1crt,Vcrt
  An1crt=An1crt/Cov
  read(NT20,*) P2crt9,P1crt9,C2crt9,hcrt9,An2crt9,Vcrt9
  An2crt9=An2crt9/Cov
else
c Call subroutine to determine critical pressure value:
  call crtP2(Xacc,Facc,Ierror)
End if
c
write(NT30,*) ' '
write(NT30,*) '*****'
write(NT30,*) 'Critical Values to Cause Structure Wrinkle'
write(NT30,*) 'at Its Root Under Inward Load'
write(NT30,*) 'P2      (Crt.)      :',P2crt
write(NT30,*) ' '
write(NT30,*) 'Critical Values When Membrane Becomes '
write(NT30,*) 'Fully Wrinkled Due to Suction At Top : '
write(NT30,*) 'P2      (Crt.)      :',P2crt
write(NT30,*) 'P1      (Crt.)      :',P1crt
If(Phil .gt. .5*Pi) then
  write(NT30,*) 'Total Height      :',hbcrt+hcrt+
& Ra*cos(Ab2crt)
  write(NT30,*) 'Total Vol.      :',Vcrt+Vbcrt+
& Ra**3*Pi*cos(Ab2crt)*(1.-cos(Ab2crt)**2/3.)
  Ang2crt=90.00
Else
  write(NT30,*) 'Total Height      :',hcrt
  write(NT30,*) 'Total Vol.      :',Vcrt
  Ang2crt=Phil*Cov
End if
If(Phil .gt. .5*Pi)then
  write(NT30,*) '***** Break Down Summary *****'
  write(NT30,*) '-----'
  write(NT30,*) ' Bottom Section '
  write(NT30,*) 'C1      (Crt.)      :',C1crt
  write(NT30,*) 'H      (Crt.)      :',hbcrt
  write(NT30,*) 'Ang(1) (Crt.)      :',180-Cov*Ab1crt
  write(NT30,*) 'Ang(2) (Crt.)      :',180-Cov*Ab2crt
  write(NT30,*) 'Volume (Crt.)      :',Vbcrt
  hcrt=hcrt+hbcrt+Ra*cos(Pi-Ab2crt)
  write(NT30,*) ' '
  write(NT30,*) ' Top Section '
End if
write(NT30,*) 'Ang(1) (Crt.)      :',Cov*An1crt
write(NT30,*) 'Ang(2) (Crt.)      :',Ang2crt
write(NT30,*) 'C2      (Crt.)      :',C2crt
write(NT30,*) 'H      (Crt.)      :',hcrt
write(NT30,*) 'Volume (Crt.)      :',Vcrt
write(NT40,2111) hcrt,P2crt,An1crt*Cov,Ang2crt,C2crt,P1crt,
& (h0-hcrt),100.00
2111 format(8(f11.4,1x))
write(NT30,*) ' '

```

```

write(NT30,*) '*****'
write(NT30,*) 'Critical Values When Membrane Becomes '
write(NT30,*) 'Orthogonal to the Plate Under Pressure P2 : '
write(NT30,*) 'P2      (Crt.)      :',P2crt9
write(NT30,*) 'P1      (Crt.)      :',P1crt9
write(NT30,*) 'C2      (Crt.)      :',C2crt9
write(NT30,*) 'H       (Crt.)      :',hert9
write(NT30,*) 'Ang(2)  (Crt.)      :',Cov*An2crt9
write(NT30,*) 'Volume  (Crt.)      :',Vert9
write(NT40,2111) hert9,P2crt9,-90.00,An2crt9*Cov,C2crt9,P1crt9,
& (h0-hert9),100.00
Rat=P2crt9/Pbct
If(Phil .gt. .5*Pi .and. Rat .gt. 1.)then
  Phi=Pi-asin(Rat**(.5*sin(Phil)))
  write(NT30,*) 'Rigid Body Settlement      :',
& Ra*(cos(Phi)-cos(Phil))
End if
write(NT30,*) ' '
write(NT30,*) '*****'
c
write(6,*) 'No. of Pressure Trials ', NT
write(6,*) 'Pressures to apply:'
write(6,*) (PP2(i),i=1,NT)
c
c Icalb keeps track of # of base-wrinkle routine call
Icalb=0
Do 42 ni=1,NT
  P2=PP2(ni)
c Check If Membrane Is Fully Wrinkled First:
  If(P2 .lt. P2crt .and. P2 .lt. 0.)then
    Itowrk1=1
  Else
    Itowrk1=0
  End if
c
Ifail=0
Ibaswr=0
If(P2 .gt. 0.)then
  Ral=P2/Pbct
  If(Ral .gt. 1.) Phi=Pi-asin(Ral**(.5*sin(Phil)))
  If(Ral .le. 1.) Phi=Phil
Else
  Phi=Phil
End if
If(abs(P2) .lt. P01)then
  write(NT30,*) 'Insufficient Pressure Force P2'
  write(6,*) 'Insufficient Pressure Force P2'
  write(6,*) '(P2 = ',P2,')'
  write(NT30,*) '*****'
  write(NT30,*) ' '
  write(6,*) 'Discard Test Pressure      ',P2
  If(ni .lt. NT) write(6,*)
& 'Pick up Next Pressure Value      '
  go to 42
Else
  call rootbnd(Xacc,Facc,Ierror,Itowrk1,Iroot,ni,C2)
  If(P2 .lt. 0. .and. Itowrk1 .eq. 0. .and.
& Phil .gt. .5*Pi) then
    Ibaswr=1
    Icalb=Icalb+1
    call baswrk(Xacc,Facc,P2,Ierrob,Iroot,Icalb,C1)
  End if

```

```

        If(Ierror .eq. 1) then
            Goto 42
        End if
    End if
    If(Iroot .eq. 0) goto 333
c
222    write(NT30,*) 'External Pressure At      : ',P2
c
        Ib=0
        If(Ibaswr .eq. 1) then
c Saving the parameters for next trial:
            Anb2Ls=Anb2
            Anb1Ls=Anb1
            Pb2Ls=Pb2
            C1Ls=C1
        End if
        If(Itowrkl .eq. 1) then
            Hdp=ht
            Xlbd=Ra*(Phi1-Ang0)
        Else
            If(P2 .gt. 0.)then
                Swklb=Ra*(Phi1-Phi)
                Hdp=ht+Ra*(cos(Ang2)-cos(Phi))
                Xlbd=Ra*(Phi1-Ang0-Phi+Ang2)
            Else
                If(Ibaswr .eq. 1)then
                    Hdp=ht+hb+Ra*cos(Ang2)
                    Xlbd=Ra*(Ang2-Ang0)
                    Xlbdb=Ra*(Anb2-(Pi-Phi1))
                Else
                    Hdp=ht+Ra*(cos(Ang2)-cos(Phi1))
                    Xlbd=Ra*(Ang2-Ang0)
                End if
            End if
        End if
        If(Ibaswr .ne. 1)then
            Rwrkl=100.*Xlbd/(Ra*(Phi1-Ang0))
        Else
            Rwrkl=100.*Xlbd/(Ra*(.5*Pi-Ang0))
            Rwrklb=100.*Xlbdb/(Ra*(Phi1-.5*Pi))
        End if
c Saving the following data for next load case calculation
        Ang2Ls=Ang2
        Ang1Ls=Ang1
        Sv1Ls=Sv1
        ItowrklLs=Itowrkl
        P2Ls=P2
        C2Ls=C2
c
        write(NT30,*) 'Final Internal pressure      : ',P1
        write(NT30,*) 'Enclosed Volume After Deformation : ',
&          Sv1
        write(NT30,*) 'Height Of The Displaced Plate    : ',Hdp
        If(Ibaswr .ne. 1)then
            write(NT30,*) 'Find C2 as                  : ',C2
            write(6,*) 'Find C2 as : ',C2,' At P2 = ',P2
            write(NT30,*) 'Length Before deformation    : ',xldb
            write(NT30,*) 'Wrinkled Meridional Length   : ',Sl
            write(NT30,*) '% wrinkled membrane         : ',Rwrkl
            write(NT30,*) 'Angle Phi(1) (deg.)          : ',
&          Ang1*Cov
            write(NT30,*) 'Angle Phi(2) (deg.)          : ',

```

```

&      Ang2*Cov
      If(P2.gt. 0. .and. Phi1 .gt. .5*Pi .and. P2/Pbcr1 .gt. 1.)
&      write(NT30,*) 'Rigid Body Settlement      :',
&      Ra*(cos(Phi)-cos(Phi1))
      write(NT30,*) ' '
      Else
        write(NT30,*) '***** Upper Section *****'
        write(NT30,*) 'Find C2 as      :',C2
        write(6,*) 'Find C2 as :',C2,' At P2 =',P2
        write(NT30,*) 'Length Before deformation (Upper):',xlbdt
        write(NT30,*) 'Wrinkled Meridional Length (Upper):',Sl
        write(NT30,*) '% wrinkled membrane (Upper):',Rwrklt
        write(NT30,*) 'Angle Phi(1) (deg.) (Upper):',
&      Ang1*Cov
        write(NT30,*) 'Angle Phi(2) (deg.) (Upper):',
&      Ang2*Cov
        write(NT30,*) 'Vertical Stretch in Upper Section :',ht
&      -Ra*(cos(Ang0)-cos(Ang2))
        write(NT30,*) '***** Lower Section *****'
        write(NT30,*) 'Find C1 as      :',C1
        write(6,*) 'Find C1 as :',C1,' At P2 =',P2
        write(NT30,*) 'Length Before deformation (Lower):',xlbdb
        write(NT30,*) 'Wrinkled Meridional Length (Lower):',Slb
        write(NT30,*) '% wrinkled membrane (Lower):',Rwrklb
        write(NT30,*) 'Angle Phi(1) (deg.) (Lower):',
&      (Pi-Anb1)*Cov
        write(NT30,*) 'Angle Phi(2) (deg.) (Lower):',
&      (Pi-Anb2)*Cov
        write(NT30,*) 'Vertical Stretch in Lower Section :',hb-
&      Ra*(-cos(Anb2)-cos(Phi1))
      End if
      write(NT40,2111) Hdp,P2,Ang1*Cov,Ang2*Cov,C2,P1,(h0-ht),Rwrkl
      write(NT30,*) '*****'
      write(NT30,*) ' '
      write(NT30,*) ' '
      If(Hdp.lt. 0.)then
        write(NT30,*) 'Calculation Terminated As Plate Decents'
        write(NT30,*) 'Under Its Base Plane'
        go to 1111
      End if
c
333      If(Iroot .eq. 0)then
        write(NT30,*) 'Fail to find C2 at P2=',P2
        write(6,*) 'Fail to find C2 at P2=',P2
        write(NT30,*) '*****'
      End if
42      continue
223      format(5(e14.5,2x))
1111 stop
      end
*****
      subroutine rootbnd(Xacc,Facc,Ierror,Itowrkl,Iroot,Icall,root)
*****
c Subroutine to search for a root bound between C21 and C22
c The found root bound is stored as (X1,X2)
*****
      parameter (max=400,IP2max=40)
      Implicit real*8(A-H,O-Z)
      real C2(max),Y(max),V(max),P1i(max),An1(max),An2(max)
      real YY(3),PP2(IP2max)
      integer IG1(max)
c

```

```

common /Pres2/PP2(IP2max)
common /Const/Pi,Cov,Ra,r0,Phi1,Ang0,N1,N2,V1,P01,Angm
common /Var/P1,P2,Ang1,Ang2,Sl,Sv1,Vd1,Vd2,Pbct,Phi,ht
common /Crt/P2crt,P1crt,C2crt,hert,Vert,An1crt,Vmax
common /Crt9/P2crt9,P1crt9,C2crt9,hert9,Vert9,An2crt9
common /Tape/NT20,NT30
common /IconP1/ICP1,Itact
common /Prevs/Ang2Ls,Ang1Ls,Sv1Ls,ItowrkLs,P2Ls,C2Ls

c
open(unit=911,file='modison.scrh')
If(N2 .gt. max) then
  write(6,*) '!!!!!!!!!!!!!!!!!!!!!!!!!!!!'
  write(6,*) 'Array Size Limit Exceeded!'
  write(6,*) ' '
  write(6,*) '!!!!!!!!!!!!!!!!!!!!!!!!!!!!'
End if
Ierror=0
Iroot=0
Isolu=0
F1=0.
Svs=V1
write(911,*) ' '
write(911,*) ' '
write(911,*) '*****'
write(911,*) 'P2 ==',P2

c
19 If(Itact .eq. 1)then
  write(6,*)
  & 'Input assumed Ratio of Deformed vol./Original vol. : '
  write(6,*) 'Under P2 ==',P2
  write(6,*) '*****'
  write(6,*) 'Previous ratio :',Sv1Ls/V1
  write(6,*) 'Under P2 ==',P2
  read(5,*) Rsv1
  Sv1=Rsv1*V1
Else
  Sv1=V1
  Rsv1=1.
End if
Iter=0

c
If(P2 .gt. 0.) Angst=asin(r0*(P2/P1)**.5/Ra)
21 Do 20 i2=1,N2+1
  C2(i2)=0.
  Y(i2)=0.
  V(i2)=0.
  IG1(i2)=0
20 continue
22 Do 10 i=1,N1
30 If(Isolu .eq. 1)then
  Ang2=An2b1-Y2*(An2b1-An2b2)/(Y2-Y1)
Else
  If(Icall .eq. 1 .and. Itowrk1 .eq. 1)then
    Ang2=Phi1-(Phi1-Angm)*i/N1
  Else
    If(ItowrkLs .eq. Itowrk1 .and. P2Ls*P2 .gt. 0.
    & .and. Itact .eq. 0)then
      If(i .eq. 1) then
        If(P2 .gt. 0.)then
          Sv1=Sv1Ls+(P2-P2Ls)*(Sv1Ls-V1)/P2
        Else
          Sv1=Sv1Ls

```

```

        End if
    End if
    If(P2 .lt. 0.) then
        If(Itowrk1 .eq. 0) then
            Ang2=Ang2Ls-(Ang2Ls-Ang0)*(i-1.)/N1
        Else
            Ang2=Ang2Ls+(Phi1-Ang2Ls)*(i-1.)/N1
        End if
    Else
        If(P2 .gt. .5*Pi)then
            Ang2=Ang2Ls+(.5*Pi-Ang2Ls)*(i-1.)/N1
        Else
            Ang2=Ang2Ls+(Phi1-Ang2Ls)*(i-1.)/N1
        End if
    End if
    Else
        If(Itowrk1 .eq. 0)then
            If(P2 .gt. 0.)then
                If(Phi1 .le. .5*Pi)then
                    Ang2=Angst+(Phi1-Angst)*(i-1.)/N1
                Else
                    Ang2=Angst+(.5*Pi-Angst)*(i-1.)/N1
                End if
            Else
                If(Phi1 .le. .5*Pi)then
                    Ang2=Phi1-(Phi1-Ang0)*i/N1
                Else
                    Ang2=.5*Pi-(.5*Pi-Ang0)*(i-1.)/N1
                End if
            End if
        Else
            Ang2=Phi1-(Phi1-Angm)*(i-1.)/N1
        End if
    End if
    End if
    End if
    An2(i)=Ang2
    loop1=0
23  If(ICP1 .eq. 1) then
        P1=P01
    Else
        P1=P01*Sv1/Sv1
    End if
    F1=F2
c
    If(Itowrk1 .eq. 0)then
        C2(i)=Ra**2*sin(Ang2)-P2*r0**2/(P1*sin(Ang2))
    Else
        C2(i)=((sin(Phi1)*Ra)**2-P2*r0**2/P1)/sin(Ang2)
    End if
c
    G1=r0**2*(1.-P2/P1)/C2(i)
    P1i(i)=P1
    V(i)=Sv1
c
    If(Isolu .eq. 0) then
        write(911,*) 'i,Asin(Ang1),P1,C2,Ang2 in root-bound scanning'
        write(911,*) i,G1,P1,C2(i),Cov*Ang2
    Else
        write(911,*) 'i,Asin(Ang1),P1,C2,Ang2 in root refining'
        write(911,*) i,G1,P1,C2(i),Cov*Ang2
    End if

```

```

      If(abs(G1) .gt. 1.)then
        IG1(i)=1
        If(P2Ls*P2 .gt. 0. .and. ICP1 .eq. 1)then
c   Ensure subsequent parameters on the same trend as the previous
          If(P2 .gt. 0. .and. C2(i) .lt. C2Ls) goto 10
          If(P2 .lt. 0. .and. C2(i) .gt. C2Ls) goto 10
        Else
          If(P2 .gt. 0.) then
            G1=-.911
          Else
            G1=.911
          End if
        End if
        If(ICP1 .eq. 1)C2(i)=r0**2*(1.-P2/P1)/G1
      End if
      If(abs(G1) .gt. 1. .or. C2(i) .lt. 0.)then
        If(i .eq. 1 .and. Itact .eq. 1) then
          write(6,*) 'C2, Asin(Ang1) :',C2(i),G1
          write(6,*) 'Retry gested initial vol. ratio (0/1) ?'
          read(5,*) NY
          If(NY .eq. 1)then
            goto 19
          Else
            goto 10
          End if
        Else
          goto 10
        End if
      End if
c
      Ang1=asin(G1)
c
c   When shell is pulled up Ang1 is always greater than Ang0
      If(P2 .lt. 0. .and. Ang1 .lt. Ang0) goto 10
c
      An1(i)=Ang1
      Da=(Ang2-Ang1)/N1
c
      Sv2=0.
      Sl=0.
      Negdr=0
      ht=0.
      Do 50 j=1,N1
        Ang=Ang2-(2.*j-1.)*Da/2.
        r=(P2*r0**2/P1 + C2(i)*sin(ang))**.5
        Sv2=Sv2+.5*Da*C2(i)*r*sin(Ang)
        ht=ht+.5*Da*C2(i)*sin(Ang)/r
50      Continue
c   Using Simpson's Rule To Evaluate Meridian Curve Length:
      An=Ang1
      Do 51 j=1,N1/2
        Do 52 ii=1,3
          Ang=An+Da*(ii-1)
          r=(P2*r0**2/P1 + C2(i)*sin(ang))**.5
          YY(ii)=.5*C2(i)/r
52      Continue
          An=Ang
          Sl=Sl+YY(1)+4.*YY(2)+YY(3)
51      Continue
          Sl=Sl*Da/3.
c
      If(Itowrk1 .eq. 1) then

```

```

      Sv2=Sv2*Pi
    Else
      If(Phi1 .gt. .5*Pi .and. P2 .lt. 0.)then
        Vuw=Ra**3*cos(Ang2)*(1.-cos(Ang2)**2/3.)
      Else
        Vuw=Ra**3*(cos(Phi)*(cos(Phi)**2/3.-1.)-cos(Ang2)*
&      (cos(Ang2)**2/3.-1.))
      End if
      Sv2=Pi*(Sv2+Vuw)
    End if
  c
  If(Itowrkl .eq. 0)then
    Y(i)=Ra*(Ang2-Ang0)-Sl
  Else
    Y(i)=Ra*(Phi1-Ang0)-Sl
  End if
  F2=Y(i)
c
  write(911,*) 'Y(i),Sl,P1,Ang1*Cov,Ang2*Cov,Iter'
  write(911,*) Y(i),Sl,P1,Ang1*Cov,Ang2*Cov,Iter
c If the total volume after deformation is inaccurate, re-evaluate.
  write(911,*) 'Sv2,Sv1',Sv2,Sv1
  write(911,*) ' '
  tolv=(Abs(Sv2-Sv1)/Sv1+abs(Sv2-Sv1)/Sv2)*.5
  If(abs(G1) .lt. 1.) then
    If(tolv .gt. .01) then
      Sv1=(Sv1+Sv2)*.5
      go to 23
    End if
    Sv1=Sv2
  End if
  If(Isolu .eq. 1 .and. ICP1 .eq. 0)then
    If((Sv2-Vd1)*(Sv2-Vd2) .gt. 0.)then
      If((Y(i)-Y1)*(Y(i)-Y2) .lt. 0.)then
        Sv1=Vd1+(Y(i)-Y1)*(Vd1-Vd2)/(Y1-Y2)
      Else
        Sv1=Vd1-Y1*(Vd1-Vd2)/(Y1-Y2)
      End if
    End if
  End if
c
  write(911,*) '*****'
c
100  format(i2,4(e14.4,2x))
      If(abs(Y(i)) .lt. Facc) then
        Iroot=1
        Isolu=1
        root=C2(i)
        goto 11
      End if
      If(Isolu .eq. 0)then
        If(Y(i)*Y(i-1) .lt. 0. .and. IG1(i-1) .ne. 1)then
c
c Once determine root bound, change from root bound searching to
c root refining within the bound
c
        write(911,*) 'An1b1,An1b2',An1(i-1)*Cov,An1(i)*Cov
        Iroot=1
        Isolu=1
        X1=C2(i-1)
        X2=C2(i)
        Y1=Y(i-1)

```

```

        Y2=Y(i)
        Vd1=V(i-1)
        Vd2=V(i)
        Pi1=Pi(i-1)
        Pi2=Pi(i)
        An1b1=An1(i-1)
        An2b1=An2(i-1)
        An2b2=An2(i)
        An1b2=An1(i)
    End if
c  When P2 exceeds P2 crt and no root is found in the fully wrinkled
c  region, skip to the next applied pressure:
        If(i .eq. N1 .and. Itowrkl .eq. 1
&          .and. P2 .lt. P2crt)then
            write(NT30,*) 'Fail to find a rootbound in fully'
            write(NT30,*) 'wrinkled domain'
            write(NT30,*) 'At P2 = ',P2
            write(NT30,*) ' '
            write(NT30,*) '*****'
            Ierror=1
            Goto 11
        End if
        If(i .eq. N1 .and. Itowrkl .eq. 0
&          .and. P2 .gt. P2crt)then
            write(NT30,*) 'Fail to find a rootbound in partially'
            write(NT30,*) 'wrinkled domain'
            write(NT30,*) 'At P2 = ',P2
            write(NT30,*) ' '
            write(NT30,*) '*****'
            Ierror=1
            Goto 11
        End if
c
    Else
        If(abs(F1-F2) .lt. Facc**2)then
            write(NT30,*)
& 'Assuming Root Found at No Function value changes'
            write(NT30,*) 'Function stagnant at ',Y(i)
            write(NT30,*) 'Assuming func. Tolerance be (Facc**2)'
&          ,Facc*2
            root=C2(i)
            Swkl=Sl
            goto 11
        End if
        If(abs(Y(i)) .lt. Facc) then
            root=C2(i)
            Swkl=Sl
            go to 11
        Else
            If(Y(i)*Y1 .lt. 0.)then
                Y2=Y(i)
                An2b2=Ang2
                Vd2=Sv1
c
            Else
                Y1=Y(i)
                An2b1=Ang2
c
                Vd1=Sv1
            End if
            Iter=Iter+1
            If(Iter .gt. N2)then
                Ierror=1
                write(NT30,*) 'Iteration fails in root finding

```

```

& process'
        write(NT30,*) 'At P2 =',P2
        write(NT30,*) ' '
        Ierror=1
        go to 11
    End if
    go to 30
End if
End if
10 Continue
11 If(Itact .eq. 1 .and. Ierror .eq. 1)then
    write(6,*) 'Give Another Try (0/1) ?'
    read(5,*) NY
    If(NY .eq. 1)go to 19
End if
return
End
*****
subroutine crtP2(Xacc,Facc,Ierror)
*****
c Subroutine to search for critical suction pressure P2 that causes
c fully wrinkled membrane and critical downward load when the plate
c is orthogonal to the membrane.
c
*****
Parameter (max=400)
Implicit real*8(A-H,O-Z)
real C2(max),Y(max),V(max),Pl1(max),An2(max),An1(max)
c
real drr(max)
common /Const/Pi,Cov,Ra,r0,Phi1,Ang0,N1,N2,V1,P01,Angm
common /paramb/Anb2,Anb1,Slb,Pb2,rb,Svb,hb
common /Var/P1,P2,Ang1,Ang2,Sl,Sv1,Vd1,Vd2,Pbert,Phi,ht
common /Crt/P2crt,P1crt,C2crt,hcrt,Vcrt,An1crt,Vmax
common /Crtb/Pb2crt,C1crt,hbert,Vbert,Ab1crt,Ab2crt
common /Crt9/P2crt9,P1crt9,C2crt9,hcrt9,Vcrt9,An2crt9
common /Tape/NT20,NT30
common /IconP1/ICP1,Itact
c
open(unit=922,file='modison.crt')
If(N2 .gt. max) then
    write(6,*) '!!!!!!!!!!!!!!!!!!!!!!!!!!!!'
    write(6,*) 'Array Size Limit Exceeded!'
    write(6,*) ' '
    write(6,*) '!!!!!!!!!!!!!!!!!!!!!!!!!!!!'
End if
Phi=Phi1
Do 5 Icert=1,2
    Ierror=0
    Iroot=0
    Isoln=0
    Iter=1
    Ip1=0
    If(Icert .eq. 1) Sv1=.5*(V1+Vmax)
    If(Icert .eq. 2) Sv1=.5*V1
c
c In Do loop 5, trial 1 calculates upward critical values
c trial 2 calculates downward critical values
c
21 Do 20 i2=1,N2+1
    C2(i2)=0.
    Y(i2)=0.
    V(i2)=0.

```

```

20     continue
22     Do 10 i=1,N1
        Iloop1=0
30     If(Ifact .eq. 1 .and. Iloop1 .ge. 2)then
        write(6,*) 'Calculated Value Sv1 , P1 & Y :',
&         Sv1,P1,Y(i)
        If(Iloop1 .gt. 4)then
            write(6,*) 'Input New Vol. :'
            read(5,*) Sv1
            Iloop1=0
        End if
    End if
    If(Icrt .eq. 1)then
        If(Isolu .eq. 1)then
            Ang1=An1b1-Y2*(An1b1-An1b2)/(Y2-Y1)
        Else
            Ang1=Angm-(Angm-Ang0)*i/N1
        End if
        If(Phil .gt. .5*Pi) then
            Ang2=Pi*.5
        Else
            Ang2=Phil
        End if
        An1(i)=Ang1
c
23     If(ICP1 .eq. 1) P1=P01
        If(ICP1 .eq. 0) P1=P01*V1/Sv1
c
        P2=P1*(r0**2-Ra**2*sin(Ang2)*sin(Ang1))/
&         (r0**2*(1.-sin(Ang1)/sin(Ang2)))
        C2(i)=((sin(Ang2)*Ra)**2-P2*r0**2/P1)/sin(Ang2)
c
    Else
8        If(Isolu .eq. 1)then
            Ang2=An2b1-Y2*(An2b1-An2b2)/(Y2-Y1)
        else
            Ang2=Phi-(Phi-Ang0)*i/N1
        End if
        Ang1=-Pi*.5
        An2(i)=Ang2
        If(ICP1 .eq. 1)P1=P01
        If(ICP1 .eq. 0)P1=P01*V1/Sv1
        P2=P1*(Ra**2*sin(Ang2)+r0**2)*sin(Ang2)/
&         (r0**2*(1.+sin(Ang2)))
        C2(i)=r0**2*(P2/P1-1.)
        Ral=P2/Pbcrt
        If(Ral .gt. 1.)then
            Phi=Pi-asin(Ral**.5*sin(Phil))
            P2=P1*(Ra**2*sin(Ang2)+r0**2)*sin(Ang2)/
&         (r0**2*(1.+sin(Ang2)))
            C2(i)=r0**2*(P2/P1-1.)
        End if
        If(C2(i) .lt. 0.) then
            write(922,*) 'Skip due to C2<0.'
            go to 10
        End if
    End if
    Da=(Ang2-Ang1)/N1
c
    h=0.
    Sv2=0.
    Sl=0.

```

```

Negdr=0
Do 50 j=1,N1
  Ang=Ang2-(2.*j-1.)*Da/2.
  r=(P2*r0**2/P1+C2(i)*sin(ang))**.5
  Sl=Sl+.5*Da*C2(i)/r
  h=h+.5*sin(Ang)*Da*C2(i)/r
  Sv2=Sv2+.5*Da*C2(i)*r*sin(Ang)
50 Continue
c
  If(P2 .gt. 0.)then
    Ral=P2/Pbcr
    If(Ral .gt. 1.) Phi=Pi-asin(Ral**.5*sin(Phi1))
    If(Ral .lt. 1.) Phi=Phi1
    h=h+Ra*(cos(Ang2)-cos(Phi))
  End if
c Vuw is related to the unwrinkled membrane enclosed volume.
  If(Icrt .eq.2)then
    Vuw=Ra**3*(cos(Phi)*(cos(Phi)**2/3.-1.)-cos(Ang2)*
& (cos(Ang2)**2/3.-1.))
    Sv2=Pi*(Sv2+Vuw)
  Else
    Sv2=Sv2*Pi
  End if
  Y(i)=Ra*(Ang2-Ang0)-Sl
  write(922,*) 'i,C2,Y(i),Ang2,Ang1,Sl,P1,P2'
  write(922,*) i,C2(i),Y(i),Ang2*Cov,Ang1*Cov,Sl,P1,P2
c
c If the total volume after deformation is inaccurate, re-evaluate.
  write(922,*) 'Sv1,Sv2',Sv1,Sv2
  tolv=(Abs(Sv2-Sv1)/Sv1+abs(Sv2-Sv1)/Sv2)*.5
  Sv1=Sv2
  If(tolv .gt. .01)then
    Iloop1=Iloop1+1
    goto 30
  End if
  write(922,*) '*****'
c
  V(i)=Sv1
  Pl1(i)=P1
  If(Isolu .eq. 0)then
    If(Y(i)*Y(i-1) .lt. 0.)then
c
c Once determine root bound, change from root bound searching to
c root searching within the bound
c
      Iroot=1
      Isolu=1
      X1=C2(i-1)
      X2=C2(i)
      Y1=Y(i-1)
      Y2=Y(i)
      Vd1=V(i-1)
      Vd2=V(i)
      Pi1=Pl1(i-1)
      Pi2=Pl1(i)
      If(Icrt .eq. 1)then
        An1b1=An1(i-1)
        An1b2=An1(i)
      Else
        An2b1=An2(i-1)
        An2b2=An2(i)
      End if

```

```

End if
c
Else
  If(abs(Y(i)) .lt. Facc) then
    If(Icrt .eq. 1) then
      C2crt=C2(i)
      P2crt=P2
      P1crt=P1
      hert=h
      Vert=Sv2
      An1crt=An1(i)
    If(Phil .gt. .5*Pi)then
      call baswrk(Xacc,Facc,P2crt,Ierrob,Iroot,1,C1)
      If(Ierrob .eq. 1)then
        C1crt=0.
        Hbert=-Ra*cos(Phil)
        Ab1crt=Phil
        Ab2crt=Phil
        Vbert=Ra**3*Pi*cos(Phil)*(cos(Phil)**2/3.-1.)
        Vs=0.
      Else
        C1crt=C1
        hbert=hb
        Ab1crt=Anb1
        Ab2crt=Anb2
        Vbert=Svb
      End if
    End if
    go to 5
  Else
    C2crt9=C2(i)
    P2crt9=P2
    P1crt9=P1
    hert9=h
    Vert9=Sv2
    An2crt9=An2(i)
    go to 5
  End if
Else
  If(Y(i)*Y1 .lt. 0.)then
    Y2=Y(i)
    If(Icrt .eq. 1)An1b2=Ang1
    If(Icrt .eq. 2)An2b2=Ang2
  Else
    Y1=Y(i)
    If(Icrt .eq. 1)An1b1=Ang1
    If(Icrt .eq. 2)An2b1=Ang2
  End if
  Iter=Iter+1
  If(Iter .gt. N2)then
    Ierror=1
    write(NT30,*) 'Iteration fails in root finding'
  write(NT30,*) 'process for critical case'
  write(NT30,*) 'At P2 =',P2
  go to 11
End if
go to 30
End if
End if
Continue
10 If(Iroot .eq. 0)then
  Ierror=1

```

```

        write(6,*) 'Root not bounded in critical P2'
        write(NT30,*) 'Root not bounded in critical P2'
        write(NT30,*) '*****'
        write(NT30,*) ' '
        End if
5      Continue

11     return
      End
*****
      subroutine baswrk(Xacc,Facc,P2,Ierrob,Iroot,Icall,root1)
*****
c Subroutine to search for a root bound between C11 and C12
c to determine the wrinkled form in the vicinity of support
c near the membrane base. The found root bound is stored as (X1,X2)
*****
      parameter (max=400,IP2max=40)
      Implicit real*8(A-H,O-Z)
      real C1(max),Y(max),Ab1(max),Ab2(max)
      real YY(3),PP2(IP2max)
      integer IG1(max)

c
      common /Pres2/PP2(IP2max)
      common /Const/Pi,Cov,Ra,r0,Phi1,Ang0,N1,N2,V1,P01,Angm
      common /Tape/NT20,NT30
      common /Prevbs/Anb2Ls,Anb1Ls,Pb2Ls,C1Ls
      common /paramb/Anb2,Anb1,S1b,Pb2,rb,Svb,hb

c
      open(unit=912,file='modison.scrb')
      If(N2 .gt. max) then
        write(6,*) '!!!!!!!!!!!!!!!!!!!!!!'
        write(6,*) 'Array Size Limit Exceeded!'
        write(6,*) ' '
        write(6,*) '!!!!!!!!!!!!!!!!!!!!!!'
      End if
      Ierrob=0
      Iroot=0
      Isolu=0
      F1=0.
      rb=Ra*sin(Phi1)
      Pb2=P2*(r0/rb)**2
      Aan=Pi-Phi1
      P1=P01
      write(912,*) ' '
      write(912,*) ' '
      write(912,*) '*****'
      write(912,*) 'P2 ==',P2

c
      Iter=0

c
21    Do 20 i2=1,N2+1
        C1(i2)=0.
        Y(i2)=0.
        IG1(i2)=0
20    continue
22    Do 10 i=1,N1
30      If(Isolu .eq. 1)then
        Anb2=Ab2b1-Y2*(Ab2b1-Ab2b2)/(Y2-Y1)
      Else
        If(Icall .eq. 1)then
          Anb2=.5*Pi-(.5*Pi-Aan)*(i-1.)/N1
        Else

```

```

        Anb2=Anb2Ls-(Anb2Ls-Aan)*(i-1.)/N1
    End if
End if
c
    Ab2(i)=Anb2
    loop1=0
    F1=F2
c
    C1(i)=Ra**2*sin(Anb2)-Pb2*rb**2/(P1*sin(Anb2))
c
    G1=rb**2*(1.-Pb2/P1)/C1(i)
c
    If(Isolu .eq. 0) then
        write(912,*) 'i,Asin(Anb1),C1,Anb2 in root-bound scanning'
        write(912,*) i,G1,C1(i),Cov*Anb2
    Else
        write(912,*) 'i,Asin(Anb1),C1,Anb2 in root refining'
        write(912,*) i,G1,C1(i),Cov*Anb2
    End if
    If(abs(G1) .gt. 1.)then
        IG1(i)=1
        If(C1(i) .gt. C1Ls) then
            goto 10
        Else
            G1=.911
        End if
        C1(i)=rb**2*(1.-Pb2/P1)/G1
    End if
c
    Anb1=asin(G1)
c
c When shell base is pulled out Anb1 is always less than Phi1
    If(Anb1 .gt. Phi1) goto 10
c
    Ab1(i)=Anb1
    Da=(Anb2-Anb1)/N1
c
    Svb=0.
    Slb=0.
    hb=0.
    Negdr=0
c Using Simpson's Rule To Evaluate Intergrals:
    Do 33 Isum=1,3
        An=Anb1
        Do 51 j=1,N1/2
            Do 52 ii=1,3
                Ang=An+Da*(ii-1)
                r=(Pb2*rb**2/P1+C1(i)*sin(Ang))**.5
                If(Isum .eq. 1)YY(ii)=.5*C1(i)/r
                If(Isum .eq. 2)YY(ii)=.5*C1(i)*r*sin(Ang)
                If(Isum .eq. 3)YY(ii)=.5*sin(Ang)*C1(i)/r
52            Continue
            An=Ang
            If(Isum .eq. 1)Slb=Slb+YY(1)+4.*YY(2)+YY(3)
            If(Isum .eq. 2)Svb=Svb+YY(1)+4.*YY(2)+YY(3)
            If(Isum .eq. 3)hb=hb+YY(1)+4.*YY(2)+YY(3)
51        Continue
33    Continue
    Slb=Slb*Da/3.
    Svb=Svb*Da/3.
    hb=hb*Da/3.
c

```

```

c Vuw is related to the unwrinkled membrane enclosed volume.
  Vuw=Ra**3*cos(Anb2)*(cos(Anb2)**2/3.-1.)
  Svb=Pi*(Svb+Vuw)
  hb=hb+Ra*cos(Anb2)
  Y(i)=Ra*(Anb2-Aan)-Slb
  F2=Y(i)

c
  write(912,*) 'Y(i),Sl,Ang1*Cov,Ang2*Cov,Iter'
  write(912,*) Y(i),Sl,Anb1*Cov,Anb2*Cov,Iter
  write(912,*) ' '

c
  write(912,*) '*****'

c
100  format(i2,4(e14.4,2x))
      If(abs(Y(i)) .lt. Facc) then
        Iroot=1
        Isolu=1
        root1=C1(i)
        goto 11
      End if
      If(Isolu .eq. 0)then
        If(Y(i)*Y(i-1) .lt. 0. .and. i .gt. 1)then
c
c Once determine root bound, change from root bound searching to
c root refining within the bound
c
        write(912,*) 'An1b1,An1b2',Ab1(i-1)*Cov,Ab1(i)*Cov
        Iroot=1
        Isolu=1
        X1=C1(i-1)
        X2=C1(i)
        Y1=Y(i-1)
        Y2=Y(i)
        Ab1b1=Ab1(i-1)
        Ab2b1=Ab2(i-1)
        Ab2b2=Ab2(i)
        Ab1b2=Ab1(i)
        End if

c
        If(i .eq. N1) then
          write(NT30,*) 'Fail to find a rootbound in partially'
          write(NT30,*) 'wrinkled domain'
          write(NT30,*) 'At P2 = ',P2
          write(NT30,*) ' '
          write(NT30,*) '*****'
          Ierrob=1
          Goto 11
        End if

c
        Else
          If(abs(F1-F2) .lt. Facc**2)then
            write(NT30,*)
            & 'Assuming Root Found at No Function value changes'
            write(NT30,*) 'Function stagnant at ',Y(i)
            write(NT30,*) 'Assuming func. Tolerance be (Facc**2)'
            & ',Facc*2
            root1=C1(i)
            goto 11
          End if
          If(abs(Y(i)) .lt. Facc) then
            root1=C1(i)
            go to 11
          End if

```

```

Else
  If(Y(i)*Y1 .lt. 0.)then
    Y2=Y(i)
    Ab2b2=Anb2
  Else
    Y1=Y(i)
    Ab2b1=Anb2
  End if
  Iter=Iter+1
  If(Iter .gt. N2)then
    Ierrob=1
    write(NT30,*) 'Iteration fails in root finding
& process'
    write(NT30,*) 'At P2 =',P2
    write(NT30,*) ' '
    Ierrob=1
    go to 11
  End if
  go to 30
End if
End if
10 Continue
11 return
End
*****

```

```

*****
*
* THIS PROGRAM SOLVES A DIFFERENTIAL EQUATION IN MEMBRANE VIBRATION ANALYSIS
*      THESIS PROBLEM
* DUMB AS IT HAS NO ADAPTIVE STEP-SIZE DETERMINATION, AND NO CODE
* TO ESTIMATE ERROR, TOTAL # OF INTEGRATION IS DETERMINED BY STEP SIZE
*****
      PROGRAM D15R2
c      driver for routine rk dum
      parameter(nvar=2)
c
      character*9 filnm(5)
      character*5 prefix
      dimension vstart(nvar)
      common /Tape/NT20,NT30,NT40,NT50,NT60
      common /const/Pi,Cov,Ra,r0,h0,fi10,Xm,P01,g,f,wfreq,eqh,ICP1
      common /Extrm/htmin,htmax
      common /Idiverg/Istop
      common /Irr/Ierr
      common /Icount/Itrial,Ipol
      external derivs
c
      data filnm/ 'prefix.out','prefix.in','prefix.plt','prefix.php'
      & , 'prefix.spm'/
c
      write(6,'(//,a,$)') 'Enter file prefix(5 Characters):'
      read(5,600) prefix
      do 5 i=1,5
          filnm(i)(1:5)=prefix
5      continue
      NT20=20
      NT30=30
      NT40=40
      NT50=50
      NT60=60
      open(unit=NT20,file=filnm(1))
      open(unit=NT30,file=filnm(2))
      open(unit=NT40,file=filnm(3))
      open(unit=NT50,file=filnm(4))
      open(unit=NT60,file=filnm(5))
c
      read(NT30,*) dx
      read(NT30,*) x1,x2
      read(NT30,*) (vstart(i),i=1,nvar)
      read(NT30,*) Xm,g,f,wfreq
      read(NT30,*) Ra,fi10,h0,P01,htmax,htmin
c      If ICP1 is 0, internal pressure obeys  $P1 = P10 * V0 / V1$ 
c      If ICP1 is 1, internal pressure is kept constant.
      Pi=3.1415926
      Cov=Pi/180.
      Istop=0
c
      fi10=fi10*Cov
      r0=Ra*sin(fi10)
c      h0=Ra*cos(fi10)
      write(NT20,*) 'Spherical Dome Radius      :',Ra
      write(NT20,*) 'Initial Internal Pressure   :',P01
      write(NT20,*) 'Mass of rigid plate         :',Xm
      write(NT20,*) 'Gravity Constant           :',g
      write(NT20,*) 'Radius of rigid plate      :',r0
      write(NT20,*) 'No-load Height of rigid plate :',h0

```

```

write(NT20,*) 'Integration Step Size      :',dx
write(NT20,*) 'Integration Time interval  :',x1,x2
write(NT20,*) 'Initial Height, Velocity  :',
&      (vstart(i),i=1,nvar)
write(NT20,*) 'Load force Amplitude      :',f
write(NT20,*) 'Load force frequency (Rad/s.) :',wfreq
c
c Ipol assures to calculate static parameters once only
Ipol=0
write(NT20,*)' Time , Deflection , Velocity '
call rk dumb(vstart,nvar,x1,x2,dx)
if(Istop .ne. 0)
& nstep=Istop
c Plot the equilibrium position:
write(NT40,*) '&'
write(NT40,*) x1,eqh
write(NT40,*) x2,eqh
600 format(A5)
stop
end
*****
subroutine derivs(x,y,dydx)
parameter(nmax=100)
dimension y(nmax),dydx(nmax)
common /const/Pi,Cov,Ra,r0,h0,fi10,Xm,P01,g,f,wfreq,eqh,ICP1
common /Tape/NT20,NT30,NT40,NT50,NT60
common /Icount/Itrial,Ipol
c
h1=y(1)
If(y(1) .lt. hmin)then
write(6,*) 'Plate descends to dome bottom'
write(6,*) 'Calculation Stop'
write(NT20,*) 'Plate descends to dome bottom'
write(NT20,*) 'Calculation Stop'
Ierr=1
go to 5
End if
call interpol(h1,P1,C2,fi1)
fi1=fi1*Cov
dydx(1)=y(2)
dydx(2)=-g+(-f*cos(wfreq*x)+P1*Pi*(r0**2-C2*sin(fi1)))/Xm
5 return
end
*****
subroutine rk dumb(vstart,nvar,x1,x2,xh)
parameter(nmax=100)
dimension vstart(nvar),v(nmax),dv(nmax)
common /Tape/NT20,NT30,NT40,NT50,NT60
common /Idiverg/Istop
common /Icount/Itrial,Ipol
do 11 i=1,nvar
v(i)=vstart(i)
11 continue
If(Ipol .eq. 1)
& write(6,*) 'Initial Values :',(v(i),i=1,nvar)
x=x1
nstep=(x2-x1)/xh
c
Velo1=vstart(2)
write(NT40,200) x,v(1)
write(NT20,200) x,v(1),v(2)

```

```

do 14 k=1,nstep
  Itrial=k
  call derivs(x,v,dv)
  call rk4(v,dv,nvar,x,xh,v,k)
  Velo2=v(2)
  x=x1+k*xh
c  If velocity changes sign, there is a local maximum amplitude:
  If(Velo1*Velo2 .le. 0.)then
    write(NT60,*) x,v(1)
  End if
c
  write(NT20,200) x,v(1),v(2)
  write(NT40,200) x,v(1)
  write(NT50,200) v(1),v(2)
  if(Istop .ne. 0) goto 100
c  if(x+xh .eq. x)pause 'Stepsize not significant in rk4dumb'
  Velo1=Velo2
14  continue
200 format(' ',3(e12.5,2x))
100 return
end
*****
subroutine rk4(y,dydx,n,x,h,yout,Itrial)
common /Idiverg/Istop
parameter (nmax=100)
dimension y(n),dydx(n),yout(nmax),yt(nmax),dyt(nmax),dym(nmax)
hh=h*.5
h6=h/6.
xh=x+hh
do 11 i=1,n
  yt(i)=y(i)+hh*dydx(i)
11 continue
  call derivs(xh,yt,dyt)
  do 12 i=1,n
    yt(i)=y(i)+hh*dyt(i)
12  continue
    call derivs(xh,yt,dym)
    do 14 i=1,n
      yt(i)=y(i)+h*dym(i)
      dym(i)=dyt(i)+dym(i)
14  continue
      call derivs(x+h,yt,dyt)
      do 15 i=1,n
        yout(i)=y(i)+h6*(dydx(i)+dyt(i)+2.*dym(i))
15  continue
      return
    end
*****

subroutine intepol(ht,P1,C2,fi1)
  PARAMETER (Npoint=200,Nfunc=4)
c
c  Npower == Highest Power of Linear Regression
c  Nfunc  == # of function to use to data modeling
c  Nsec   == # of Section of broken-down function

real xx(Npoint),x(Npoint),y(Nfunc,Npoint),yy(Npoint)
common /Tape/NT20,NT30,NT40,NT50,NT60
common /const/Pi,Cov,Ra,r0,h0,fi10,Xm,P01,g,f,wfreq,eqh,ICP1
common /Extrm/htmin,htmax
common /Irr/Ierr
common /Icount/Itrial,Ipol

```

```

c
c Ipol assures to calculate static parameters once only
  Ipol=Ipol+1
  If(Ipol .eq. 1) then
c
    read(NT30,*) Ndat
    If(Npoint .lt. Ndat)then
      write(6,*) 'Not Enough Space in Data Array X,Y'
      write(NT20,*) 'Not Enough Space in Data Array X,Y'
      stop
    End if
    Do 15 i=1,Ndat
      read(NT30,*) x(i),(y(k,i),k=1,Nfunc)
15  Continue
c Searching for height of static equilibrium :
    If(wfreq .ne. 0.)then
      Totfor=Xm*g
    Else
      Totfor=Xm*g+f
    End if
    EqP2=Totfor/(Pi*P01*Ra**2)
    If(EqP2 .eq. 0.)then
      eqh=h0
    Else
      Do 10 i=1,Ndat
        xx(i)=y(4,Ndat-i+1)
        yy(i)=x(Ndat-i+1)
10      Continue
        call locate(xx,Ndat,EqP2,loca)
        call value(xx(loca),xx(loca+1),yy(loca),
&      yy(loca+1),EqP2,eqh)
        End if
        write(6,*) 'EqP2,eqh',EqP2,eqh
      End if
c
c There are 3 functions to interpolate:
    if(ht .eq. h0)then
      P1=P01
      C2=0.
      fi1=fi01
      go to 26
    End if
    call locate(x,Ndat,ht,loca)
    call value(x(loca),x(loca+1),y(1,loca),
&      y(1,loca+1),ht,P1)
    call value(x(loca),x(loca+1),y(2,loca),
&      y(2,loca+1),ht,C2)
    call value(x(loca),x(loca+1),y(3,loca),
&      y(3,loca+1),ht,fi1)
26 Return
    End
*****
c
c Subroutine to carry out interpolation or extrapolation:
  subroutine value(x1,x2,y1,y2,x,y)
    real x,y
    y=y1+(x-x1)*(y2-y1)/(x2-x1)
    Return
  End
*****
c subroutine for interpolation location
  subroutine locate(x,Ndat,ht,loca)

```

```
Parameter (Npoint=200)
real x(Npoint)
c
Do 10 i=1,Ndat
  If(ht .gt. x(i) .and. ht .lt. x(i+1))then
    loca=i
    go to 5
  end if
  If(ht .lt. x(1))then
    loca=1
    go to 5
  End if
  If(ht .gt. x(Ndat))then
    loca=Ndat-1
    go to 5
  End if
10 continue
5 return
end
```

:

\*\*\*\*\*

No. of Pressure Trials : 3

Applied Pressure as factors of Initial Internal

Pressure:

-80.0000 -8.00000 5.00000

\*\*\*\*\*

Radius of sphere	:	10.0000000000000
Radius of rigid plate	:	2.5000000000000
Meridional Angle at the root(deg.)	:	150.00013369027
Initial internal pressure	:	10.0000000000000
Curve divisions In The Wrinkled		
Region for Numerical Integration	:	300
Max allowable # of trials	:	100
Tolerance of C2 (root)	:	1.0000000000000D-03
Tolerance of Length Summation	:	1.0000000000000D-02

Original Enclosed Volume	:	4131.7817225053
Original Height Of The Plate(Exact)	:	18.342713013405
Maximun Height Of The Plate	:	23.520648724993
Volume at the Maximun Height	:	769.71045413967
Ang(1) and Ang(2) at This Max. Height	:	83.932908249594

\*\*\*\*\*

Critical Values to Cause Structure Wrinkle  
at Its Root Under Inward Load

P2 (Crt.)	:	39.999983094007
-----------	---	-----------------

Critical Values When Menbrane Becomes  
Fully Wrinkled Due to Suction At Top :

P2 (Crt.)	:	-120.94499866947
P1 (Crt.)	:	10.0000000000000
Total Height	:	20.548589116226
Total Vol.	:	3496.1953708082

\*\*\*\*\* Break Down Summary \*\*\*\*\*

#### Bottom Section

C1 (Crt.)	:	175.19647216797
H (Crt.)	:	8.7057978156419
Ang(1) (Crt.)	:	144.95921975345
Ang(2) (Crt.)	:	100.600023618614
Volume (Crt.)	:	884.87069285982

#### Top Section

Ang(1) (Crt.)	:	27.780660197282
Ang(2) (Crt.)	:	90.0000000000000
C2 (Crt.)	:	175.59062194824
H (Crt.)	:	16.869557072225
Volume (Crt.)	:	2039.9385750238

\*\*\*\*\*

Critical Values When Menbrane Becomes

Orthogonal to the Plate Under Pressure P2 :

P2 (Crt.)	:	84.996223069054
P1 (Crt.)	:	10.0000000000000
C2 (Crt.)	:	46.872638702393
H (Crt.)	:	2.7486436472271
Ang(2) (Crt.)	:	89.550146262865
Volume (Crt.)	:	2246.9102627314
Rigid Body Settlement	:	1.8135696295069

```

*****
External Pressure At          : -800.000000000000
Final Internal pressure       : 10.00000000000000
Enclosed Volume After Deformation : 1616.1442995233
Height Of The Displaced Plate : 23.488413357893
Find C2 as                   : 528.82043457031
Length Before deformation     : 23.653137448579
Wrinkled Meridional Length    : 23.804277564882
% wrinkled membrane           : 100.000000000000
Angle Phi(1) (deg.)          : 73.200019579945
Angle Phi(2) (deg.)          : 96.891390143860
*****

External Pressure At          : -80.000000000000
Final Internal pressure       : 10.00000000000000
Enclosed Volume After Deformation : 2077.0096831986
Height Of The Displaced Plate : 18.436621998908
***** Upper Section *****
Find C2 as                   : 145.08784484863
Length Before deformation (Upper) : 8.3919972089288
Wrinkled Meridional Length (Upper) : 8.3853436445392
% wrinkled membrane (Upper) : 63.6666666666667
Angle Phi(1) (deg.) (Upper) : 22.811242631728
Angle Phi(2) (deg.) (Upper) : 62.560167203961
Vertical Stretch in Upper Section : 1.0147145322301D-01
***** Lower Section *****
Find C1 as                   : 142.85282897949
Length Before deformation (Lower) : 4.2935159000000
Wrinkled Meridional Length (Lower) : 4.2843092592311
% wrinkled membrane (Lower) : 41.0000000000000
Angle Phi(1) (deg.) (Lower) : 148.33066768779
Angle Phi(2) (deg.) (Lower) : 125.40007887726
Vertical Stretch in Lower Section : 5.7852670384301
*****

External Pressure At          : 50.000000000000
Final Internal pressure       : 10.00000000000000
Enclosed Volume After Deformation : 3847.1636859640
Height Of The Displaced Plate : 13.946116818493
Find C2 as                   : 30.514400482178
Length Before deformation     : 6.3822884938893
Wrinkled Meridional Length    : 5.6816883436820
% wrinkled membrane           : 26.982841104120
Angle Phi(1) (deg.)          : -55.013360683167
Angle Phi(2) (deg.)          : 47.057368755518
Rigid Body Settlement         : 0.36870750604545
*****

```